Nucleophilic Addition to Oligomeric Arene Complex Cations

A Thesis

Submitted to the Faculty of Graduate Studies
in Partial Fulfillment of the Requirements
for the Degree of Master of Science
in the Department of Chemistry

University of Manitoba
Winnipeg, Manitoba

Debbie Armstrong

April 1996

ISBN 0-612-12961-6

Name _____

Dissertation Abstracts International and *Masters Abstracts International* are arranged by broad, general subject categories. Please select the one subject which most nearly describes the content of your dissertation or thesis. Enter the corresponding four-digit code in the spaces provided.

Organic Chemistry
SUBJECT TERM

0490
SUBJECT CODE

UMI

Subject Categories

THE HUMANITIES AND SOCIAL SCIENCES

COMMUNICATIONS AND THE ARTS
Architecture 0729
Art History 0377
Cinema 0900
Dance 0378
Fine Arts 0357
Information Science 0723
Journalism 0391
Library Science 0399
Mass Communications 0708
Music 0413
Speech Communication 0459
Theater 0465

EDUCATION
General 0515
Administration 0514
Adult and Continuing 0516
Agricultural 0517
Art 0273
Bilingual and Multicultural 0282
Business 0688
Community College 0275
Curriculum and Instruction 0727
Early Childhood 0518
Elementary 0524
Finance 0277
Guidance and Counseling 0519
Health 0680
Higher 0745
History of 0520
Home Economics 0278
Industrial 0521
Language and Literature 0279
Mathematics 0280
Music 0522
Philosophy of 0998
Physical 0523
Psychology 0525
Reading 0535
Religious 0527
Sciences 0714
Secondary 0533
Social Sciences 0534
Sociology of 0340
Special 0529
Teacher Training 0530
Technology 0710
Tests and Measurements 0288
Vocational 0747

LANGUAGE, LITERATURE AND LINGUISTICS
Language
- General 0679
- Ancient 0289
- Linguistics 0290
- Modern 0291

Literature
- General 0401
- Classical 0294
- Comparative 0295
- Medieval 0297
- Modern 0298
- African 0316
- American 0591
- Asian 0305
- Canadian (English) 0352
- Canadian (French) 0355
- English 0593
- Germanic 0311
- Latin American 0312
- Middle Eastern 0315
- Romance 0313
- Slavic and East European 0314

PHILOSOPHY, RELIGION AND THEOLOGY
Philosophy 0422
Religion
- General 0318
- Biblical Studies 0321
- Clergy 0319
- History of 0320
- Philosophy of 0322

Theology 0469

SOCIAL SCIENCES
American Studies 0323
Anthropology
- Archaeology 0324
- Cultural 0326
- Physical 0327

Business Administration
- General 0310
- Accounting 0272
- Banking 0770
- Management 0454
- Marketing 0338

Canadian Studies 0385
Economics
- General 0501
- Agricultural 0503
- Commerce-Business 0505
- Finance 0508
- History 0509
- Labor 0510
- Theory 0511

Folklore 0358
Geography 0366
Gerontology 0351
History
- General 0578
- Ancient 0579
- Medieval 0581
- Modern 0582
- Black 0328
- African 0331
- Asia, Australia and Oceania 0332
- Canadian 0334
- European 0335
- Latin American 0336
- Middle Eastern 0333
- United States 0337

History of Science 0585
Law 0398
Political Science
- General 0615
- International Law and Relations 0616
- Public Administration 0617

Recreation 0814
Social Work 0452
Sociology
- General 0626
- Criminology and Penology ... 0627
- Demography 0938
- Ethnic and Racial Studies 0631
- Individual and Family Studies 0628
- Industrial and Labor Relations 0629
- Public and Social Welfare 0630
- Social Structure and Development 0700
- Theory and Methods 0344

Transportation 0709
Urban and Regional Planning 0999
Women's Studies 0453

THE SCIENCES AND ENGINEERING

BIOLOGICAL SCIENCES
Agriculture
- General 0473
- Agronomy 0285
- Animal Culture and Nutrition 0475
- Animal Pathology 0476
- Food Science and Technology 0359
- Forestry and Wildlife 0478
- Plant Culture 0479
- Plant Pathology 0480
- Plant Physiology 0817
- Range Management 0777
- Wood Technology 0746

Biology
- General 0306
- Anatomy 0287
- Biostatistics 0308
- Botany 0309
- Cell 0379
- Ecology 0329
- Entomology 0353
- Genetics 0369
- Limnology 0793
- Microbiology 0410
- Molecular 0307
- Neuroscience 0317
- Oceanography 0416
- Physiology 0433
- Radiation 0821
- Veterinary Science 0778
- Zoology 0472

Biophysics
- General 0786
- Medical 0760

EARTH SCIENCES
Biogeochemistry 0425
Geochemistry 0996
Geodesy 0370
Geology 0372
Geophysics 0373
Hydrology 0388
Mineralogy 0411
Paleobotany 0345
Paleoecology 0426
Paleontology 0418
Paleozoology 0985
Palynology 0427
Physical Geography 0368
Physical Oceanography 0415

HEALTH AND ENVIRONMENTAL SCIENCES
Environmental Sciences 0768
Health Sciences
- General 0566
- Audiology 0300
- Chemotherapy 0992
- Dentistry 0567
- Education 0350
- Hospital Management 0769
- Human Development 0758
- Immunology 0982
- Medicine and Surgery 0564
- Mental Health 0347
- Nursing 0569
- Nutrition 0570
- Obstetrics and Gynecology .. 0380
- Occupational Health and Therapy 0354
- Ophthalmology 0381
- Pathology 0571
- Pharmacology 0419
- Pharmacy 0572
- Physical Therapy 0382
- Public Health 0573
- Radiology 0574
- Recreation 0575
- Speech Pathology 0460
- Toxicology 0383

Home Economics 0386

PHYSICAL SCIENCES
Pure Sciences
Chemistry
- General 0485
- Agricultural 0749
- Analytical 0486
- Biochemistry 0487
- Inorganic 0488
- Nuclear 0738
- Organic 0490
- Pharmaceutical 0491
- Physical 0494
- Polymer 0495
- Radiation 0754

Mathematics 0405
Physics
- General 0605
- Acoustics 0986
- Astronomy and Astrophysics 0606
- Atmospheric Science 0608
- Atomic 0748
- Electronics and Electricity 0607
- Elementary Particles and High Energy 0798
- Fluid and Plasma 0759
- Molecular 0609
- Nuclear 0610
- Optics 0752
- Radiation 0756
- Solid State 0611

Statistics 0463

Applied Sciences
Applied Mechanics 0346
Computer Science 0984
Engineering
- General 0537
- Aerospace 0538
- Agricultural 0539
- Automotive 0540
- Biomedical 0541
- Chemical 0542
- Civil 0543
- Electronics and Electrical 0544
- Heat and Thermodynamics ... 0348
- Hydraulic 0545
- Industrial 0546
- Marine 0547
- Materials Science 0794
- Mechanical 0548
- Metallurgy 0743
- Mining 0551
- Nuclear 0552
- Packaging 0549
- Petroleum 0765
- Sanitary and Municipal 0554
- System Science 0790

Geotechnology 0428
Operations Research 0796
Plastics Technology 0795
Textile Technology 0994

PSYCHOLOGY
General 0621
Behavioral 0384
Clinical 0622
Developmental 0620
Experimental 0623
Industrial 0624
Personality 0625
Physiological 0989
Psychobiology 0349
Psychometrics 0632
Social 0451

THE UNIVERSITY OF MANITOBA

FACULTY OF GRADUATE STUDIES

COPYRIGHT PERMISSION

NUCLEOPHILIC ADDITION TO OLGOMERIC ARENE COMPLEX CATIONS

BY

DEBBIE ARMSTRONG

A Thesis/Practicum submitted to the Faculty of Graduate Studies of the University of Manitoba in partial fulfillment of the requirements for the degree of

MASTER OF SCIENCE

Abstract

Addition of hydride and cyanide anions to a series of mono-, di- and polycyclopentadienyliron arene complex cations with etheric bridges was investigated. Reaction of the di-iron complexes with sodium borohydride resulted in the formation of a number of adducts. o-, m-, p-Methyl- and o,o-dimethylphenoxy, thiophenoxybenzene cyclopentadienyliron complexes were used as models to allow for the characterization of the analogous di-iron complexes. The isomeric structures of these adducts were identified using HH COSY and CH COSY NMR techniques. Hydride addition results indicated that the etheric or thioetheric substituents have the predominant effect over the methyl group, leading to a higher addition ratio for the meta-, followed by the ortho-, then the para-position. The products identified from the reaction of the hydride ion with the thiophenoxy compounds were similar to those found for the etheric complexes, but were slightly more selective. It was also clear that in the di-iron system, hydride addition to each complexed arene ring took place independently. The addition of the cyanide anion to di- and poly-iron arene systems was more selective than that of the hydride anion. Reaction of sodium cyanide with p-methyl or o-methyl substituted arene complexes led to the formation of one adduct, with the cyanide being added to the meta-position of the etheric bridges. However, cyanide addition to the di-iron complex, with a methyl substituent attached at the meta-position of each complexed arene, led to the formation of a mixture of adducts. Cyanide addition to the poly-iron system with p-substituted arenes proved to be very selective, allowing for the formation of one adduct. Selective addition of the cyanide anion to various alkylarylsulfonyl di-iron complexes gave rise to one adduct ortho to the electron-withdrawing sulfonyl group. Oxidative demetallation with 2,3-dichloro-5,6-dicyano-1,4-

benzoquinone (DDQ) yielded the functionalized uncomplexed polyaromatic ether with cyano groups in good yield. This study provides a foundation for the chemical alteration of the organic and polymeric systems as well as an understanding of nucleophilic preference to specific sites on an aromatic system that is interacting with a metal moiety.

Acknowledgments

I would like to thank my supervisor Dr. A. S. Abd-El-Aziz for his support, guidance and patience throughout the course of my work. I also wish to thank Dr. H. M. Hutton for his encouragement, and guidance with my work.

Special thanks to S. Bernardin and C. R. de Denus for all their help with the preparation of various complexes as well as support during the writing of my thesis. I wish to thank all the people who provided moral support and patience through the duration of my project, K. Koczanski, K. Epp, Y. Lei, K. Drouillard, S. Smith, A. White, W. Boraie, G. Fisher-Smith, T. Wolowiec, and Dr. D. Vanderwel. I would like to thank the University of Manitoba, Chemistry Department, and the College of Graduate Studies, for giving me the opportunity to pursue this project. I would like to give thanks to the University of Winnipeg for providing me with the facilities necessary to reach this goal.

Last but not least, I would like to thank all my friends and family for all the support and encouragement. Thank you all.

Contents

List of Figures

List of Tables

1.0 Introduction

The need for the development of simple methods to functionalize organic compounds in order to activate these compounds by introducing reactive groups to the system, has led to the investigation of nucleophilic substitution and addition reactions of organo-transition metal complexes [1]. Nucleophilic functionalization via substitution or addition reactions does not usually occur with unsaturated hydrocarbons, due to the electron-rich nature of these compounds [2]. Complexation of benzene analogs to metallic moieties increases the reactivity towards nucleophilic substitution of addition reactions; this can be attributed to metal-ligand bonding effects where the electron density of an aromatic ring or unsaturated hydrocarbon is pulled towards the positively-charged metal, thus promoting attack from a variety of nucleophiles (such as CN^-, H^-, and R^-). The hapto (donor molecule) number and the parity of the ligand, influence the transfer of electron density in the metal-ligand bond [3]. The use of organotransition metal systems with chromium, manganese, or iron has developed into an extremely versatile area [4].

1.1 Synthesis and reactivity of arene cyclopentadienyliron complexes

The (arene)Fe^+ complex where the ligand is a cyclopentadienyl ring (Cp), was first prepared by Nesmeyanov and his group in 1963 [5-8]. Synthesis of these organoiron complexes occurs via the ligand exchange reaction as shown in Scheme 1, in which ferrocene reacts with an aromatic hydrocarbon at 80-165 ^oC in the presence of excess $AlCl_3$ and Al(s), resulting in the substitution of one cyclopentadienyl ring (Cp) by the hydrocarbon to give $[(C_6H_6)FeCp]^+$. The arenes that undergo ligand exchange include toluene, chlorobenzene, anilines, xylenes, and biphenyls.

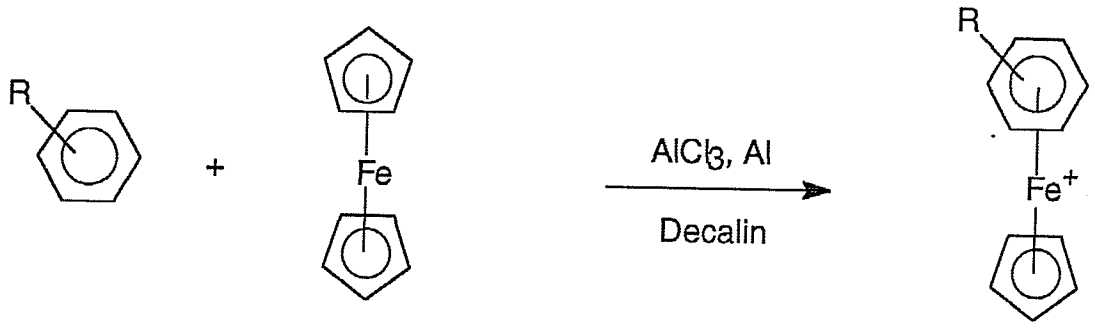

Mono or Disubstitued

R = CH_3, Cl

Scheme 1

Numerous NMR studies on the characteristics of these metal systems illustrating the effect of the metal on complexation where the predominant Cp peak in ^1H NMR shifts 1-2 ppm downfield upon complexation with the metal in ferrocene. As well, it can be seen that the arene protons shift 1 ppm upfield from the uncomplexed structure. Similar shifting patterns are observed in ^{13}C NMR [9]. The complexed aromatic peaks are shifted upfield to 80-100 ppm with the quaternary carbons at ca. 100 ppm from the uncomplexed structures (ca. 120-140 ppm and the quaternary carbon at 135 ppm). This effect of the metal on the arene ring has been attributed to metal-ligand π^*- back donation, ligand π-σ donation and ligand σ-metal donation [10].

The reaction of nucleophiles with the metal systems mentioned above can result in up to six possible products due to the following processes:

(1) Decomplexation by attack at the metal center,

(2) Addition of nucleophile to arene ring complex,

(3) Electron transfer,

(4) Nucleophilic substitution of halogens,

(5) Ring opening, and

(6) Deprotonation of alkyl side chains.

Nucleophilic addition to arene complexes, substitution of halogens, and deprotonation of side chains will be addressed in this work.

1.2 Nucleophilic addition reactions

1.2.1 Introduction

Davies et al. reviewed nucleophilic additions to organometallic complexes consisting of unsaturated hydrocarbon ligands [3]. They established a set of rules by which the site of nucleophilic attack could be predicted on the basis of a series of ligands. These rules are outlined below.

Rule 1: Attack of nucleophiles favor even coordinated polyenes consisting of zero unpaired electrons in the highest occupied molecular orbital (HOMO).

Rule 2: There is preference for addition to occur at open polyenes in comparison to closed polyenes.

Rule 3: The site of addition for even open polyenes is at the terminal carbon atom.

This investigation will not explore the reaction of open polyenes, and so only Rule 1 can be applied. According to Rule 1, the nucleophile will attack the benzene ring in the cationic complex η^6-benzene-η^5-cyclopentadienyliron. Within the Hückel approximation, the HOMOs of odd polyenes are of equal energies and nonbonding, but the HOMOs of even polyenes are bonding and therefore more stable than the orbitals of the odd polyenes. These rules will be demonstrated in sequence in Scheme 2. First the hydride nucleophile should attack an even polyene rather than an odd. Second, addition should demonstrate a preference to attack at an open

polyene rather than a closed polyene and thirdly, the site would be at the terminal carbon.

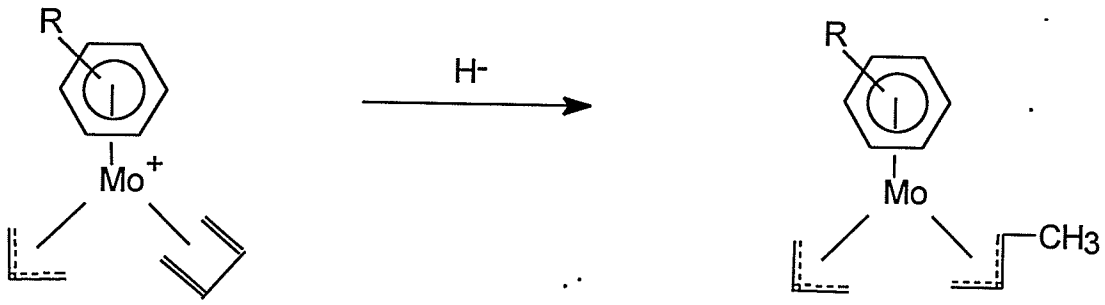

Scheme 2

These rules are easily applied to the simple situation described above but do not allow for prediction of the position on a complexed arene ring (C_6H_5R). Several studies of nucleophilic addition to organometallic complexes were conducted in order to predict and ultimately control the regioselectivity of nucleophilic attack, using carbanions, hydrides, phosphorus and nitrogen contained compounds. Arene rings bound to cationic metal moieties such as chromium tricarbonyl, molybdenum tricarbonyl, tungsten tricarbonyl, ruthenium cyclopentadienyl, manganese tricarbonyl, or iron cyclopentadienyl systems become activated towards nucleophilic attack. Ironcyclopentadienyl complexes were chosen for our research based on their to its low toxicity, high stability, low cost, and ease of complexation / Decomplexation [10, 11]. The addition of nucleophiles to hydrocarbons would extend the uses of these compounds [1, 3, 4] (Scheme 3).

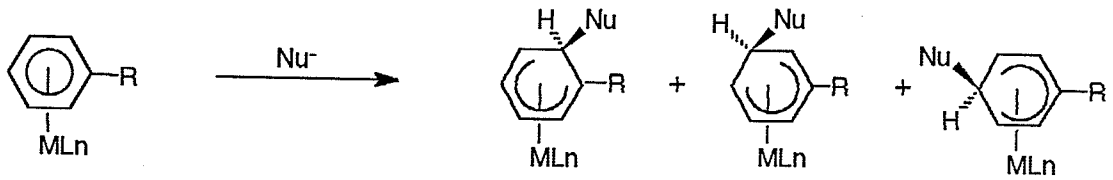

MLn = $(CO)_3Cr$, $(CO)_3Mn^+$, $(C_6H_6)Re^+$, $CpIr^{+2}$, $CpRu^+$, $(C_6H_6)Ru^+$, $(C_6H_6)Fe^{+2}$, $CpFe^+$, etc.

Nu^- = H^-, CN^-, Et^-, Ph^-, D^-, MeO^-

Scheme 3

These studies have revealed novel routes to functionalized organotransition metal complexes as well as the liberated organic compounds [1, 3, 4]. Addition occurs on the exo-face of the arene ligand, as confirmed by NMR and X-ray crystallographic studies [12-18].

1.2.2 Arene Fe^+Cp Complexes

Nucleophilic addition of the hydride anion to ironcyclopentadienyl systems has been investigated [19]. Addition of the hydride anion to $[C_6H_5XFeCp]^+$ cations occurs exclusively exo at the arene ring, with the position of attack dependent on the substituent X [19]. In the case of X = Cl, Me, OMe, and COOMe, the reaction with H^- afforded a mixture of ortho (o-), meta (m-), para (p-) and ipso products. When X = Me, the o-, m-, and p-adducts were formed in approximately a 1:1:1 ratio indicating the small influence a methyl group has on the site of addition [19]. The positions of the protons in ^1H NMR spectrum varied from 2.5-6.5 ppm due to the reduction of π-electron circulation within the ring. The inductive electron release by the methyl groups is responsible for the low shielding of the arene and

cyclopentadienyl protons. Since electron density is asymmetrically distributed over the cyclohexadienyl ligand, the chemical shift is characteristic of its point of attachment. Addition to a substituted position on the ring has been proposed as sterically unfavorable; as well, the release of σ-electrons from methyl group(s) makes it an unfavorable position for attack [19]. For X = OMe, the adduct was formed with a mixture of 1 : 5 : 3, ortho : meta : para products. This regioselectivity was explained as a significant resonance interaction between the nonbonding pair of electrons of oxygen and the arene π system [20]. This ππ - ππ overlap results in a donation of electron density from oxygen to the ortho and para positions. It can also be assumed that electron withdrawal by the metal coordinated to the arene ring would emphasize the polarity of this character slightly. The overall effect of this electron donation from the oxygen would reduce the local positive charge at positions ortho and para to the methoxy substituent, therefore addition occurs meta. Similar reactions with X = Cl and COOMe illustrate attack of the anion in the order of ortho > meta > para positions. Inductive electron withdrawing groups in the ground state of these cations would increase the local positive charge at the ortho positions relative to the meta and para positions [21, 22]. These results are in agreement with theoretical predictions [23].

Sutherland et al. studied hydride addition products with various substituted $[C_6H_5XFeCp]^+$ complexes [24-30]. Fifteen complexes were examined and they were able to establish characteristic properties of the substituent and determine the most likely position of attack by nucleophiles. If the substituent X was a strong electron-donating group (eg: X = NR_2), the adducts formed in both the meta and para positions. In contrast, if X was a strong electron-withdrawing group (eg: X = NO_2) the position of nucleophilic attack was ortho to the substituent X. The other 13 samples demonstrated

mixtures of adducts in the ortho, meta, para, and ipso positions [24] (Scheme 4).

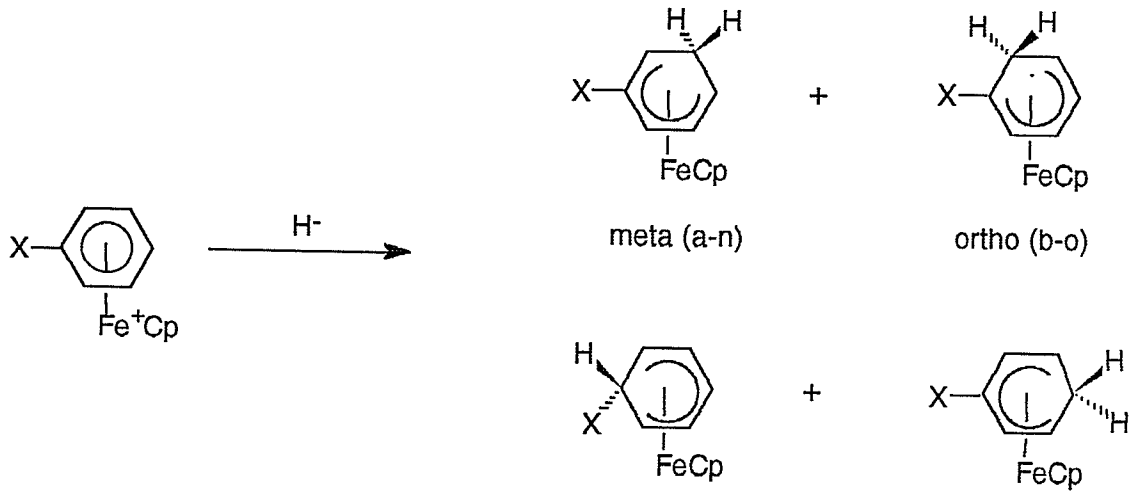

	X		X
a	$N(Me)_2$	i	Ph
b	OPh	j	Cl
c	OMe	k	CO_2Me
d	SC_6H_4 p-Me	l	COPh
e	CH_2Ph	m	CN
f	CMe_3	n	$SO_2C_6H_4$ p-Me
g	Me	o	NO_2
h	Ft		

The results in Scheme 4 were in agreement with those predicted using MO calculations. It was concluded that electronic, steric, and free valency effects all play a role in the position of site activation towards the nucleophile [24]. In general, the nucleophile attacks on the exo face of the arene ring, i.e. away from the metal. The dihedral angle (90°) at which the nucleophile is positioned, along with its ring carbon and an adjacent carbon, does not allow for coupling of this group to any position on the ring except for the endo position. Thus we have very specific coupling patterns which makes it easier to solve the structure of the adduct. If the nucleophile is the hydride anion then H(exo) appears at the highest field position of all the protons whereas

H(endo) appears in the range of 2.4-2.8 ppm. The protons adjacent to the position of addition usually appear between 2-2.92 ppm whereas the remaining arene protons appear at low field. The ^{1}H spectrum generally is a first order coupled spectrum with minimal second order characteristics, however as the number of isomers increase, complexity of the spectrum increases due to significant peak overlap.

The $(C_6H_5X)Fe^{+}Cp$ complexes discussed above show considerable variation in the position of interaction with the nucleophile and differ only in the substituent. In order to determine the extent of the effect of the substituents, further investigation was in order [31]. Electron-donating groups (+I) contain an unshared electron pair on an atom(s) connected to an unsaturated system, which results in a shift of electron density from the substituent to the unsaturated system [2]. On the other hand, electron-withdrawing groups (-I) contain electronegative atom(s) that may multiply bind to an unsaturated system resulting in a shift of electron density from the unsaturated group to the electronegative atom(s) [2]. Both groups display different effects, but these must first be defined. Inductive effects are those that describe the polarization of a bond by a nearby electronegative or electropositive center and acts as a collective effect, (e.g.: the polarization of one bond caused by the polarization of another in order to disperse the positive charge). The final effect is a resonance effect (or mesomeric effect) which define the shift in the distribution of electron density from the original structure. Electron withdrawing groups are described as (-R) and electron donating groups defined by (+R) [2]. The terms donation and withdrawal are used to denote the change in the electronic characteristics of a group when a hydrogen is replaced by a molecule or atom. Consider the complex $(C_6H_5X)Fe^{+}Cp$ where X=Cl; the reaction with H^{-} results in addition at the

ortho position primarily whereas anisole (X=OMe) yields the meta product. This has been justified using the rationale of inductive and resonance effects of the substituents [23]. The groups studied were classified and compared to experimental data as follows.

X	Electronic Effect	Ratio of Products ortho : meta : para
Cl	-I > +R	4 : 1 : 0
OMe	-I < +R	0.2 : 1 : 0.6
Me	+I	1 : 1 : 1
COOMe	-I -R	13 : 1 : 1.1

Inductive electron donation has no influence for methyl groups but the meta directing property of OMe shows the importance of the +R effect by which the positive nature in the ortho and para positions are reduced through donation of π-electron density from the oxygen atom. The lack of activity of the para position in the chloro-substituted complex could also be attributed to the +R effect. This is in accordance with the -R effect of the ester group when the para position is slightly activated but clearly is stronger in the ortho position [23].

Cyanide addition to substituted (η^6-arene-η^5-cyclopentadienyl)iron cations has also been studied, although on a smaller scale compared to other nucleophiles. Sutherland et al. established a procedure where they could control the substitution versus addition of CN^- of one reaction. When cyanide reacted with $[(C_6H_5Cl)FeCp]^+$, time was the factor which controlled the product formed. When the reaction time was 30 min., addition ortho to the chloro substituent was the only product detected. However, when the reaction was left for 3 hours, the product showed substitution at the chloro group, as well as ortho addition. Oxidative demetallation procedures yielded 2-chlorobenzonitriles and phthalonitriles for the 30 min. and 3 hour reactions, respectively [29]. Similar products were obtained even with -OR groups on the ring. Once the metal moiety was removed, 3-methoxy and 3-

phenoxyphthalonitriles were obtained. Similarly, 2,6-dichlorotoluene yielded pure addition product or a mixture with the substitution product. The oxidizing agent of choice was 2,3-dichloro-5,6-dicyano-1,4-benzoquinone (DDQ) [30]. Similar studies on the reaction of cyanide with $Fe^{+}Cp$ complexes have involved the use of electron-withdrawing groups (NO_2, $SO_2C_6H_4$(p-Me), CO_2Me and CN), in order to exert greater regio control over the site of addition. Under identical reaction conditions as outlined for hydride addition, CN adducts formed selectively ortho to the strong withdrawing substituent (Scheme 5).

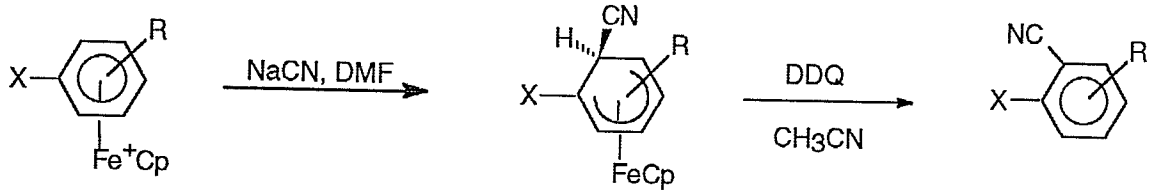

R = H, CH_3 X = NO_2, CN, p-$SO_2C_6H_4Me$, Cl

Scheme 5

Studies of complexed aromatic and heterocyclic compounds focused on the functionalization with cyanide and ketone enolate anions [30]. The only product detected exhibited addition ortho to the electron withdrawing substituent on the arene ring. For the heterocyclic compound, position 4 (or ortho) to the ketone on a xanthone type compound was the site of addition. DDQ again was the best reagent to liberate the functionalized organic or heterocyclic compound.

Steric effects resulting from the methyl groups ortho to the electron-withdrawing substituent of arene complexes have been reported with hydride addition [28]. When ortho positions were hindered, addition in the meta and para positions increased. It was proposed that steric, electronic and free valency effects all play a role in nucleophilic addition reactions [23, 24]. However, cyanide and acetonyl addition did not display the same sensitivity towards steric factors; addition in this case occurred in the ortho position only, or ipso to the methyl group. Recall that hydride adducts form predominantly ortho to electron withdrawing groups and both cyanide and acetonyl ions give selective attack at the site ortho to the substituent [30] (Scheme 6).

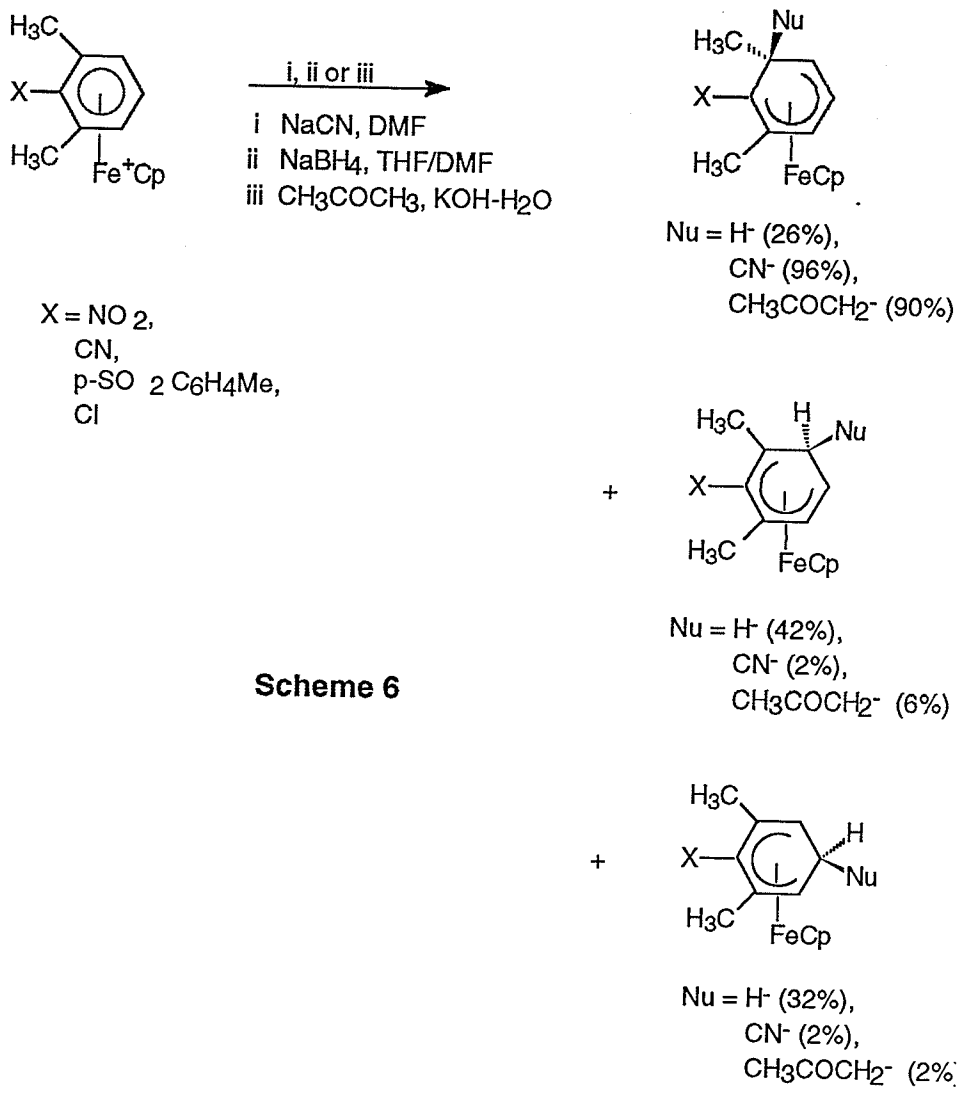

Scheme 6

Therefore steric factors alone do not account for variations in the site of attack. Electronic and free valency effects [31, 32], along with the nature of the nucleophile, also contribute to the overall product distribution. There does not seem to be a trend that can be generalized for all addition reactions other than the correlation of the inductive and resonance effects of the substituent, however even here there are inconsistencies. It may be that the nature of the nucleophile may have more influence over position of attack than any other factor.

Functionalization of cyclopentadienyl(naphthalene)iron (II) complexes via nucleophilic addition has recently been reported [33]. Reaction with alkyllithium and Grignard reagents yielded the 19 electron complex [(η^5-Cp)(η^6-naphthalene)Fe(I)]. Introduction of methoxy groups to naphthalene was proposed in order to inhibit the reduction of these complexes, in hope that the reaction path would change. It was found that reaction of this complex with organolithium reagents produced a series of isomers as illustrated in Scheme 7.

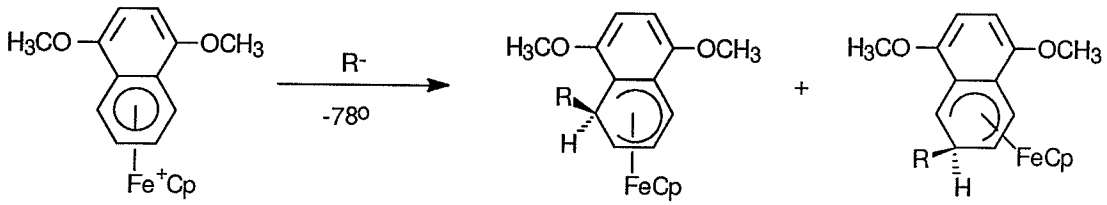

a **b**

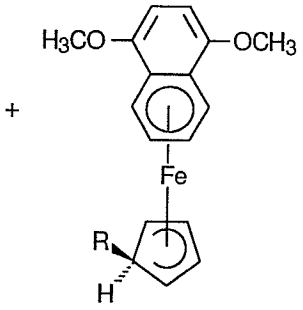

c

Nucleophile	Ratio of Products
$NaBH_4$	a(69) : b(31) : c(0)
MeLi	a(72) : b(17) : c(11)
PhLi	a(61) : b(26) : c(13)
AllylLi	a(75) : b(7) : c(18)
$Li(CHS(CH_2)_3S)$	a(0) : b(66) : c(34)
Bu^tLi	a(0) : b(0) : c(100)

It is obvious that stabilized primary carbon nucleophiles and hydride anions add exclusively to the naphthalene ligand to give exo products in the 5

> 6 positions, unless the nucleophile is bulky. Addition at the Cp ligand increases as the size and reactivity of the nucleophile increases. Products of this study were identified using X-ray crystallographic and NMR techniques [33, 34].

Popular reactions of nitroarenes with nucleophiles such as the Janovsky reaction illustrate the addition of carbanions derived from various ketones [25, 35]. The significance of these reactions is the utilization of nitroarenes; for example, addition to m-dinitro or 1,3,5-trinitrobenzene would result in the formation of a carbon-carbon bond ortho to a nitro substituent [25, 35]. Janovsky reactions require the presence of two or more electron withdrawing groups in order for the reaction to take place, but a metal moiety can replace one of the electron withdrawing groups. For example; the η^6-nitrobenzene-η^5-cyclopentadienyliron cation reacted with the acetonyl anion to give the Janovsky adduct 1-5-η^5-1-nitro-6-exo-(2-oxo-1-propyl)-cyclohexadienyl)(η^5-cyclopentadienyl)iron [25]. This reaction resulted in addition at the same site, ortho to the substituent, when the nitro group was replaced by CN, p-$SO_2C_6H_4CH_3$ or COC_6H_5. If the nitro group was replaced by a chloro substituent then a mixture of ortho, meta, and para adducts were formed in the ratio of 12.7 : 1 : 1.1, indicating the importance of the inductive effect of an electron-withdrawing substituent. Treatment of these products with ammonium ceric nitrate yielded the organic compound. Similar nucleophiles such as nitromethyl, cyanomethyl, and phenylethynyl anions also demonstrated selective ortho addition to complex arenes which contain an electron-withdrawing group [36]. In contrast, nucleophiles such as alkyl, dichloromethyl, and trichloromethyl anions displayed no selectivity under the same conditions, and resulted in the formation of all three isomers. It seemed quite promising to introduce chlorinated alkyl groups to the ring. The

dichloromethyl adduct formed predominantly at the position ortho to the substituent. These chlorinated organic products are of synthetic importance in the production of heterocyclic compounds [36]. Oxidative-demetallation was successful using DDQ.

1.2.3 Arene $Cr(CO)_3$ complexes

Due to the ease of complexation of the $(CO)_3Cr$ moiety with aromatic systems, the vast majority of research in this field has involved the use of these types of complexes [4, 37]. Addition of nucleophiles to (arene)$Cr(CO)_3$ has led to the formation of anionic [$(CO)_3$Cr(cyclohexadienyl)] intermediates which could not be obtained through substitution reactions unless a strong leaving group was present. These adducts are air sensitive and usually undergo oxidative demetallation without isolation, allowing for the functionalization of the arene compounds [4]. A novel characteristic of the cyclohexadienyl intermediates is the increased reactivity towards electrophilic reagents, enhancing the flexibility of this methodology. In general, the electrophiles demonstrate selectivity consistant with that of the nucleophile. The reaction appears to be general although only a few examples have been reported [4]. The only drawback in the use of these chromium complexes is the weak electrophilicity of the arene ring; thus, strong nucleophiles containing ester, nitrile, sulfur, and carbanions stabilized by lithium are necessary for reaction to occur which in fact introduces competition for addition to the arene ring [38].

Regioselectivity has been the subject of many studies in which correlations have been suggested to facilitate predictions with a reasonable degree of accuracy. To summarize, arenes containing electron-donating substituents (eg: NR_2, OMe, F) favored addition to the site meta to the

substituent, with a small amount of ortho product. As the substituent weakens in its donating- or withdrawing-abilities the selectivity of the nucleophile decreases, indicating the role of inductive and resonance effects. Thus for methyl or chloro substituents, a mixture of meta ~ ortho > para products were detected that varied depending on the nucleophile [20]. Substituents such as F_3C, and Me_3Si resulted in para addition with a small amount of meta products. Some substituents, such as CO and CN, not only activate the ring towards nucleophilic addition but are also susceptable to attack themselves [39]. In the case of naphthalene complexes, it was found that if sufficient equilibration time was allowed, mixtures of products could become solely one product. When metal moieties activate heterocyclic ring systems there is high selectivity for both the 4 and 7 positions, but mixtures of these products can be forced to equilibrate solely to one product [4] (Scheme 8).

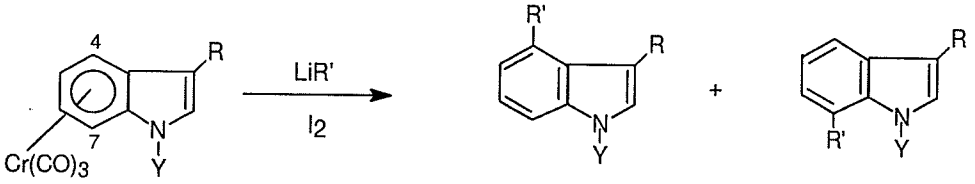

LiR'	R	Y			
CMe_2CN	H	Me	99	:	1
1,3-dithianyl	H	Me	14	:	86
CMe_2CN	CH_2SiMe_3	Me	17	:	83
CMe_2CN	CH_2SiMe_3	$CH_2SiBu^tMe_3$	95	:	5

Scheme 8

The rate of this intermolecular equilibration is affected by various reaction conditions including solvent change, the use of K^+ versus Li^+ reagents, and temperature change [4]. Steric effects of the carbonyl ligands have been proposed as influencing site activation. The arene carbons

eclipsed with a CO ligand are predicted to be more electrophilic, and thus more receptive to nucleophiles [4]. For most systems, this is an acceptable explanation where donor substituents favor meta due to polarity of the donor group and the eclipsing carbonyl groups. Similarly, accepting groups favor ortho and para adduct formation which is influenced by both the polarity of the substituent and the anti conformation of the carbonyl ligands.

1.2.4 Arene $Mn^{+}(CO)_3$ complexes

Tremendous effort has been directed toward the use of cationic metal moieties such as $(CO)_3Mn^{+}$, $CpFe^{+}$ or $(C_6H_6)Fe^{2+}$ for the activation of arenes, allowing for the formation of neutral functionalized cyclohexadienyl complexes. Reactivity of $[(\eta^6\text{-arene})Mn(CO)_3]^{+}$ complexes is high and show similar trends in selectivity as $Cr(CO)_3$. Double nucleophilic addition is one of many projects of interest, and can be achieved with a variety of metal complexes. Nucleophilic attack on $[(\eta^6\text{-arene})Mn(CO)_3]^{+}$ yielded three products through attack at the ring, at CO, and at the metal, with the release of a ligand [40]. These results were consistent with a competing photochemical reaction taking place, which was identified later. Interest in this discovery led to mechanistic studies on the subject [41]. A method to classify the relative electrophilic reactivities through the comparison of various nucleophiles to a number of metallic moieties was also developed [38]. An arene coordinated to $Ru(C_6H_6)^{2+}$ was determined to be 6,000,000 times more electrophilic than one bound to $Fe^{+}Cp$. The order of decreasing activating abilities is as follows: $Fe(C_6H_6)_2^{2+}$ > $Ru(C_6H_6)_2^{2+}$ > $Mn(CO)_3$+ > $Mn(CO)_2PPh_3$ > $FeCp^{+}$ > $Cr(CO)_3$ [38]. Along with arene rings, heterocyclic systems can be activated towards nucleophilic attack. Heterocyclic compounds like indole are important due to their regular appearance as a

basic structural unit in many natural products [42]. The metal moiety can bind either rings but the nitrogen must be deprotonated in order for the metal to coordinate to the five-membered ring. This piano-stool structure is sensitive to both weak and strong nucleophiles allowing for limitless reaction possibilities before and after the metal is removed. They react in a manner similar to the analogous Cr complexes in that C(4) and C(7) are the most electrophilic positions. Selective products can be obtained if the group on nitrogen is controlled [42]. Overall it has been established that this route of functionalization via a manganese intermediate is a useful and effective method based on the ease of formation, addition, and oxidative demetallation. The use of $(CO)_3Mn^+$ species as an activating group has led to the synthesis of a number of potential biologically active chiral compounds [43-45]. Scheme 9 displays the reaction of nucleophiles with $(arene)Mn(CO)_3^+$ complexes to produce antibiotic stilbenes which can also be obtained from the extraction of *Xenorhabdus* (bacteria), although less efficiently.

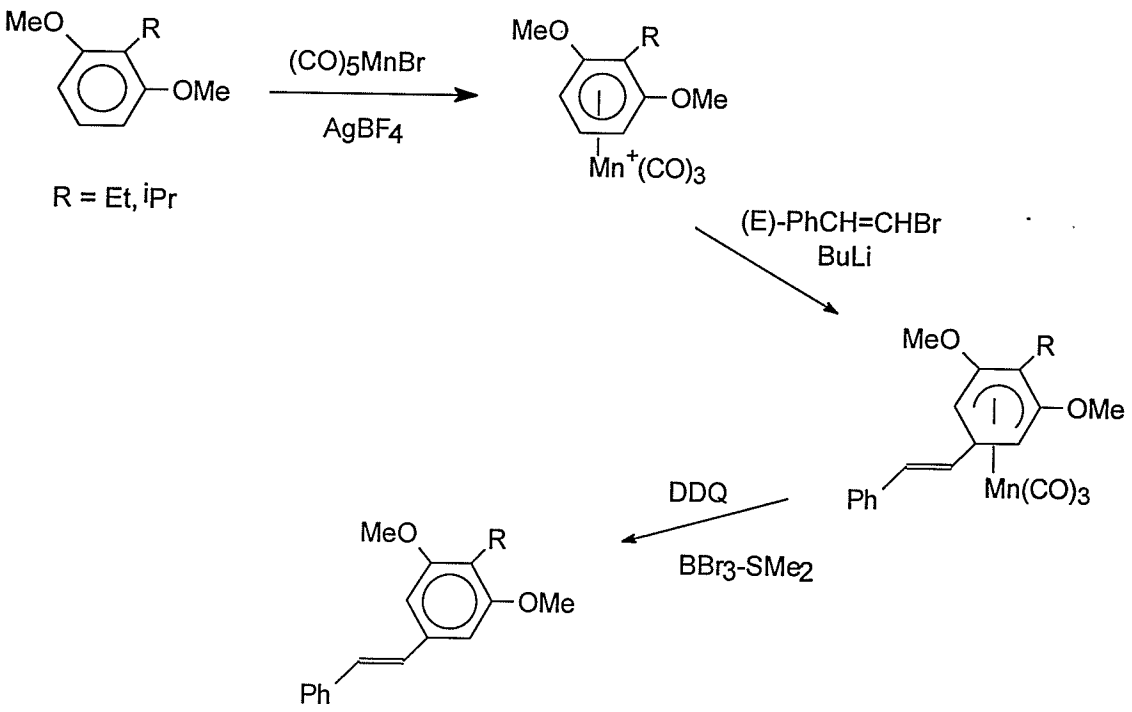

Scheme 9

This is only one example of many which displays the significance of these methods.

1.2.5 Arene $Fe(CO)_3$ complexes

Addition to arene $Fe(CO)_3^+$ complexes is of interest due to its equivalency to cyclohexenone cations in retrosynthetic analysis [46-48]. Reaction of these complexes with cyanide anions have been investigated in order to direct addition to a site which is hindered by a methyl group [49, 50]. Other research has involved the development of a method which generates a quaternary carbon surrounded by functional groups contained in a six-membered ring. This work is directed towards the generation of precursors for biological products like steroids and erythromycin [51].

1.2.6 Bis(arene) metal complexes and their reaction with nucleophiles

Cyclohexadienyl phosphonium ring adducts of the form $[(C_6H_6{\cdot}PR_3)(C_6H_6)M]^{2+}$ (M=Fe, Ru, Os) can be prepared quite easily due to the high reactivity of both the bis(arene) complex and the tertiary phosphine. Addition to both rings was never detected even when the phosphine was in large excess. Addition, as usual, occured on the exo-face of the arene ligand. The goal of this study was to develop a new method to couple aromatic molecules using coordinated benzene as the electrophile in electrophilic aromatic substitution reactions [52, 53]. $[Bis(arene)Fe]^{+2}$ cationic systems which contain methyl or phosphine substituted rings have undergone nucleophilic addition of carbanions generating carbon-carbon bonds. Polymerization and fragmentation occured, yielding partially complexed compounds [52, 53]. The reaction of $(C_6H_3Me_3)_2Fe^{2+}$ with LiPh, $LiBu^t$, and $LiCHCH_2$ type reagents yielded two adducts; one per ring which can then be oxidized to yield two free arene molecules [1]. Reaction of these methylated complexes with base can deprotonate the side chain, generating a nucleophile which is free to attack other complexes in solution. In more cyclic compounds deprotonation can also occur resulting in the formation of new double bonds or new routes of modification through alkylation reactions [53-55].

1.2.7 Double nucleophilic addition reactions

Double nucleophilic addition to complexes containing Mn, Co, and Ir has also been examined [38, 56-58]. The process involves an initial nucleophilic attack, followed by the reactivation of the neutral complex, and finally a second nucleophilic attack. The $[(\eta^6\text{-arene})Mn(CO)_3]$ cationic

systems can undergo double nucleophilic addition to aromatic molecules to yield difunctionalized cyclohexadienes. Initially, the first nucleophile reacts with the arene ring to form a neutral adduct. In order for this system to undergo a second addition the cationic complex must be regenerated, which can be achieved by the reaction with NO^+ to replace a CO ligand. These newly generated complexes are in fact more electrophilic than the initial tricarbonyl structure, and therefore undergo reaction with phosphorus, nitrogen and hydrogen donor nucleophiles, producing the desired cyclohexadiene compound.

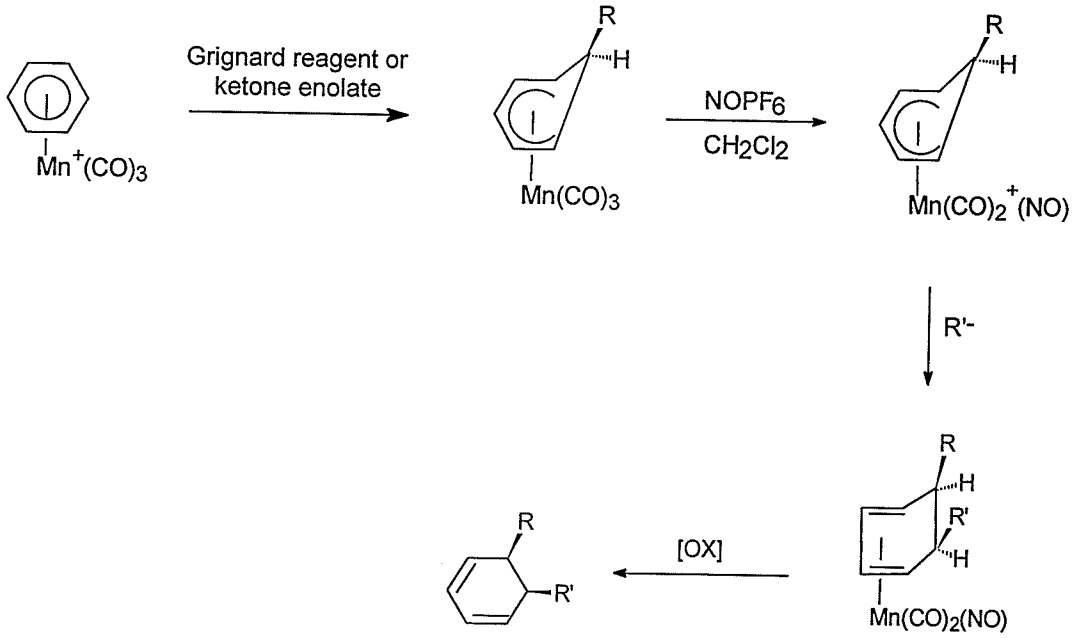

Scheme 10

The ease of preparation of manganese complexes as well as their diversity in reaction with nucleophiles has led to the formation of stable cyclohexadiene compounds [59]. A limitation of this method is in the reaction of carbanions, which may undergo reaction with the CO ligands, or electron transfer with the newly generated complex [38]. If one of the CO ligands was replaced by a

PMe_3 ligand, the chiral metal center would be developed rendering the complex more resistant to reduction due to steric factors and its reduction of the activation energy [38]. However, this allows for the formation of diastereoisomers. It was found that the major isomer featured addition on the side on which the NO ligand was situated. Once the second nucleophile was introduced to the complex, endo addition of D^-, H^-, and COR^- anions was observed. This was attributed to the presence of an electrophilic CO, however, this condition cannot be generalized to other metal complexes. Other interests with $Mn^+(CO)_3$ systems lie in the functionalization of heterocyclic compounds [41, 42, 59].

1.3 Substitution reactions

1.3.1 Introduction

The reactivity of aryl halides towards nucleophiles is enhanced by the presence of an electron-withdrawing substituent on the ring. The role of this group is to pull the electron density of the ring towards itself leaving the ring open to reaction with nucleophiles. This has the opposite effect than an electron-donating group. As discussed above, the electron-withdrawing group can be substituted by a metal moiety coordinated to each carbon in the arene ring is bound coordinately to each carbon equally. Nucleophilic substitution can easily occur with the $[(\eta^6\text{-}C_6H_5Cl)Fe^+Cp]$ [60-64]. This displacement of the chloro substituent provides a synthetically useful method which is dependent on the nature of the nucleophile and the substituent. This is one route to the functionalization of organic compounds. The usual approach to these reactions is initial formation of the complex followed by the modification of the ligand and finally, liberation of the free modified arene from the metal center as depicted in Scheme 11.

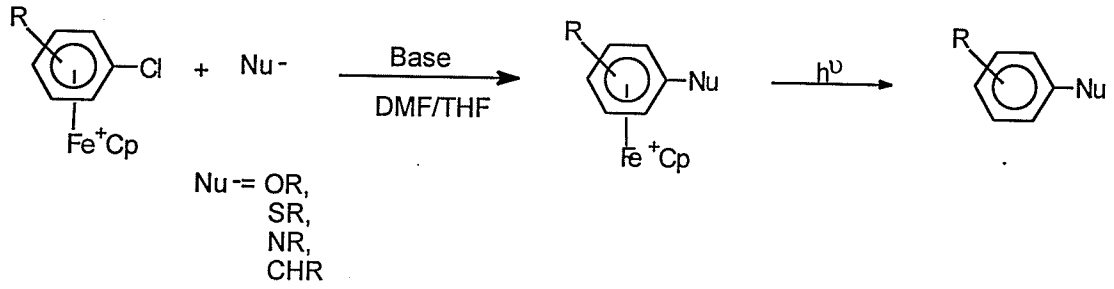

Scheme 11

1.3.2 Synthesis of S, SO_2 and O bridged complexes

A series of diiron complexes containing etheric and sulphonyl linkages with methyl and chloro substituents were prepared (Scheme 12 and 13) [10].

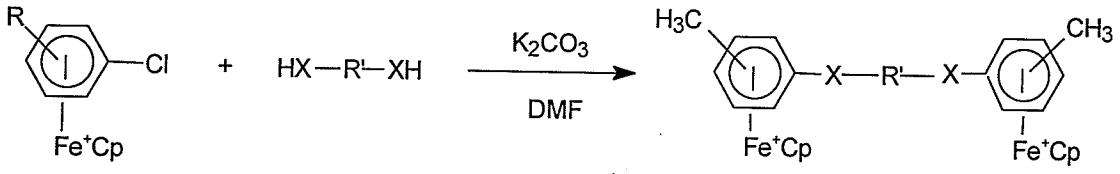

= O, O R = 4-Me, 3-Me, 2-Me, 2,6-$(Me)_2$ R' = C_6H_4

= S, S R = 4-Me, 4-Cl R' = $(CH_2)_n$ n = 2,4,6

= O, S R = 4-Me R' = C_6H_4

Scheme 12

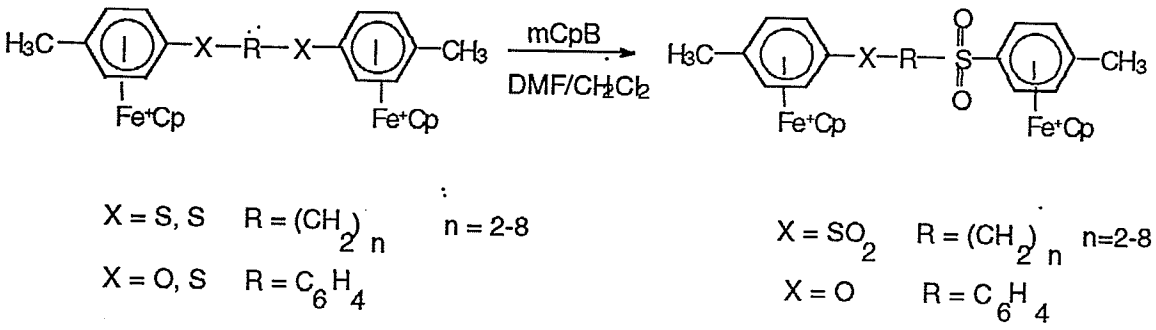

Scheme 13

The etheric diiron complexes have undergone hydride addition in order to determine the factors affecting the position of attack on the arene rings. Due to the complexity of the NMR of these bimetallic adducts it was necessary to prepare the analogous monometallic species as a model for the NMR studies. The first substitution of a chloro substituent on an arene complex by a oxygen, nitrogen, or sulfur nucleophile was completed by Nesmeyanov and co-workers [65, 66], as well as Khand et al. [20]. Scheme 14 illustrates the method used to prepare various methyl substituted (η^6-phenoxy-η^5-cyclopentadienyl)iron(II) benzene hexafluorophosphate salts.

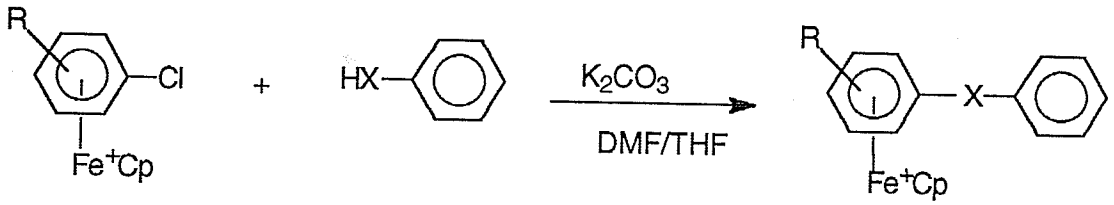

Scheme 14

An efficient synthetic route to poly-cyclopentadienyliron arene cations has recently been developed [67]. These complexes are referred to by the number of metal moieties ($Fe^{+}Cp$) contained. For example, the system which consists of three iron moieties, five aromatic rings, two methyl groups and five oxygen atoms will be referred to as the trimetallic complex. Scheme 15 illustrates the preparation of the trimetallic complex, whereas Scheme 16 and 17 demonstrate, respectively, the general synthesis of the more complicated even and odd polymetallics respectively.

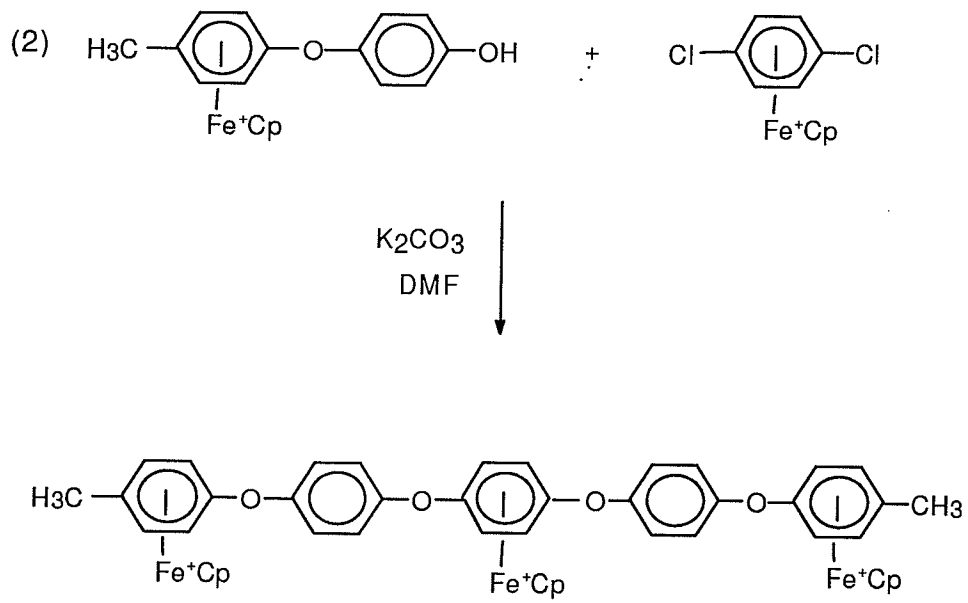

Scheme 15

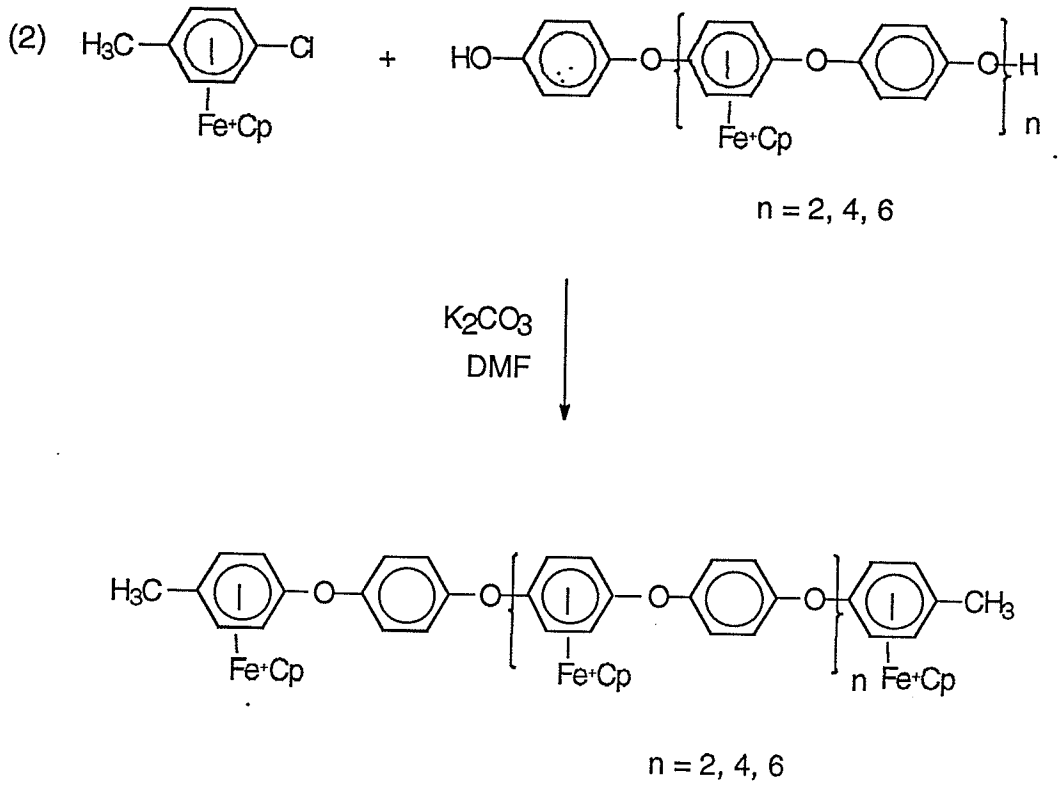
(2)
H3C
Cl
Fe+Cp
+
HO
O
O
O
H
n
Fe+Cp
n = 2, 4, 6
K2CO3
DMF
H3C
O
O
O
O
CH3
Fe+Cp
Fe+Cp
n Fe+Cp
n = 2, 4, 6

Scheme 16

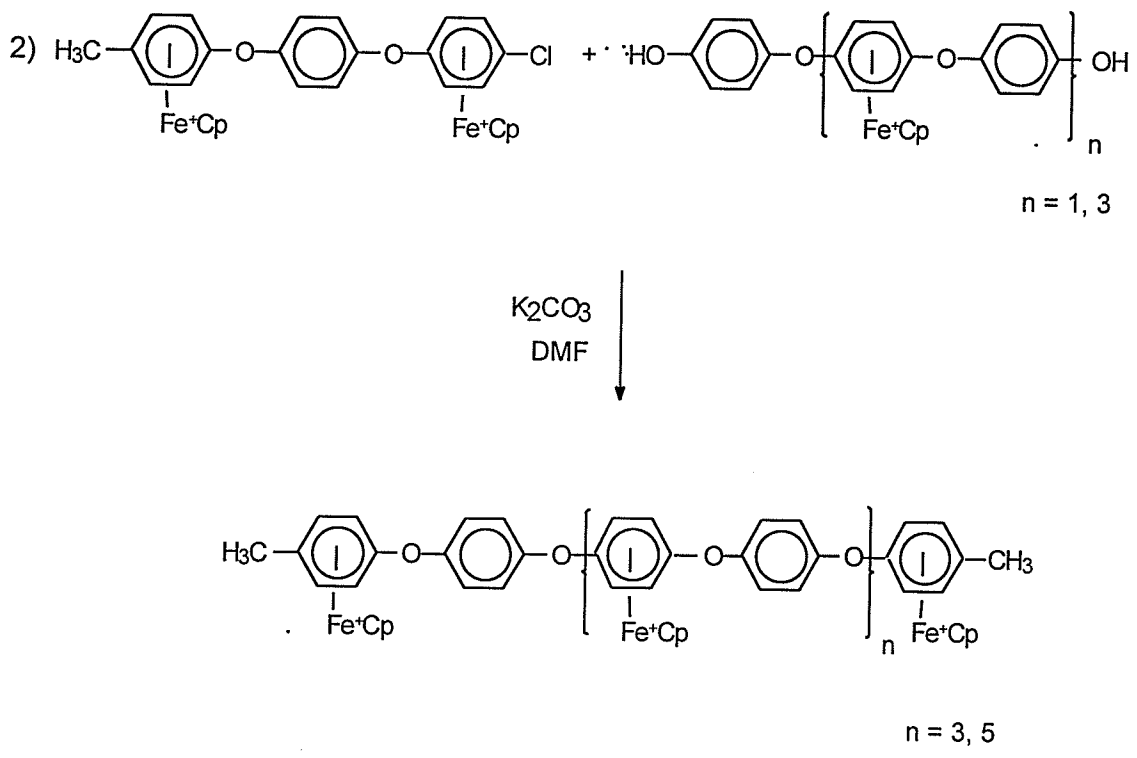

Scheme 17

1.4 NMR techniques

Nuclear Magnetic Resonance (NMR) spectroscopy is based upon the absorption of radio waves by certain nuclei in molecules when they exist in a strong magnetic field. When considering the nuclei of atoms they are grouped according to having spin or not having spin. A nucleus with spin gives rise to a small magnetic field which is referred to as a nuclear magnetic moment. A generated magnetic field from a permanent magnet is symbolized by H_0 and its direction is represented by an arrow as a vector would be. If the molecules are placed in the magnetic field, the magnetic moment of each hydrogen nuclei aligns itself in one of two directions with respect to the external field. These directions are parallel or in the same

antiparallel which the magnetic moment of the proton opposes the external field. The parallel state is more stable and lower in energy than the antiparallel state. If a frequency of radio waves is introduced a fraction of the parallel protons absorb energy and flip to the higher energy state. At this point the nucleus can lose absorbed energy to its surroundings and return to the lower energy state. If the sample continues to absorb energy then a signal in the spectrum is generated. The magnetic field is complied of both the applied field and a combination of induced molecular magnetic fields which are generated in the bonds of the molecule by H_o. The protons of a molecule flip at different combinations of H_o and radio frequency because they are in different magnetic environments. This effect allows us to obtain a spectrum of the different types of protons. For example, protons which absorb energy at lower H_o give rise to an absorption peak downfield whereas absorption at higher energy gave rise to a peak upfield.

NMR was the method proven to be the most useful in the identification and characterization of nucleophilic addition products. Over the last few decades improvement of NMR magnets and techniques has developed new routes for structure determination. As the complexity of compounds increase, higher resolution and more detailed spectroscopy is in demand. Control of pulse sequences as well as the introduction of time intervals between the initial pulse and the signal acquisition result in one or two dimensional NMR. Conventional NMR or 1-D NMR is actually in two dimensions when considering a Cartesian coordinate system with the second dimension representative of the peak intensity. In accordance, the 2-D spectrum describes a three dimensional system where the plane perpendicular to the page acts as the third dimension. 1-D spectra (^1H and ^{13}C) are attained through experiments which involve a single pulse immediately followed by a

signal acquisition and Fourier transformation of the FID (free induction decay). The FID represents the exponentially decaying sine wave with a frequency equal to the difference between the applied frequency and the resonance frequency for that nucleus. This signal is built up after a series of repetitive pulses with signal acquisition and accumulation between pulses has been acquired. For 2-D NMR, multiple pulse sequences followed by time intervals before the acquisition creates series of evolution periods. In the simple example of chloroform, the experiment begins with a pulse, interval (t_1), 90° ($\pi/2$), acquisition pulse, acquisition (t_2), and Fourier transformation of t_2 and t_1 where t_1 is the evolution period.

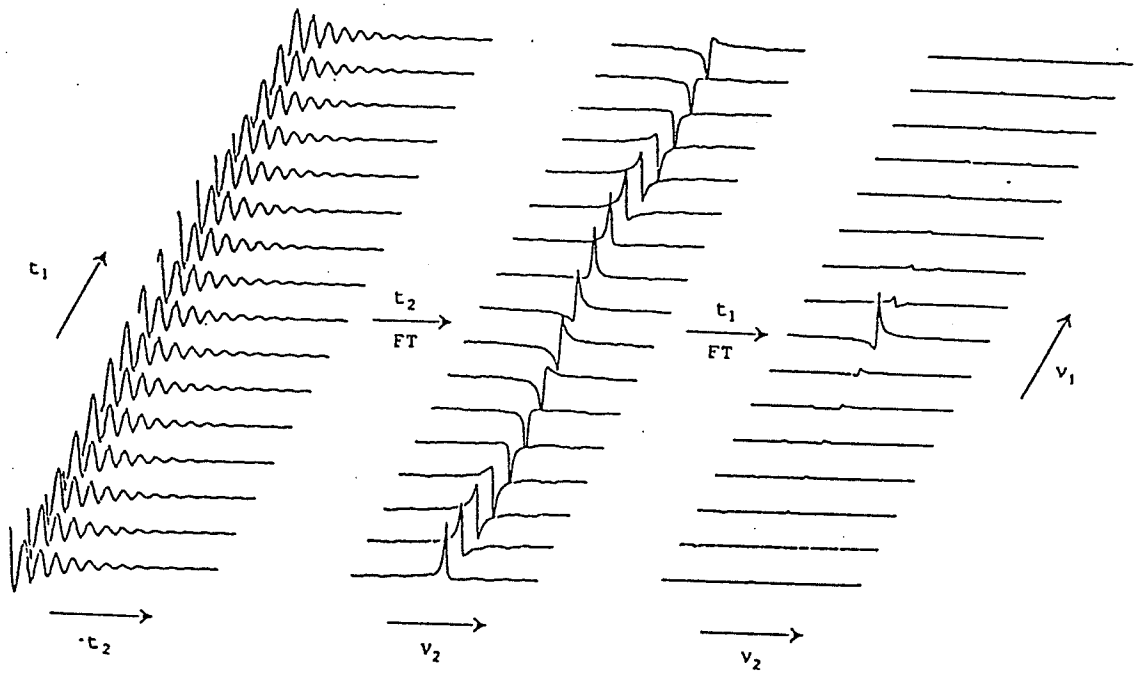

Figure 1(a)

THE CONTOUR PLOT

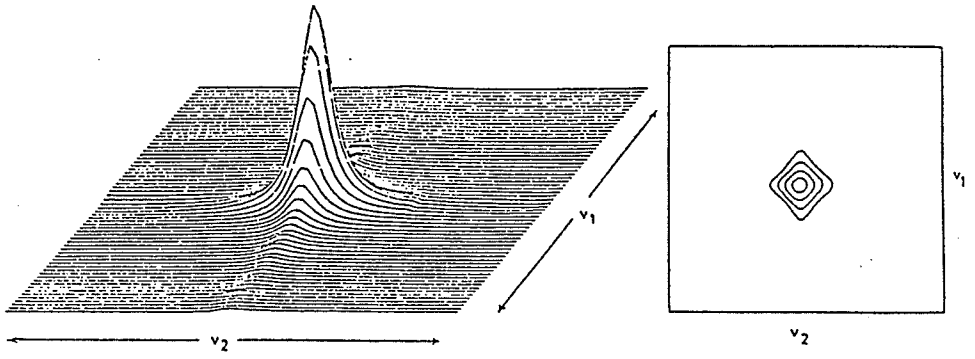

Figure 1(b)

For the one-dimensional experiment this t_2 period is held constant, but for the two-dimensional experiment this period changes incrementally after every FID has been acquired. Thus a series of FID's are generated over a range of evolution times which are transformed with respect to t_2 yielding a set of 1D spectra as a function of t_2. A second transformation with respect to t_1 gives the 2-D spectrum as demonstrated in Figure 1(a). Figure 1(b) illustrates the contour slice taken to generate a useful spectrum [68, 69]. This is a simple example of the popular correlated spectroscopy (COSY) spectrum in which the spectrum appears along the diagonal. Peaks that appear off the diagonal are referred to as crosspeaks which arise when the frequencies v_1 and v_2 differ. v_2 represents chemical shift frequencies as well as coupling frequencies involved in the t_1 period. Therefore the contour plot of these equal and unequal frequencies gives the spectrum on the diagonal as well as identical sets of peaks on either side of the spectrum. These signals or crosspeaks of identical shape and size indicate proton coupling, thus the structure can be solved by vertical and horizontal lines drawn at a 90° angle of the crosspeak to the two signals on the diagonal which are coupled. The COSY spectrum gives all structural information necessary to characterize the structure under investigation from the ^1H-^1H couplings which can be traced back to the carbon chain. The example of HH COSY (or homonuclear correlated spectroscopy) is only one of many techniques available. CH COSY (or heteronuclear correlated spectroscopy) is a method in which connectivities can clarify which H(s) are bound to a specific carbon atom. This spectrum is slightly different in that the ^1H spectrum is presented on the vertical axis and the ^{13}C spectrum is presented on the horizontal axis. The relationship between proton and carbon atoms are illustrated as a crosspeak

contour at the intersection of a horizontal line drawn from a proton peak and a vertical line drawn from a carbon peak. This discussion covers the scope of the techniques used for this research, but note that these only introduce the numerous techniques available [68, 69].

The demand for the developement of simple methods for functionalization of organic and polymeric systems has led us to the study of nucleophilic substitution and addition reactions. Previous investigations of the functionalization of polyaromatic arene complexes via nucleophilic substitution were successful [10, 67, 70-72]. The present work examines the functionalization of a series of methyl substituted mono- , di- and polycyclopentadienyliron complexes via nucleophilic addition of hydride and cyanide anions.

Hydride addition was initiated with the bimetallic systems in order to determine if there was an influential role the two metal moieties would have towards selective addition products. Methyl groups were employed in order to control the primary site activated towards the incoming nucleophile. Full spectral analysis is presented with the correlation between the analogous mono- and di-iron systems.

Addition of reactive nucleophiles was the main goal of this research. This methodology of nucleophilic addition provides a simple synthetic route to the functionalization of organic and polymeric aromatic systems. The term functionalization refers to the method which introduces a specfic molecule which can later undergo further reactions to modify the product. The cyanide anion is an example of an effective nucleophile which offers the possibility for a wide range of further reactions. The reaction of the cyanide nucleophile with a variety of arene $Fe^{+}Cp$ systems has been investigated.

2.0 Results and discussion

2.1 Hydride addition

2.1.1 Isomeric (η^6-methylphenoxy-η^5-cyclopentadienyliron)benzene hexafluorophosphate.

Hydride addition to bis(cyclopentadienyliron) arene di-cations resulted in the formation of a number of isomers. Due to the complexity of the NMR spectra of these adducts, the mono-iron systems were used as models for this investigation. While hydride addition to $CpFe^+$ complexes of monosubstituted arenes has been carefully examined [24], hydride addition to disubstituted arene complexes has yet to be reported. Reactions of (η^6-isomeric phenoxytoluene-η^5-cyclopentadienyliron) cations with an excess of sodium borohydride gave rise to a mixture of adducts, as illustrated in Scheme 18. The spectral data were complicated by the number of isomers present; thus it was necessary to characterize the products using HH COSY and CH COSY techniques. For proton assignment, the chemical shifts of the individual isomers were determined from the connectivities in the HH COSY spectrum. Once this information was obtained, ^{13}C chemical shifts were then assigned using CH COSY.

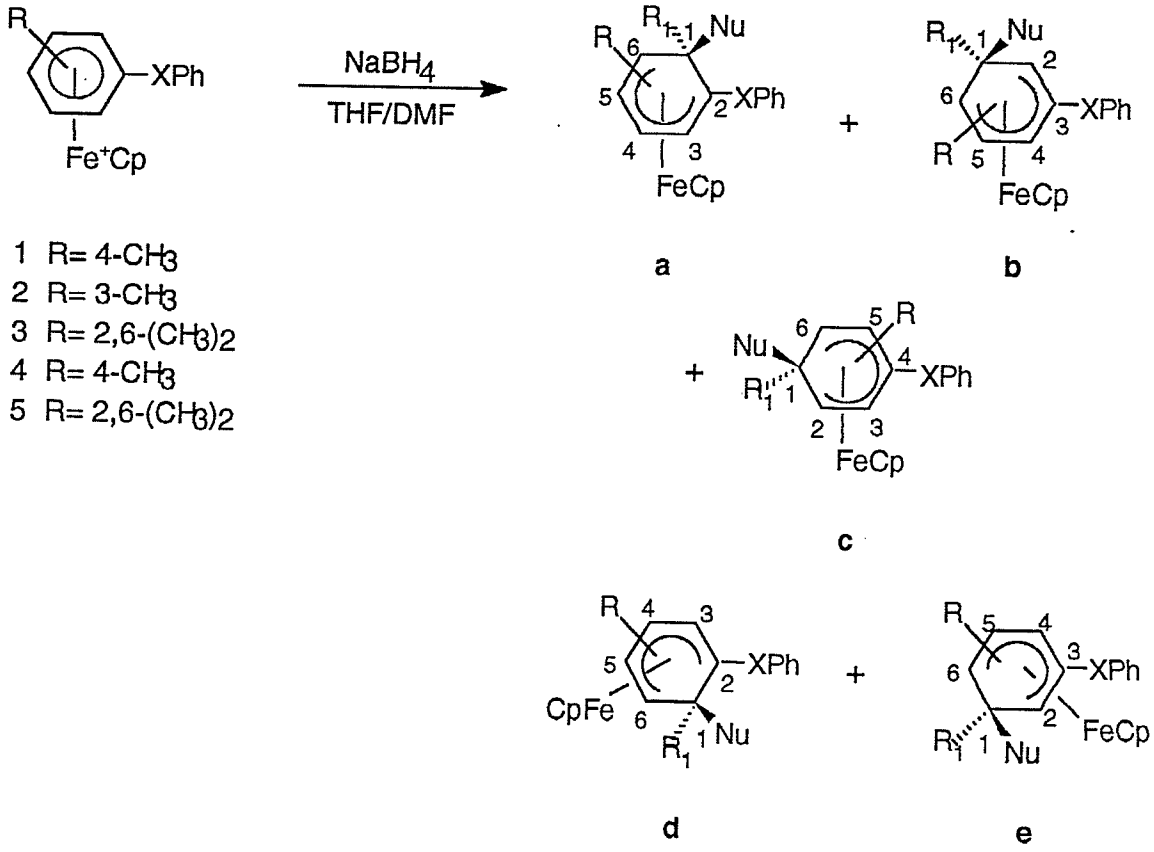

1 R= 4-CH_3
2 R= 3-CH_3
3 R= 2,6-$(CH_3)_2$
4 R= 4-CH_3
5 R= 2,6-$(CH_3)_2$

Addition Products (relative percentage)

Complex	Adduct	X	a	b	c	d	e
1	6	O	R_1=H (30)	R_1=H (66)	R_1=CH_3 (4)		
2	7	O	R_1=H (29)		R_1=H (24)	R_1=H (15)	R_1=H (32)
3	8	O	R_1=CH_3 (7)	R_1=H (59)	R_1=H (27)		
4	9	S	R_1=H (46)	R_1=H (54)			
5	10	S	R_1=CH_3 (5)	R_1=H (63)	R_1=H (32)		

Scheme 18

It has been established that a phenoxy substituent attached to the $CpFe^+$ arene complex directs the addition to meta > ortho > para, whereas a methyl substituent directs ortho > meta > para [38, 45, 51, 52, 54]. As shown

in Scheme 18, the ratio of adducts for complexes (**1**)-(**3**) demonstrates that the phenoxy group has the predominant effect, since it is a stronger electron-donating substituent than the methyl group. It should be noted that when the site of addition is reported to be meta, this indicates that addition has occurred meta to the predominant substituent, i.e. oxygen, sulfur or sulfone as opposed to the methyl, chloro or thiophenoxy group.

For Complex (**1**) the major adduct (**6b**) (66%) was formed at the position meta to the phenoxy substituent and ortho to the methyl substituent. This was clarified by first evaluating the splitting pattern and coupling constants for the peaks in the range of 1-6.5 ppm. From integration of the ^{1}H spectrum as well as knowledge of the possible adducts formed (Scheme 18), we could then utilize the information provided from the two-dimensional spectra. On the x and y axes of the HH COSY spectrum lies the ^{1}H NMR spectrum; each peak on the proton spectrum is represented by a peak along the diagonal. In this case the large cross shaped peak, in Figure 2, at 1.39 ppm will be the starting point. If two lines are drawn, one vertically and the other horizontally across the entire spectrum from the peak at 1.39 ppm, they will intersect other signals that are off the diagonal which are referred to as crosspeaks. The intersection of two lines at a cross peak indicate that the two points from which these lines originated on the diagonal are coupled to each other, and thus belong to the same structure. If lines are drawn for each peak on the diagonal, then all connectivities can be established. It can clearly be observed that the peak at 1.39 ppm is related to peaks at 6.11, 4.02, 1.93, 2.44, 2.46 and 4.27 ppm, whereas the peak at 1.79 ppm is related to peaks at 2.06, 2.78, 2.62, 4.30, 4.41 and 5.73 ppm. Once these initial relationships are discovered, the structure can be confirmed by working backwards, i.e. begin tracing the connections with the peak at 6.11 ppm on

the diagonal and repeat with the other related peaks. All peaks show connectivity with each other reinforcing the analysis. The same was done with all peaks coupled to the 1.79 ppm peak. Notice that we now have splitting patterns, coupling constants, related peaks, and proposed structures of these products. The next step is to fit the data to the structures. Of the three possible structures outlined in Scheme 18, (**6b**) contains the most aromatic proton which would be expressed as a doublet with coupling of 5-6 Hz in the downfield region of 6-6.5 ppm. In the proton NMR there exists a doublet at 6.11 ppm with a coupling constant of 5.1 Hz. The next CH to identify would be adjacent to the most aromatic proton with similar integration and coupling. This peak is represented by a doublet at 4.02 ppm with a coupling constant of 5.1 Hz. The connectivity between these peaks in the HH COSY spectrum provides verification of this assignment. The methyl group on this structure is the most aliphatic in nature as compared to others except in the case of structure (**6c**), thus the large singlet at 1.39 ppm (Peak A) is a methyl peak. From the connectivity established from the HH COSY, this methyl peak is connected to the peaks 6.11 and 4.02 ppm, thus must belong to the structure (**6b**) because (**6c**) would not have a peak as downfield as 6.11 ppm. Therefore it can be concluded that this methyl group is a constituent of (**6b**) with confirmation provided by integration. The exo and endo protons can be identified first by coupling constants (J=9-13 Hz), then connected to the rest of the structure, and finally checked with integration. The peaks at 1.93 and 2.44 ppm display a coupling constant of 10.7 Hz, characteristic of exo/endo coupling, and have similar integration to each other and the other hydrogens that they are related to in structure (**6b**). The aliphatic hydrogen at 2.46 ppm adjacent to the site of addition was located based on the connectivities found in the HH COSY (endo H at 2.44 ppm).

The final peak to identify in this structure is the cyclopentadienyl peak (Cp), which can be assigned at 4.27 ppm. The product in which the site of nucleophilic attack was ortho the phenoxy substituent (**6a**); can be characterized in the same manner as described above. The singlet at 1.79 ppm, is the methyl for (**6a**), due to the increased aromaticity of the methyl position, a downfield shift is observed from the methyl group on (**6b**). Determination of the connectivities from the HH COSY in Figure 2 suggests that the exo proton (doublet) appears at 2.06 ppm with a coupling constant of 9.8 Hz and the endo proton (doublet of doublets) appears at 2.78 ppm (J=9.8 Hz). Through integration, the Cp peak appears at 4.30 ppm and the most aromatic hydrogen which is adjacent to a methyl substituent is a doublet at 5.73 ppm. The peak adjacent to the phenoxy substituent is depicted at 4.41 ppm (doublet) with coupling of 5.1 Hz. The remaining hydrogen to be depicted which lies adjacent to the site of addition, appears as a doublet at 2.62 ppm. It was then possible to conclude that the second most abundant isomer (**6a**) (30%) was ortho to the phenoxy group and meta to the methyl substituent. Trace amounts of the product ipso to the methyl substituent (para to the phenoxy substituent), (**6c**) (4%), were detected, with a small Cp peak at 4.32 ppm and a methyl peak at 1.29 ppm; however, the amount present was too low to trace out the connectivities and to observe any carbon peaks. Once the chemical shifts for the ^{1}H NMR were assigned, the ^{13}C chemical shifts could be used to confirm these structures. Due to the number of isomers present, ^{13}C assignment was difficult, due to the structural similarity with many peaks in the aliphatic and complexed aromatic regions. This is why it was necessary to use CH COSY techniques. Figure 3 illustrates the CH COSY of adducts (**6a-c**). The ^{1}H and ^{13}C NMR spectra are located along the x and y axes of the plot respectively. To begin, a vertical

line was drawn from a proton peak down the entire spectrum. This line crosses an intense signal which indicates a correlation between that specific proton and the carbon to which it is bound. The carbon can be identified by drawing a line 90° to the vertical line across the spectrum. For structure (**6b**), the methyl group is connected to the carbon at 24.89 ppm which is in the range of an aliphatic methyl group. The endo and exo protons exist on one carbon, which is shown in the CH COSY to be present at 33.11 ppm. The most aromatic proton on the ring appears at 6.11 ppm and its corresponding carbon at 69.67 ppm. The proton coupled to the proton at 6.11 ppm appears at 4.02 ppm and its corresponding carbon peak appears at 75.24 ppm. This region of 4-6.5 ppm is characteristic of complexed aromatic protons. The Cp protons for this structure show connection to the carbon at 74.64 ppm and the proton adjacent to the site of addition relates to the carbon at 18.79 ppm. The quaternary carbons labelled 3 and 6 in Scheme 21 are found at 91.87 and 21.75 ppm respectively. The aliphatic nature of carbon 6 is expected, due to the loss in the aromaticity of the ring. The carbon chemical shifts of the structure (**6a**) correspond well to the characteristic regions that were identified for adduct (**6b**). Using the same methodology as described above, the methyl peak was associated with the ^{13}C peak at 21.75 ppm, and the endo and exo peaks corresponded to the carbon positioned at 31.72 ppm. The proton peak at 2.62 ppm was found in the aliphatic region at 29.07 ppm and the two aromatic protons showed connection to the peaks at 74.15 and 70.71 ppm respectively. The quaternary carbons are represented at 35.99 and 75.11 ppm for C2 and C5 respectively. The carbon denoted as C2 appears high field due to the aliphatic nature of the arene ring at this position. For the purpose of identification, the site of hydride addition has been designated position one,

give the phenoxy group the lowest possible number. Tables 1 and 2 contain the detailed ^{1}H and ^{13}C NMR spectral data.

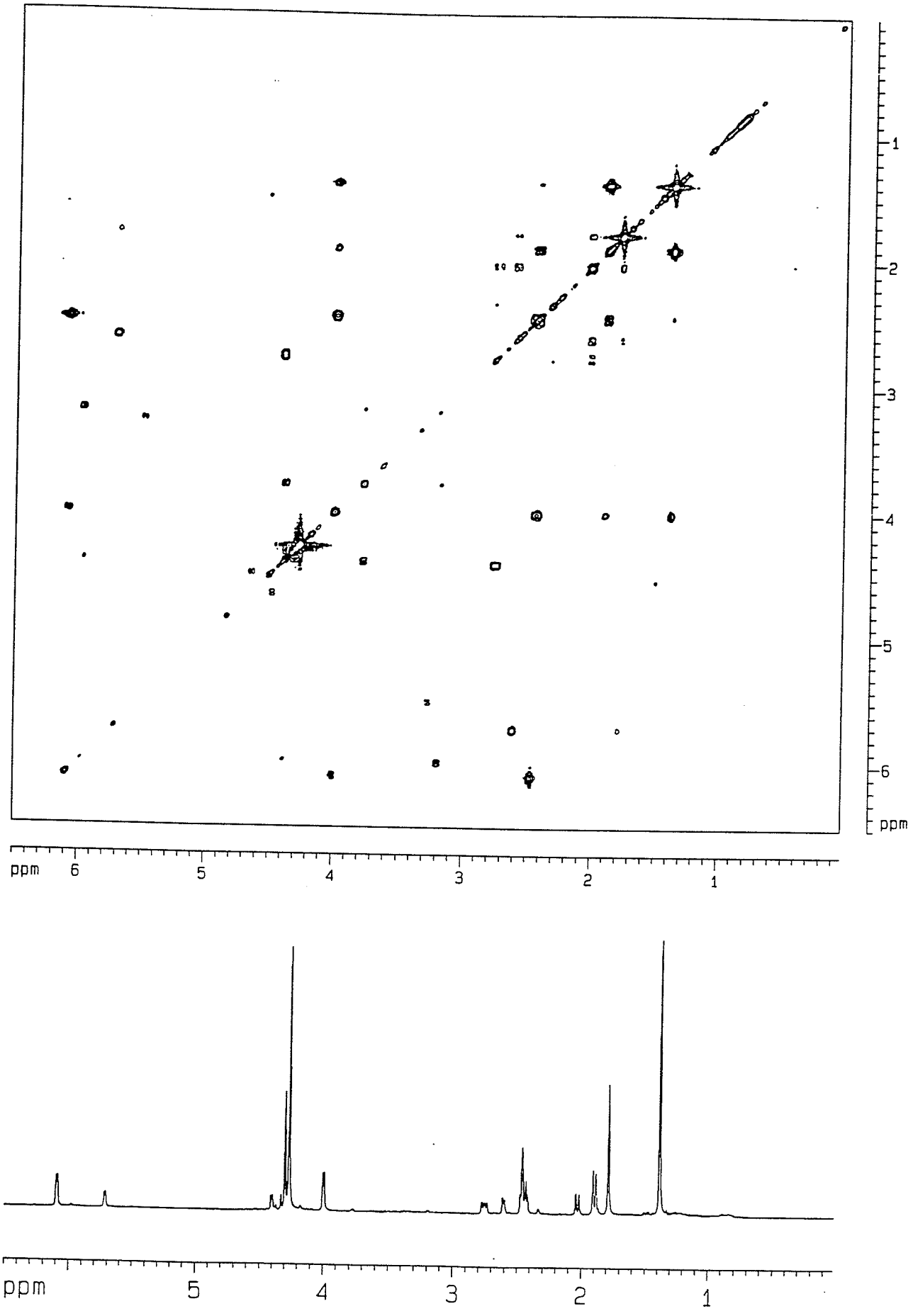

Figure 2: HH COSY of adduct (6).

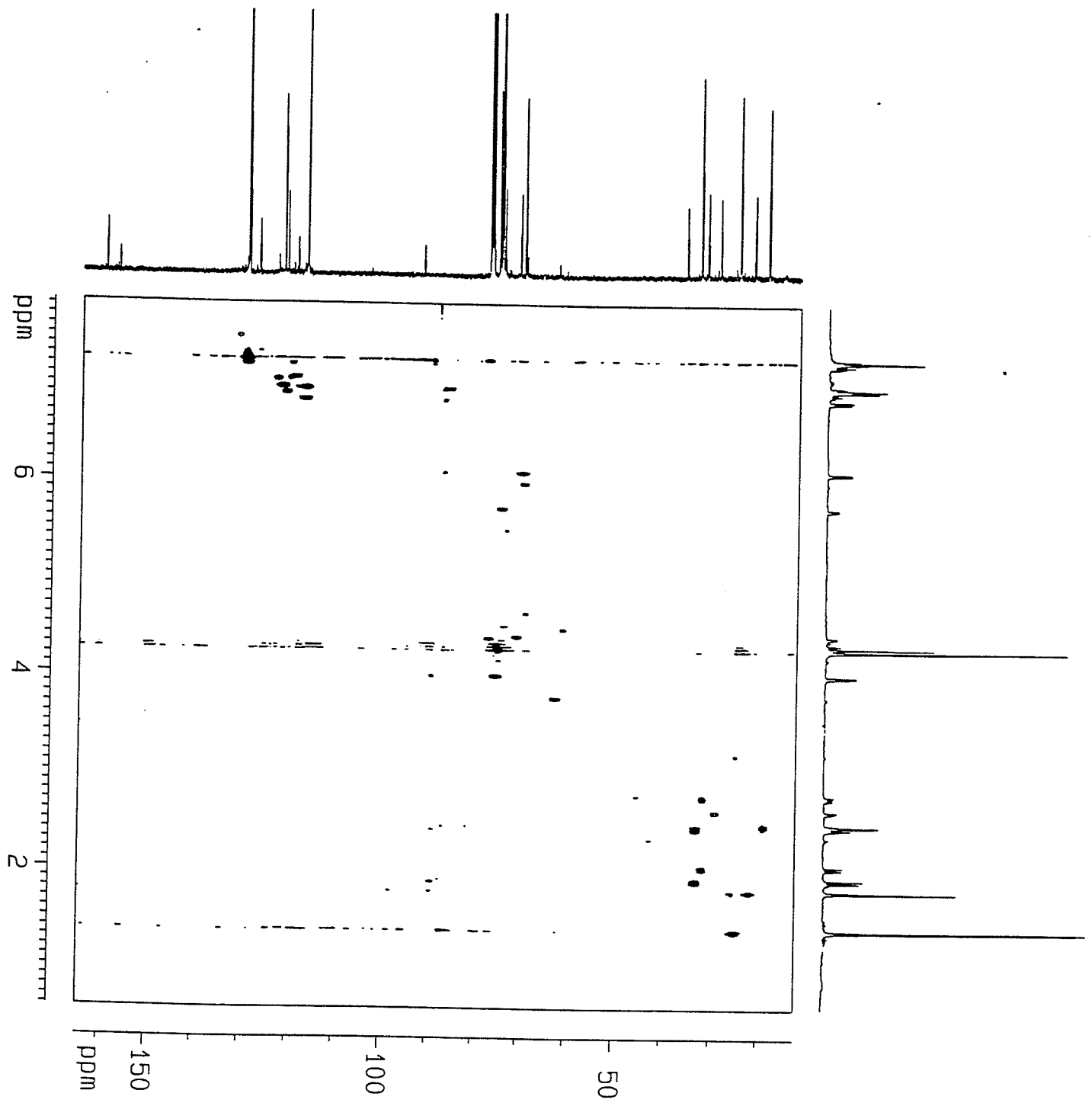

Figure 3: CH COSY of adduct (6).

Table 1: ^1H NMR data for the adducts 6, 7, 8, 9 and 10.

Adduct	CH_3	H(1-exo)	H(1-endo)	H(2)	H(3)	H(4)	H(5)	H(6)	Cp
6a	1.79	2.06	2.78	-------	4.41	5.73	-------	2.62	4.30
	s	*(d, 9.8, ex-en)*	*(dd, 9.8, en-ex; 5.9, en-6)*		*(d, 5.1)*	*(d, 5.1)*		*(d, 5.9, 6-en)*	*s*
6b	1.39	1.93	2.44	2.46	-------	6.11	4.02	-------	4.27
	s	*(d, 10.7, ex-en)*	*m*	*m*		*(d, 5.1)*	*(d, 5.1)*		*s*
7a	1.53	2.16	2.69	-------	4.41	5.67	3.91	-------	4.29
	s	*(d, 12.5, ex-en)*	*(d, 12.5, en-ex)*		*(d, 5.1)*	*m*	*(d, 5.1)*		*s*
7c	1.39	1.74	2.38	-------	4.56	-------	4.33	1.94	4.26
	s	*m*	*m*		*s*		*(d, 6.1)*	*(t, 6.5, 6-en, t, 6.2)*	*s*
7d	2.55	1.98	2.74	-------	4.40	-------	4.11	1.95	4.30
	s	*m*	*(dd, 12.5, en-ex, 5.8, en-6)*		*s*		*(d, 5.7)*	*(t, 5.8, 6-en, t, 5.7)*	*s*
7e	1.85	1.71	2.53	2.38	-------	6.23	-------	2.10	4.28
	s	*(d, 13.8, ex-en)*	*m*	*(d, 6.5, 2-en)*		*s*		*(d, 6.4, 6-en)*	*s*
8a	1.25, 1.94	1.86	-------	-------	-------	5.80	4.09	2.09	4.24
	s	*s*				*(d, 5.9)*	*(t, 5.9)*	*(d, 5.9)*	*s*
8b	1.30, 2.51	1.82	2.37	-------	-------	-------	4.24	2.03	4.18

	s	*(d, 12.2, ex-en)*	*(dd,12.2, en-ex; 6.1, en-6)*				*(d, 6.2)*	*(t, 6.3, 6-en, t, 6.3)*	*s*
8c	1.96 *s*	1.57 *(d, 12.8, ex-en)*	2.35 *(dt, 13.1, en-ex 7.0, en-2,6)*	1.79 *m*	-------	-------	-------	1.79 *m*	4.26 *s*
								m	*s*

Adduct	CH_3	H(1-exo)	H(1-endo)	H(2)	H(3)	H(4)	H(5)	H(6)	Cp
9a	1.82 *s*	1.80 *m*	2.46 *m*	-------	4.69 *(d, 4.8)*	6.01 *(d, 4.8)*	-------	2.55 *(d, 6.3, 6-en)*	4.31 *s*
9b	1.44 *s*	1.86 *(d, 12.1, ex-en)*	2.42 *m*	2.59 *(d, 6.7)*	-------	6.16 *(d, 4.8)*	4.03 *(d, 4.8)*	-------	4.29 *s*
10b	1.58, 2.70 *s*	1.71 *(d, 12.8, ex-en)*	2.41 *(dd, 12.7, en-ex, 6.4, en-6))*	-------	-------	-------	4.34 *(d, 6.3)*	2.28 *(t, 6.4, 6-en, t, 6.3)*	4.19 *s*
10c	1.96 *s*	1.70 *m*	2.45 *m*	2.17 *(d, 6.9, 2-en)*	-------	-------	-------	2.17 *(d, 6.9, 6-en)*	4.15 *s*

All samples run in $CDCl_3$ (ppm from solvent peak at 7.26 ppm).
Uncomplexed aromatic peaks in the 7-8 ppm region.
Coupling constants (Hz) are of adjacent aromatic protons unless otherwise indicated. (ex refers to exo, and en refers to endo).

Table 2: ^{13}C NMR of the adducts 6, 7, 8, 9 and 10.

Adduct	CH_3	C (1)	C (2)	C (3)	C (4)	C (5)	C (6)	Cp
6a	21.75	31.72	35.99	70.71	74.15	75.11	29.07	74.78
6b	24.89	33.11	18.79	91.87	69.67	75.24	21.75	74.64
7a	25.45	36.96	38.72	71.64	70.67	68.14	24.78	75.05
7c	23.21	32.39	28.90	73.90	90.82	73.51	16.25	74.75
7d	20.94	31.45	31.40	71.87	78.20	71.43	24.78	74.91
7e	21.80	27.59	24.55	89.89	73.01	77.96	18.00	74.57
8b	19.97, 16.52	34.28	29.66	98.20	88.00	78.82	17.93	75.37
8c	20.91	28.35	20.11	86.18	94.81	86.18	20.11	76.17
9a	21.96	29.56	36.87	80.12	83.32	87.03	28.23	75.22
9b	25.14	33.68	25.60	94.20	84.64	79.70	26.82	75.01
10b	20.36, 21.32	34.16	36.81	95.89	88.20	79.90	21.54	75.77
10c	23.71	26.14	26.64	88.25	97.70	88.25	26.64	74.80

Samples were run in $CDCl_3$ (ppm from solvent peak at 77.00 ppm)
Adduct 8a was too small to characterize by ^{13}C NMR.
Uncomplexed aromatic peaks appear at 120 -140 ppm.

For complex (**2**) where one meta position was hindered by a methyl group, the largest number of adducts formed. This makes the HH COSY complicated with many overlapping regions. Figure 4 illustrates the HH COSY of the adducts (**7**) and the lines drawn show the connectivities for each isomer. Before the structures can be solved, all of the possible structures must be considered (Scheme 18). The ^{1}H NMR spectrum looks as though it is made up of four isomers, due to the number of Cp peaks and what appears to be four methyl peaks at 1.39, 1.53, 1.85 and 2.55. First the connectivities were determined for each methyl group following the same method described previously. The peak at 1.39 ppm was found to be related to peaks situated at 1.74, 2.38, 4.56, 4.33, 1.94, and 4.26 ppm. The peak at 1.53 ppm was related to peaks at 2.16, 2.69, 4.41, 3.91, 4.29 and 5.67 ppm. The peak at 1.85 ppm was connected to the peaks 1.71, 2.53, 2.38, 6.23, 2.10, and 4.28 ppm. The final set connected the peak at 2.55 ppm with peaks 1.98, 2.74, 4.40, 4.11, 1.95, and 4.30 ppm. The largest methyl peak appears at 1.85 ppm, and so this structure was thought to be the simplest to solve. The position of this methyl peak in the aliphatic region is not next to the site of addition, as it would appear at higher field, nor is it at the most aromatic point, or it would appear down field; thus it must be meta to the site of addition. The occurrence of ipso products are rare and appear in small quantities; therefore, the most probable structure would be (**7e**). In order for this structure to be a true isomer, the methyl peak would have to show connection to a singlet in the aromatic region, which is observed at 6.23 ppm. The relationship with a peak at 4.28 ppm was detected, which represents the Cp peak of this isomer. The endo and exo protons are positioned at 2.53 ppm and 1.71 ppm respectively. The final protons on the ring to assign are those protons adjacent to the site of addition, the peak at 2.10 ppm (neighboring a

methyl group) and 2.38 ppm (adjacent to the phenoxy group). So the overall structure (**7e**) has a methyl group at 1.85 ppm, Cp at 4.28 ppm, a singlet at 6.23 ppm, endo protons overlapping at 2.53 ppm and exo proton at 1.71 as a doublet with a coupling constant of 13.8 Hz. The last two doublets appear at 2.38 and 2.10 ppm, representing the positions ortho to the site of addition. Confirmation of this analysis is provided by the CH COSY. The assigned endo and exo protons demonstrate connectivity to the same carbon at 27.59 ppm on the carbon spectrum. The methyl group appears at 21.80 ppm. The aliphatic protons adjacent to the site of addition appear connected at 24.55 ppm and 18.00 ppm. These differ because of the different substituents positioned around the ring. The aromatic CH is down field at 73.01 ppm along with the Cp carbons at 74.57 ppm. The quaternary carbons C3 and C5 appear at 89.89, and 77.96 ppm respectively. The second largest methyl peak at 1.53 ppm has a chemical shift characteristic of a methyl group ortho to the site of addition. This peak shows connection to a doublet at 2.16 ppm (J=12.5 Hz) which has a strong connecting signal to the proton at 2.69 ppm (J=12.5 Hz). Both peaks are doublets thus the endo proton is only coupled to the exo proton, evidence that the proposed structure is correct (**7a**). We also expect an aromatic triplet and two aromatic doublets associated with this structure. A peak with a distorted triplet splitting pattern is related to two doublets at 3.91 ppm and 4.41 ppm. The final peak is the Cp found at 4.29 ppm. Confirmation of the structure (**7a**) with CH COSY shows that the endo and exo protons are correctly assigned because they both relate to a peak at 36.96 ppm. The methyl group appears at 25.45 ppm, and the Cp peak at 75.05 ppm. The aromatic protons relate to peaks with chemical shifts of 71.64, 70.67 and 68.14 ppm. The quaternary carbons, C2 and C6 appear in the aliphatic region at 38.72 and 24.78 ppm respectively, due to their

positions adjacent to the site of addition. The methyl peak at 1.39 ppm, was the third largest isomer detected and its corresponding structure (**7c**) is as shown in Scheme 18. This structure is in agreement with the appearance of the methyl group in the aliphatic region. The peaks that show connectivity to this methyl peak are found at 1.74 and 2.38 ppm, which represent the exo and endo protons of this structure, which couple together in the CH COSY to one carbon peak at 32.39 ppm. The remaining protons will have the same splitting pattern as (**7d**) but chemical shifts will vary because the ether and methyl substituent have switched positions. These peaks were found at 4.56 (singlet), and 4.33 ppm (doublet, J=6.1 Hz). The final aliphatic peak was found at 1.94 (triplet, J=6.2 Hz). The CH COSY data suggested the assignment of the methyl group as 23.21 ppm, and the Cp peak as the peak at 74.75 ppm. The two aromatic protons displayed connectivity to carbon atoms appearing at 73.90 and 73.51 ppm, whereas the remaining CH appears at 16.25 ppm. The quaternary carbons C2 and C4 appear at 28.90 and 73.51 ppm respectively. The least abundant isomer present is the structure with a methyl group in an aromatic position on the ring, due to the low field chemical shift (2.55 ppm). With reference to Scheme 18, the only possible structure is (**7d**). The connectivities found using the HH COSY spectrum show that this methyl peak is related to a large singlet in the Cp region at 4.30 ppm and a doublet in this region at 4.11 ppm. There is a connection to a singlet at 4.40 ppm. The endo and exo protons appear in the aliphatic range at 2.74 and 1.98 ppm with a coupling constant of J = 12.5 Hz. The hydrogen next to the position of addition is found to be responsible for the peak at 1.95 ppm. ^{13}C NMR confirms this analysis with the methyl peak at 20.94 ppm, and the endo and exo carbon at 31.45 ppm. The aromatic protons are found at 71.87 and 71.43 ppm for C3 and C5 respectively. The

final CH appears in the aliphatic region at 24.78 ppm. The quaternary carbons C2 and C4 appear in separate regions due to the partial loss of aromaticity of the ring: 31.40 and 78.20 ppm.

In summary the major isomer was (**7e**) (32%) where addition occurred at the free meta position. Isomer (**7a**) (29%), was the next most abundant isomer, in which addition was in the ortho position with respect to both substituents. Addition at the other ortho position yielded minor amounts of the isomer (**7d**) (15%). The final isomer detected was (**7c**) (24%) where the site of addition was para to the phenoxy substituent and ortho to the methyl group. Figure 4 illustrate the HH COSY for the adducts (**7a,c-e**). For detailed ^{1}H and ^{13}C spectral NMR data, refer to Tables 1 and 2.

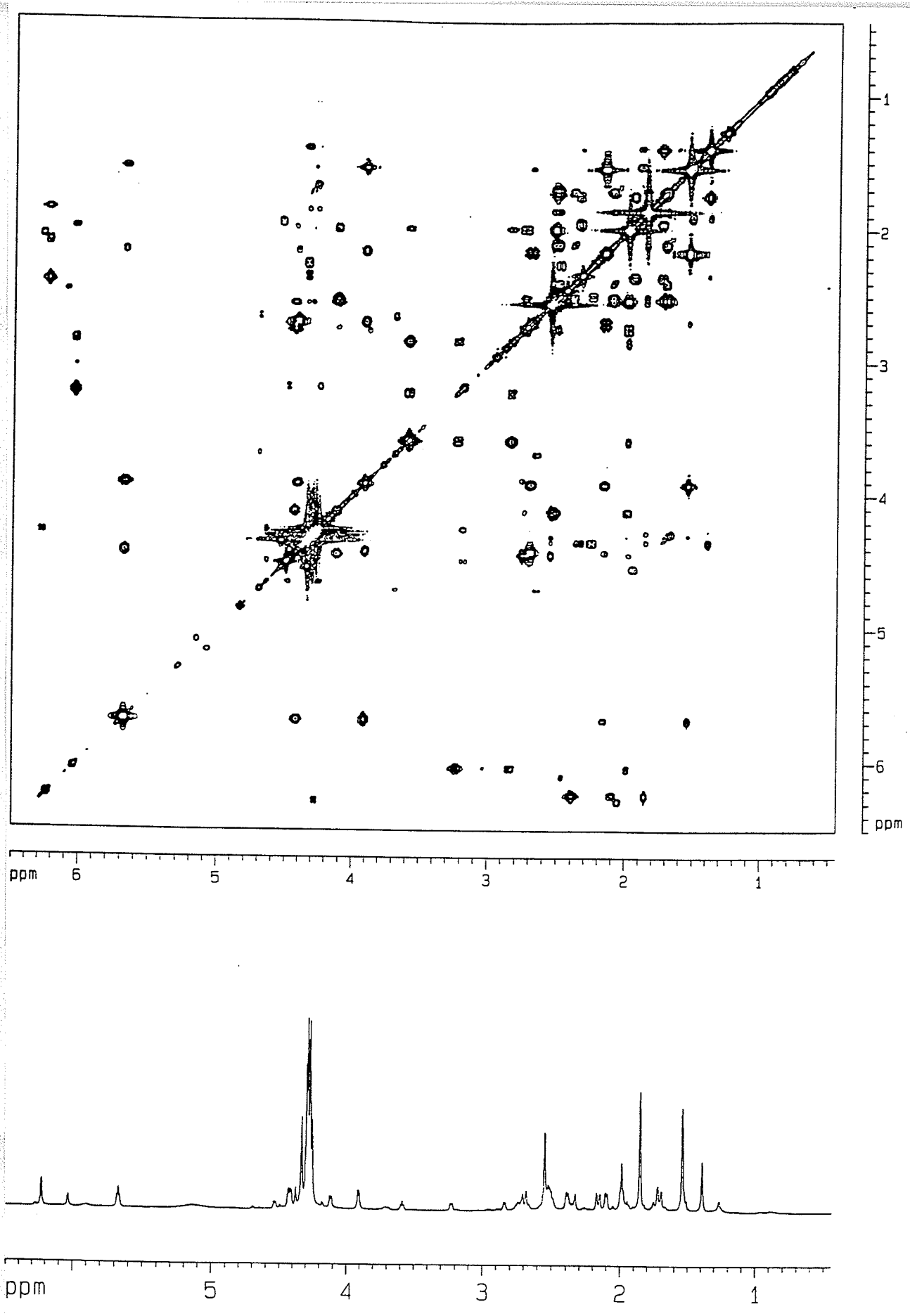

Figure 4: HH COSY of adduct (7).

Complex (**3**), in which the positions ortho to the phenoxy substituent are hindered by methyl groups, did not produce as complicated a spectrum as the above adducts, once reacted with the hydride anion. There are three predominant peaks in the aliphatic range, 1.30, 2.51, and 1.96 ppm. The HH COSY (Figure 5) indicates that peaks 1.30 and 2.51 ppm are connected, and are therefore two methyl groups of equal intensities. Referring to Scheme 18, adduct (**8b**) is the most probable structure, with two different methyl groups. The difference in chemical shifts of these peaks indicates that one is positioned para to the site of addition and the other is ortho with the phenoxy meta to this site. The most aromatic proton on this structure would be located in the Cp range and was found at 4.24 ppm. Based on integration, the Cp chemical shift was assigned as 4.18 ppm. The endo and exo protons appear at 2.37 and 1.82 ppm respectively. These chemical shifts were confirmed by CH COSY (Figure 6). The endo and exo carbon is found to be present at 34.28 ppm. The methyl groups were connected to the carbon appearing at 19.97 and 16.52 ppm. The Cp is the most predominant peak at 75.37 ppm and the slightly aromatic proton displays connectivity with a carbon atom at 78.82 ppm. The quaternary carbons vary in range due to the loss of aromaticity of the ring and are observed at 29.66, 98.20, and 88.00 ppm. The second most abundant isomer has two equivalent methyl groups at 1.96 ppm. In reference to Scheme 18, there are two possibilities of site of nucleophilic attack: para to the phenoxy group or ipso to the phenoxy group. The probability of ipso products are low therefore we will assume the structure is equivalent to (**8c**). The CH COSY should not show connectivity of the methyl peak to any aromatic protons but rather to Cp, two equivalent aliphatic protons, and endo and exo protons. Experimentally, this is what was detected: Cp (4.26 ppm), $H_{2,6}$ (1.79 ppm), endo (2.35 ppm, J=13.1 Hz)

and exo (1.57 ppm, J=12.8 Hz). These were confirmed by carbon assignment, where the endo and exo carbon was found at 28.35 ppm. The methyl peak was located at 20.91 ppm and the Cp at 76.17 ppm. The two CHs located ortho to the site of addition appeared at 20.11 ppm. The final structure identified was (**8a**) but in very small amounts as is generally the case with ipso addition. The methyl peaks appear at 1.25 and 1.94 ppm. The exo proton is located at 1.86 ppm. Relating peaks of (**8a**) to a doublet at 5.80 ppm illustrates the chemical shift of the most aromatic proton and 4.09 ppm for the aromatic complexed proton. The CH adjacent to the site of addition (H6) was found at 2.09 ppm. This assignment could not be confirmed by ^{13}C NMR because these peaks were present in small amounts were not observed in the spectrum. To summarize, the major position of addition was at the meta position with respect to the phenoxy group (**8b**) (60%), as illustrated in Scheme 18. Addition para to the phenoxy and meta to the methyl substituents, (**8c**) (28%), gave rise to the second most abundant isomer. The minor isomer, (**8a**) (12%), resulted when addition ipso to the methyl group took place. Figures 5 and 6 represent the ^{1}H and ^{13}C NMR spectra for the isomers of (**8**). The ^{1}H and ^{13}C NMR data of the addition products (**8a-c**) are listed in Tables 1 and 2.

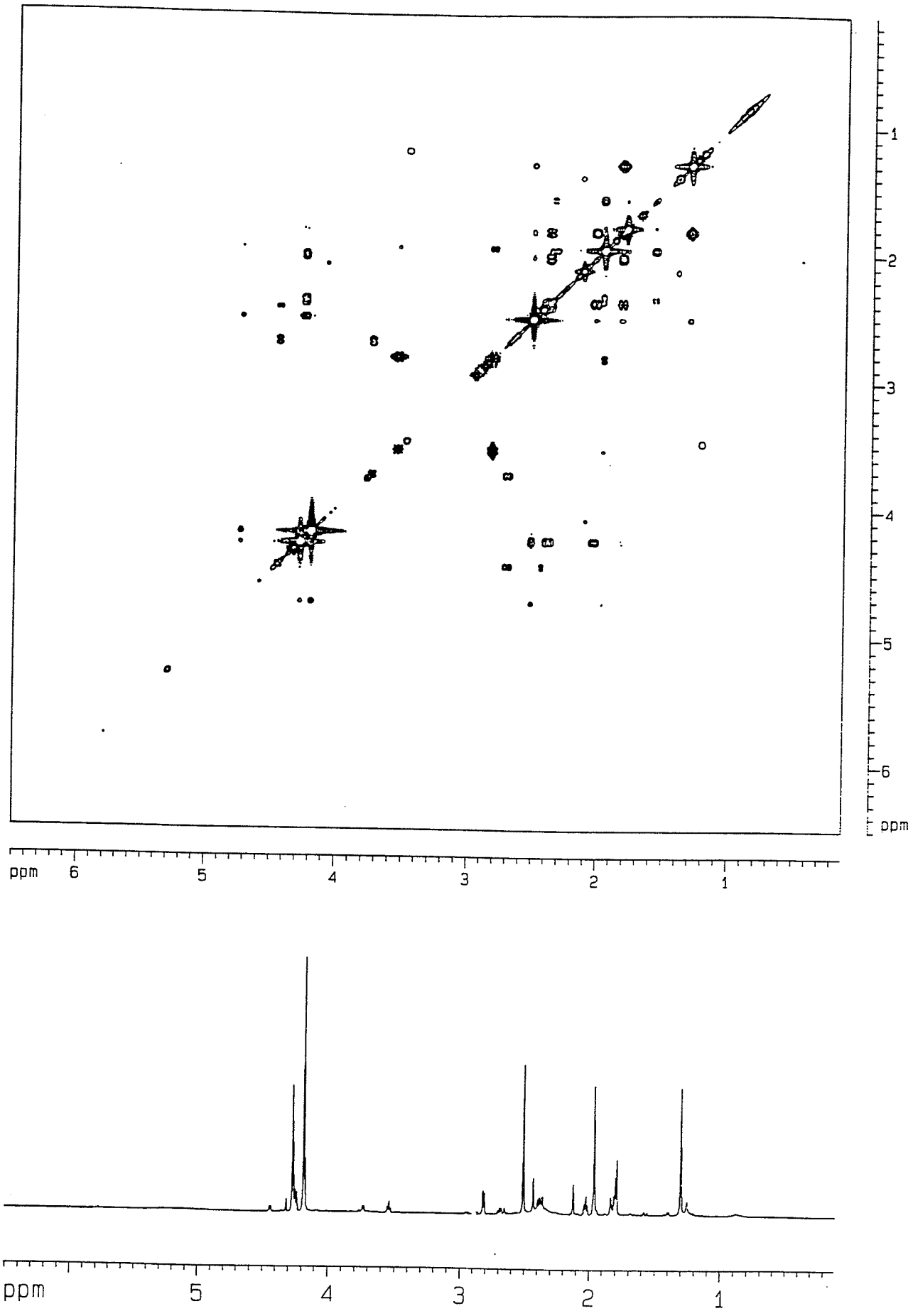

Figure 5: HH COSY of adduct (8).

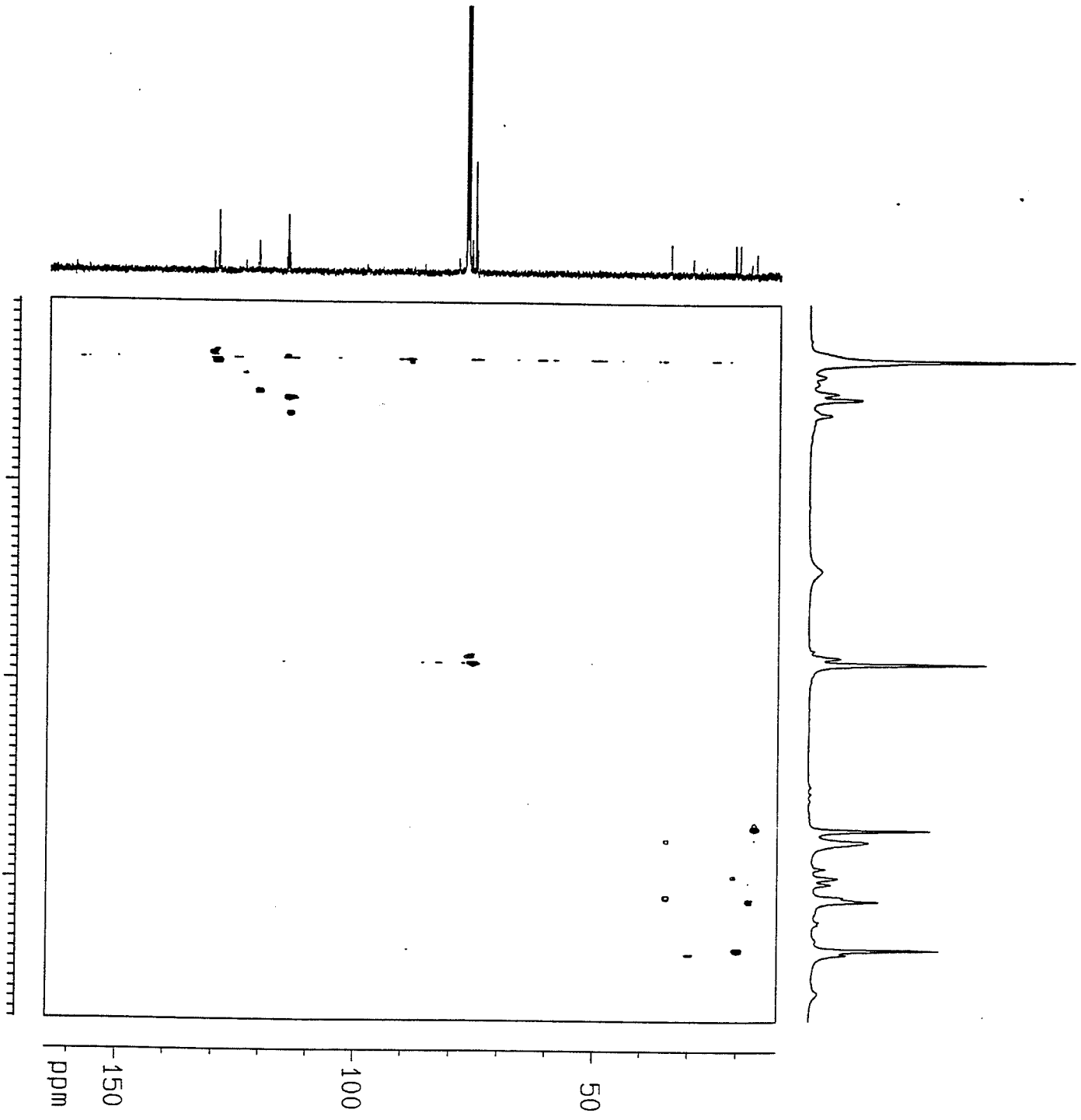

Figure 6: CH COSY of adduct (8).

2.1.2 Isomeric (η^6-methylthiophenoxy-η^5cyclopentadienyliron)benzene hexafluorophosphate.

In order to compare the effect of the etheric linkage on the regioselectivity of the system, thioether linkages were also studied. Thiophenoxy groups should direct the same as the phenoxy group: meta > ortho > para. In all cases the phenoxy system activated the meta site towards nucleophiles, even in the situation where one position was hindered. The reaction of complex (**4**) with $NaBH_4$ resulted in the formation of two isomers (**9a**) (46%) and (**9b**) (54%) (Scheme 18). Two dimensional techniques were not necessary due to the reduced number of isomers as well as the increased resolution of the spectra for both ^1H and ^{13}C NMR. These are identical isomers as obtained with (**6a**) and (**6b**). Structure (**9b**) has a methyl group in the position adjacent to the site of nucleophilic attack therefore appears at a higher field position (1.44 ppm) as compared to (**9a**) where the methyl group is meta to this site, where it was located at 1.82 ppm. These chemical shifts are consistent with the etheric isomers of (**6**). The most aromatic protons were found in the complexed aromatic region at 6.01 and 6.14 ppm for (**9a**) and (**9b**) respectively. The downfield shift of (**9b**) as compared to (**9a**) is expected, due to the adjacent thiophenoxy group (Scheme 18). The assignment of the Cp peaks at 4.31 and 4.29 ppm for (**9a**) and (**9b**) were based on the integration. The slightly aromatic protons appear in the Cp region at 4.69 ppm for (**9a**) and 4.03 ppm for (**9b**). The chemical shifts differ due to the position of the thiophenoxy substituent. The aliphatic region is slightly more complicated than the rest of the spectrum with a large amount of overlap due to the slight increase in shielding caused by the presence of the sulfur substitutent. The exo and endo protons for the isomer (**9a**) are located at 1.80 and 2.42 ppm; for isomer (**9b**) they are positioned at

1.86 and 2.46 ppm. ^{13}C chemical shifts were determined using the trends and relationships found in adduct (**6**). The methyl peaks for (**9a**), 19.97 ppm, and (**9b**), 25.14 ppm, correlate well with those in (**6a**) and (**6b**), as do the endo/exo carbons situated at 29.56 and 33.68 ppm. The Cp peaks for these structures are found at 75.22 (**9b**), and 75.01 ppm (**9a**), which are slightly higher than those in adduct (**6**), but well within the Cp range. The aromatic carbons demonstrate a downfield shift from those in the phenoxy adducts from 69.67 to 84.64 ppm, 75.24 to 79.70, and 91.87 to 94.20 ppm for (**6b**) to (**9b**). The same relationship was found for isomer (**a**); from 74.15 to 83.32, 75.11 to 87.03, and 70.71 to 80.12 ppm. This downfield shift can also be observed with the protons adjacent to the site of nucleophilic addition; 18.79 (**6b**) to 25.60 (**9b**) ppm, but the (**a**) isomer seems unaffected. This effect is due to the slightly stronger shielding effect of sulfur compared to oxygen. Note that the meta isomer is present in slightly larger amounts, therefore the directing ability of the thioether substituent activates the meta > ortho site towards nucleophilic addition. Figures 7 and 8 represent the ^{1}H and ^{13}C NMR of the adducts (**9a-b**). The NMR chemical shifts and coupling constants are given in Tables 1 and 2.

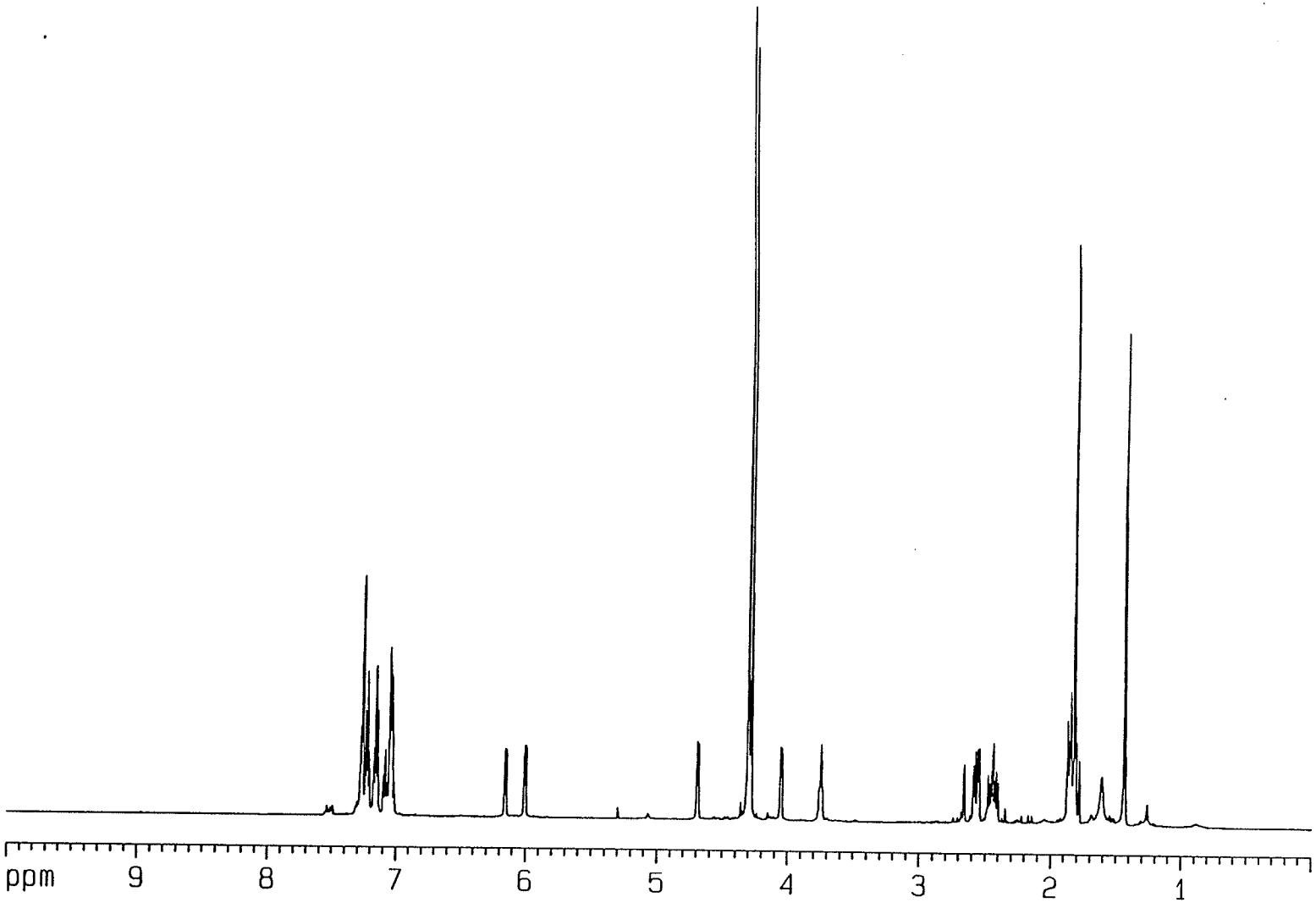

Figure 7: ^{1}H NMR of adduct (9).

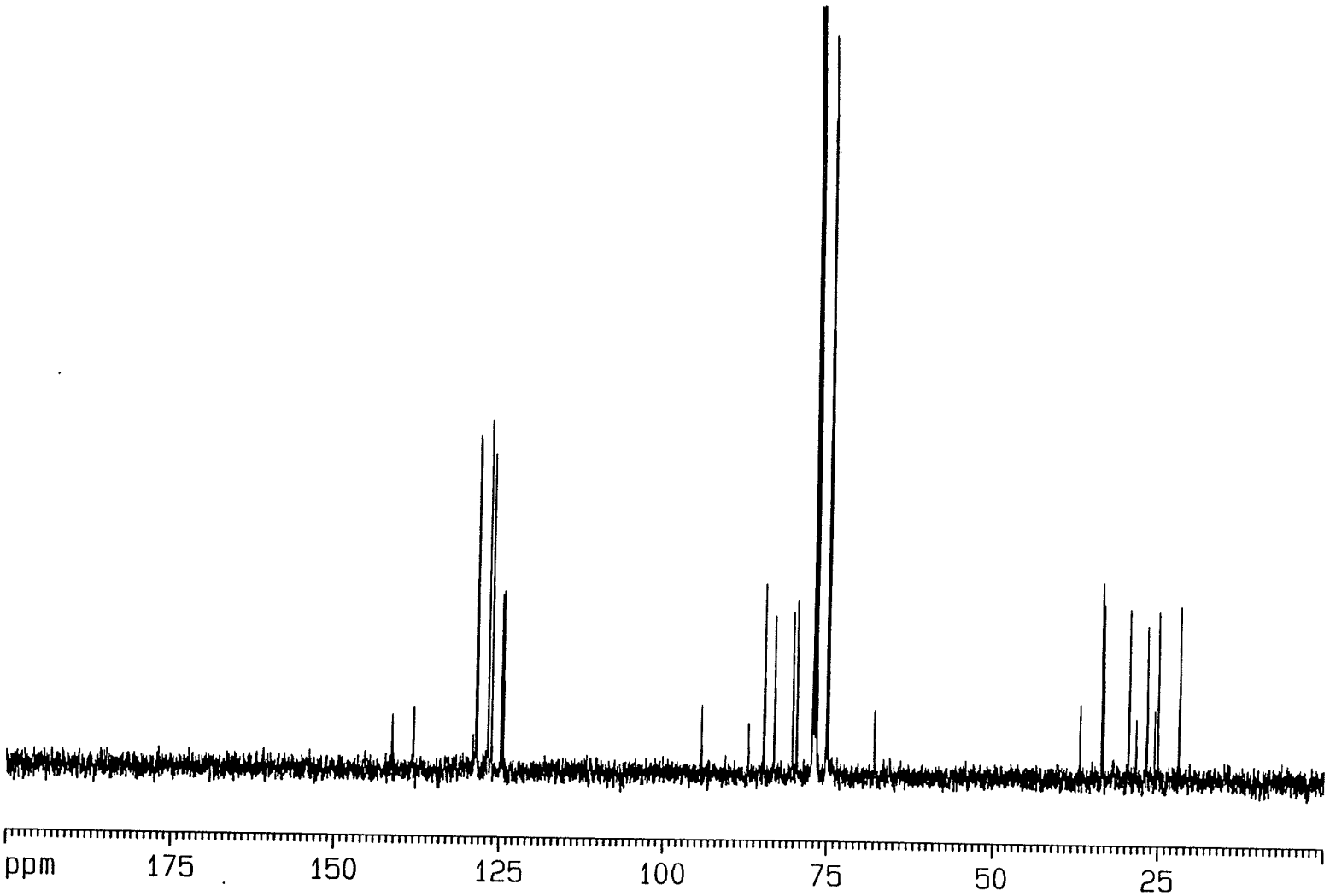
ppm
175
150
125
100
75
50
25

Hydride addition with complex (**5**) resulted with the major isomer (**10b**) (63%) in the meta position. The second isomer was (**10c**) (30%) where the adduct formed para to the thioether group. Trace amounts of ipso product (**10a**) (7%) were detected, but clearly not enough to evaluate (Scheme 18). These isomeric adducts were not difficult to analyze once the analogous oxygen structures were clear; therefore two-dimensional techniques were not necessary. There are notable downfield shifts in the NMR from the phenoxy compounds to the thiophenoxy compounds, but the shifts are within the appropriate ranges. The methyl groups appear at 1.58 and 2.70 ppm (**10b**) and 1.96 ppm (**10c**). The endo and exo protons appear in the aliphatic region at 2.41 and 1.71 ppm (**10b**) and 2.45 and 1.70 for (**10a**). The partially aromatic proton is found at approx. 4.34 ppm and the protons adjacent to the site of addition are located at 2.28 (**10b**), and 2.17 (**10c**) ppm. Methyl peaks are located in the aliphatic region at 20.36 and 21.32 ppm (**10b**) and 23.71 ppm (**10c**). The endo and exo carbon appears at 34.16 and 26.14 ppm for (**10b**) and (**10c**) respectively. The other aliphatic protons and quaternary carbons appear in the range of 21.54-36.81 ppm. The aromatic quaternary carbons appear in the range of 79.9-97.7 for C-Me and C-SPh carbons. All peaks in the ^{1}H and ^{13}C NMR correlate well with the analogous phenoxy adducts, and selectivity does not change greatly. However, these sulfur complexes gave excellent resolution in NMR, notably better than oxygen. In summary, the meta site is the preferred site for addition (Scheme 18). Attempts to separate the various isomers above by means of column chromatography were unsuccessful due to the instability of these products. At room temperature, the products are stable for approx. 8 hours. After this point the adducts begin to decompose and the NMR is no longer reliable. Every sample was analyzed within 3 hours of preparation. Figure 9 and 10 illustrate

the ^{1}H and ^{13}C NMR spectra for the adduct (**10**). Tables 1 and 2 include the detailed spectroscopic data.

Figure 9: ^{1}H NMR of

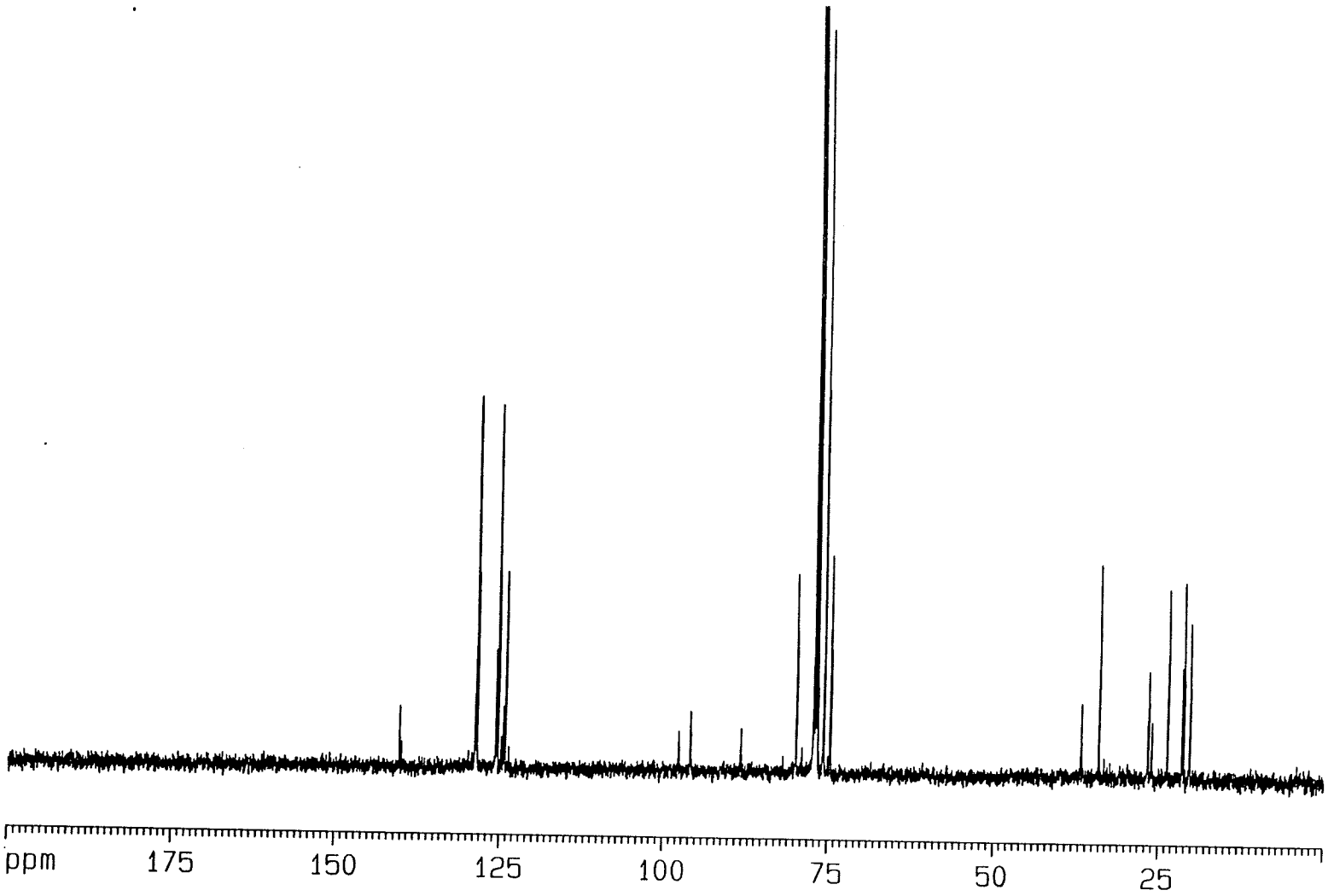

Figure 10: ^{13}C NMR of adduct (10).

The ether and thioether bridges have similar directing power, and thus similar predominant adducts formed. In this study NMR measurements show that the ether/thioether substituents have a larger overall influence on the charge distribution in the meta position on the arene complex. The substituents on the complexes complement each other with respect to the charge distribution around the ring. Methyl groups direct ortho and ether/thioether direct meta; this is the position in which the major adduct is formed. The second position the methyl group will influence is meta with respect to itself whereas the ether/thioether links activate the ortho position. The results obtained correlate with the directing abilities of the combined substituents.

2.1.3 Isomeric 1,4-bis(η^6-methylphenoxy-η^5- cyclopentadienyliron) benzene dihexafluorophosphate.

Reaction of 1.0 mmol of 1,4-bis[(η^6-4-methylphenoxy-η^5-cyclopentadienyl)iron]benzene cation (**11**) with 5.0 mmol of sodium borohydride produced a mixture of isomers, as shown in Scheme 19.

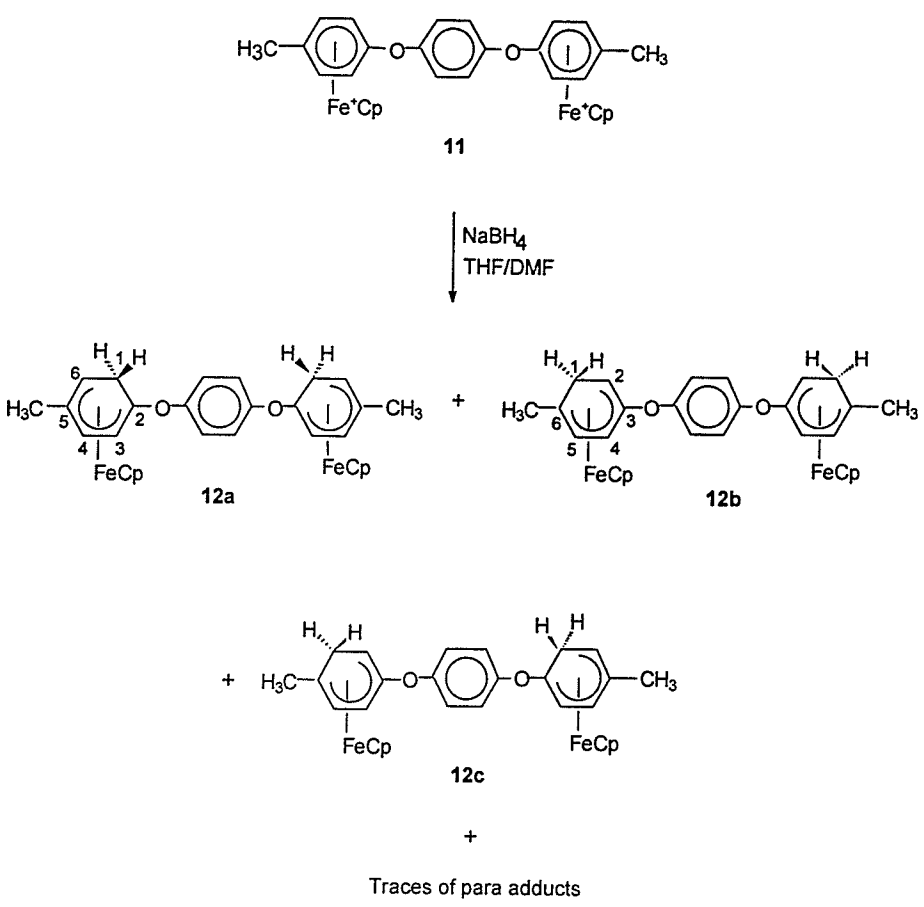

Scheme 19

The major product is the meta isomer (59%), along with ortho (35%) and a trace of para (6%). Since the complexed arene rings are separated by phenylene as shown in Scheme 19, the addition to each of these rings should be independent. Thus a variety of symmetrical (addition the same on both rings) and asymmetrical (addition different on both rings) adducts should be obtained as well as the possibility of diastereoisomers. There is no significant change in the chemical shifts between the protons or carbons of one cyclohexadienyl ring and the other; thus these rings are independent of each other, so addition to one ring has no influence on the site of addition on the remaining ring. Since there is no observable interaction between the two arene rings, it is not possible to identify the adduct on both arene rings of one

structure. It can be concluded that addition occurs on both rings as indicated by the Cp (cyclopentadienyl ligand) shift from 5.2 to 4.5 ppm as well as the complexed aromatic protons from 6.5 to the range of 1-6.5 ppm. The position of nucleophilic attack on each ring can be determined from the NMR spectrum. It was not possible to distinguish between the chemical shift for the ortho-ortho isomer (**12a**) and ortho-addition of the asymmetric isomer (**12c**). The relative percentage of the adduct was calculated from the NMR spectra for each isomer. These numbers represent the total specific adduct formed in the mixture but do not at all represent the ratio of symmetrical to unsymmetrical products. For instance, the meta isomer was calculated to be 59%, which was the total of meta addition in the meta-meta (**12b**), meta-ortho (**12c**) and the trace meta-para. It is also important to note that we cannot observe diastereomers for these adducts. The ^{1}H and ^{13}C NMR chemical shifts are listed in Tables 3 and 4, where (**12a**) and (**12b**) represent the symmetrical ortho and meta isomers, respectively, as well as the ortho and meta addition of the asymmetrical structure (**12c**). The chemical shifts in ^{1}H and ^{13}C NMR spectra displayed the exact positions as the analogous mono-iron adducts. Adduct (**12**) will be used as the example for the di-iron complexes to compare shifts with the mono-iron isomers. The methyl groups on the isomer (**12b**) were located at 1.36 ppm, while the mono-iron methyl for this isomer (**6b**) was 1.39 ppm. The endo and exo protons of (**12b**) are found at 1.85 and 2.41 ppm respectively, and in (**6b**), 1.93 and 2.44 ppm. The proton adjacent to the site of attack appears at 2.43 ppm (**12b**) and 2.46 ppm in (**6b**). The aromatic protons appear at 6.05 and 3.97 ppm in (**12b**), and 6.11 and 4.02 ppm in (**6b**). The Cp rings follow the same trend, 4.24 ppm in (**12b**) and 4.27 ppm in (**6b**). The carbon chemical shifts for the methyl group appear at 24.87 ppm in (**12b**) and 24.89 ppm in (**6b**). The endo/exo carbons

are 33.10 for (**12b**) and 33.11 for (**6b**). This relationship continues for the aromatic carbons; 91.87, 69.67, and 75.24 for (**6b**) and 93.85, 68.98, and 75.10 for (**12b**). The quaternary carbons, at 18.79 and 21.75 ppm of the monoiron system and 18.30 and 20.79 ppm for the di-iron system, are similar. The adducts (**6a**) and (**12a**) display similarity as the (**b**) isomers did. The methyl peaks are found at 1.79 ppm for (**6a**) and 1.77 ppm for (**12a**) with their corresponding carbon peaks at 21.75 ppm for (**6a**) and 21.74 ppm for (**12a**). The exo and endo protons for (**6a**) are 1.93 and 2.44 ppm and the corresponding chemical shifts for (**12a**) are 2.00 and 2.75 ppm. The carbon peaks for the endo/exo carbons on (**6a**) and (**12a**) are at 31.72 ppm and 31.67 ppm respectively. The aromatic protons and their corresponding carbons are 4.41 ppm, 5.73 ppm and 70.71 ppm and 74.15 ppm for the isomer (**6a**). For the adduct (**12a**) these peaks appear at 4.31 ppm, 5.65 ppm and 70.12 ppm and 73.89 ppm. The protons adjacent to the site of addition appear in the proton range of 2.60-2.62 ppm and 29.07-29.06 ppm for the carbon region of the mono- and di-iron adducts. The quaternary carbons for (**6a**) and (**12a**) appear in the range of 35.92-35.99 and 75.11-74.96 ppm. The significance of these numbers and the range in which they appear is how they describe the structure of the adduct. All methyl protons appear as expected in the aliphatic region of 1-3 ppm and their carbons in the range of 20-30 ppm. The addition of the hydride anion induces a loss of aromaticity to the complexed ring, thus generating a 1-6.5 ppm range in which the ring protons appear. The exo and endo protons are not equivalent, and thus differ in chemical shift and interaction with the other protons on the ring. There are two methods to identify one from the other: either based on chemical shift because exo protons are always found upfield from the endo proton, or by the splitting pattern, which will differ because the endo proton

couples to adjacent protons, whereas the exo proton only couples with the endo hydrogen. A final clue to determine endo/exo chemical shifts is to measure coupling constants, since they have distinct J values of 9-13 Hz. These last two criteria are effective when the number of isomers is small. The exo protons are found in the range of 1.59-2.16 ppm and the chemical shifts of the endo protons appear from 2.34-2.78 ppm. The carbon chemical shift of the endo/exo carbon is in the aliphatic range at 27.59-36.96 ppm, depending on the position of the substituents on the ring. In general, the protons adjacent to the site of addition are aliphatic and appear in the range of 1.83-2.62 ppm and the corresponding aliphatic carbon range extends from 16.25-29.07 ppm. The chemical shifts for proton and carbon depend on the position of the substituent, but exist in the aliphatic regions of the spectrum. Quaternary carbon chemical shifts range in the spectrum from 20-97 ppm; where the chemical shift is dependent on the aromaticity of the ring. The C-O carbon is found in the range of 31-97 ppm. If the site of addition is ortho to this phenoxy substituent then it will appear in the aliphatic region, but if the position of attack is meta to the phenoxy group, where the ring is aromatic, then the chemical shift of this quaternary carbon will be around 95 ppm. This is also the case for C-Me quaternary carbons where the position of nucleophilic attack is the primary influence on chemical shift. If addition was ortho to a methyl group, then the carbon peak would appear in the aliphatic carbon range around 24 ppm, whereas if the methyl group was meta to the site of addition, the carbon would appear around 75 ppm. The aromatic protons of the ring in the C4 and C5 or C3 positions generally appear in the complexed aromatic range of 3.89-6.23 ppm for proton NMR and 70-90 ppm for the carbon NMR. These are the protons furthest away from the site of addition; therefore this part of the ring relates to the original complex with

slightly less aromatic character. The general trend indicates definite chemical shift characteristics which can aid in the structure determination of other addition products, involving other nucleophiles. We have also established that the two rings on a bimetallic complex do not interact, and therefore do not influence reactions at the other ring. Figures 11 and 12 illustrate the HH COSY and ^{13}C NMR of adduct (**12**).

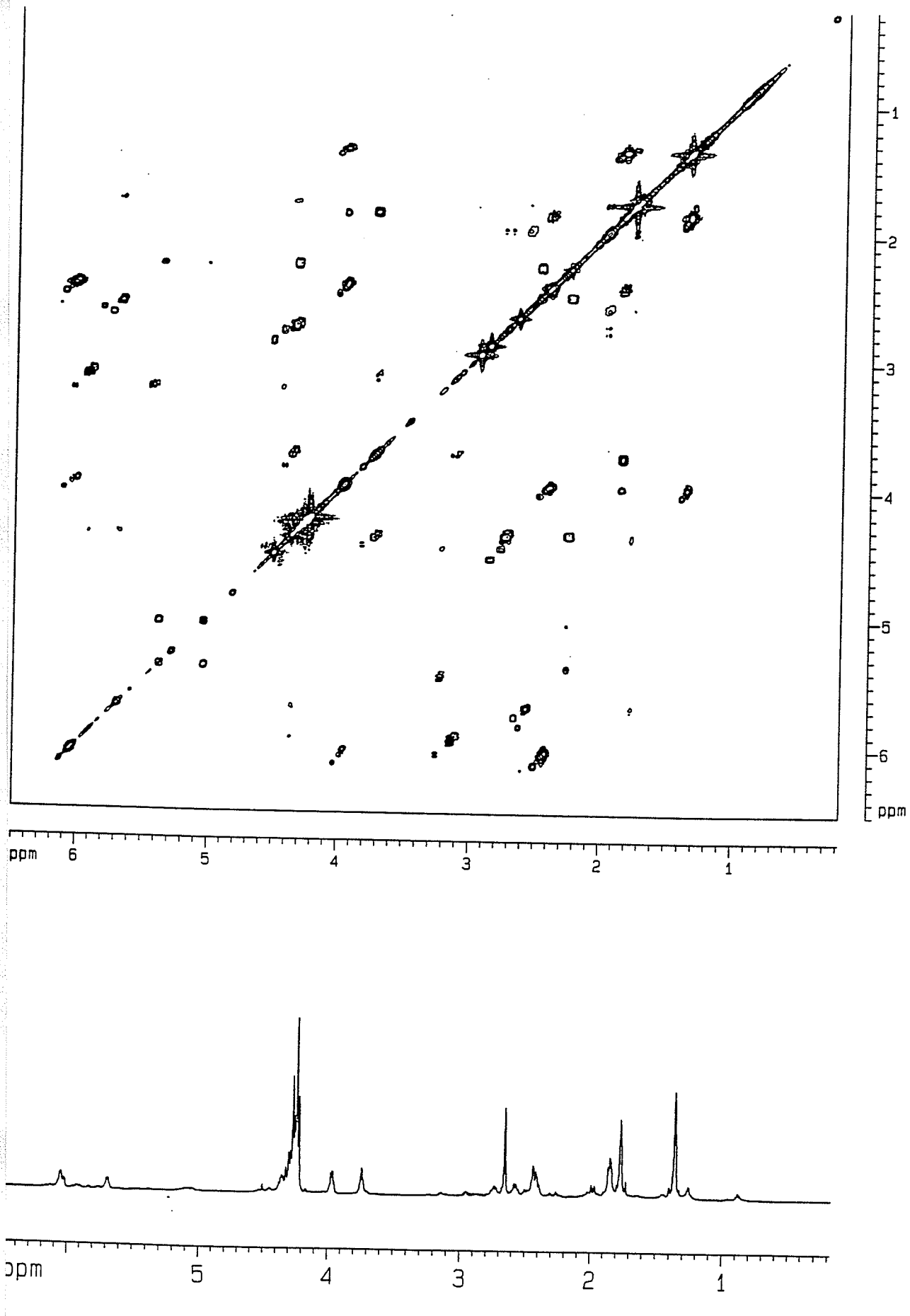

Figure 11: HH COSY of adduct (12).

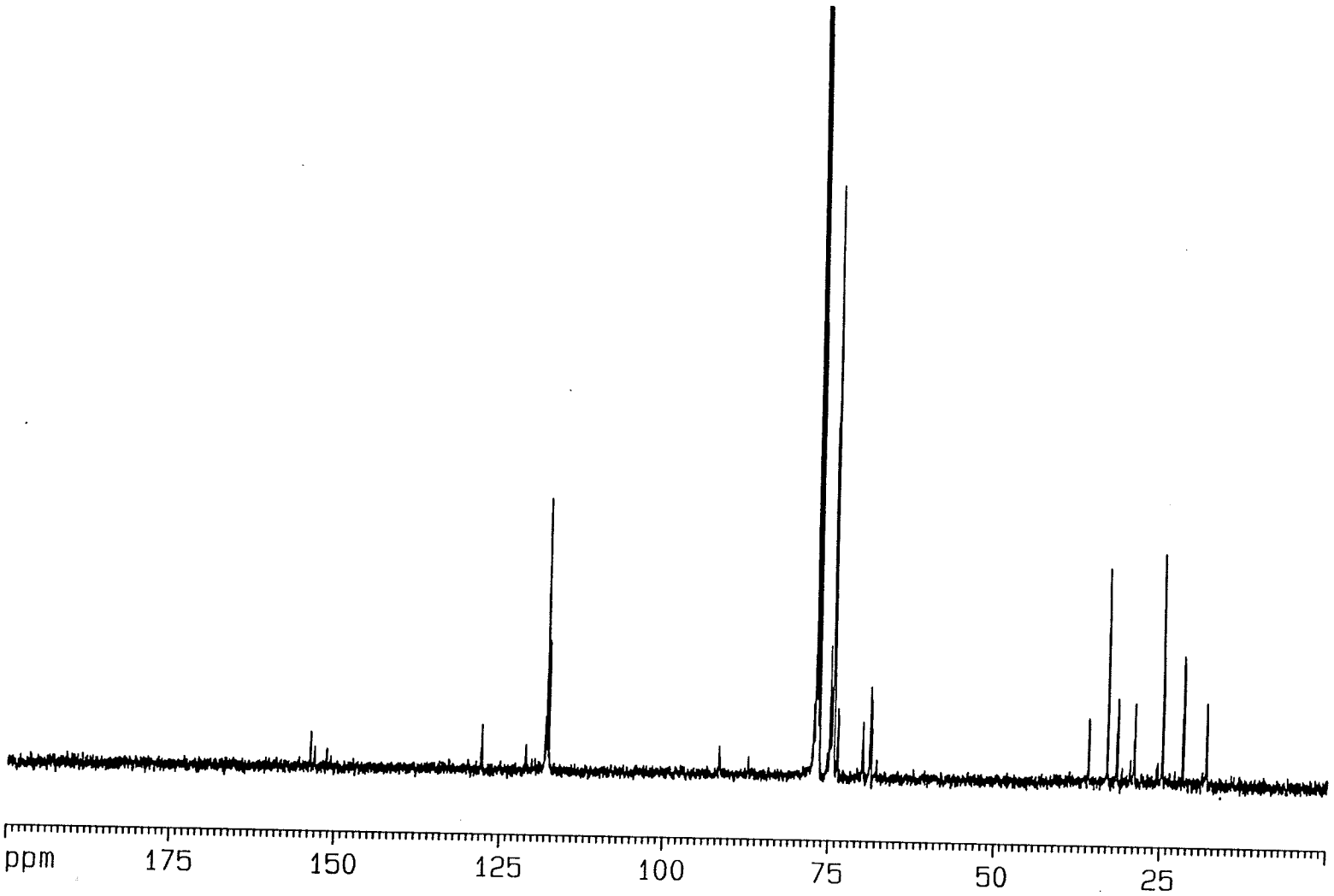

Figure 12: ^{13}C NMR of adduct (12).

Table 3: ^1H NMR data for the adducts 12, 14 and 15.

Adduct	CH_3	H(1-exo)	H(1-endo)	H(2)	H(3)	H(4)	H(5)	H(6)	Cp
12a	1.77	2.00	2.75	-------	4.31	5.65	-------	2.60	4.27
	s	*(d, 11.3, ex-en)*	*(dd, 10.8, en-ex; 5.9, en-6)*		*(d, 5.6)*	*(d, 5.6)*		*(d, 5.9, 6-en)*	*s*
12b	1.36	1.85	2.41	2.43	-------	6.05	3.97	-------	4.24
	s	*(d, 10.7, ex-en)*	*m*	*(d, 6.0, 2-en)*		*(d, 5.7)*	*(d, 5.7)*		*s*
14a	1.51	2.13	2.66	-------	3.89	5.64	4.40	-------	4.26
	s	(d, 10.7, ex-en)	(d, 10.7, en-ex)		(d, 5.5)	(t, 5.5)	(d, 5.5)		s
14b	1.83	1.67	2.48	2.36	-------	6.17	-------	2.07	4.24
	s	(d, 14.4, ex-en)	m	(d, 6.5)		s		(d, 6.6)	s
14c	1.36	1.71	2.34	-------	4.53	-------	4.30	1.91	4.23
		m	*m*		*m*		*m*	*m*	*s*
16a	1.63, 2.70	1.66	2.39	-------	-------	-------	4.16	2.03	4.14
	s	*(d, 12.5, ex-en)*	*(dd, 13.4, en-ex; 7.3, en-6)*				*(d, 6.4)*	*m*	*s*
16b	2.18	1.59	2.34	1.83	-------	-------	-------	1.83	4.17
	s	*m*	*(dd, 12.1, en-ex, 7.3, en-2,6)*	*m*				*m*	*s*

All samples run in $CDCl_3$ (ppm from solvent peak at 7.26 ppm).
Uncomplexed aromatic peaks in the 7-8 ppm region.
Coupling constants (Hz) are of adjacent aromatic prot

Table 4: ^{13}C NMR of the adducts 12, 14 and 16.

Adduct	CH_3	C (1)	C (2)	C (3)	C (4)	C (5)	C (6)	Cp
12a	21.74	31.67	35.92	70.12	73.89	74.96	29.06	74.65
12b	24.87	33.10	18.30	93.85	68.98	75.10	20.79	74.53
14a	25.49	36.89	36.43	71.39	70.29	70.00	25.62	74.90
14b	21.85	27.60	24.51	89.92	72.21	76.22	20.97	74.41
14c	24.81	31.36	26.61	73.84	89.99	72.82	17.39	74.78
16a	19.96, 16.41	34.94	29.74	97.37	89.45	78.17	16.95	75.35
16b	19.45	27.63	19.45	88.42	94.45	88.42	19.45	75.88

Samples were run in $CDCl_3$ (ppm from solvent peak at 77.00 ppm)

Uncomplexed aromatic peaks are in the 120 - 140 ppm region.

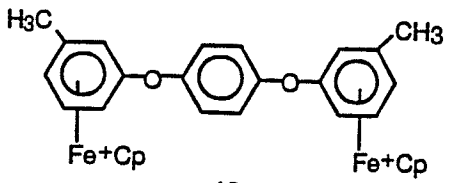

13

$NaBH_4$
THF/DMF

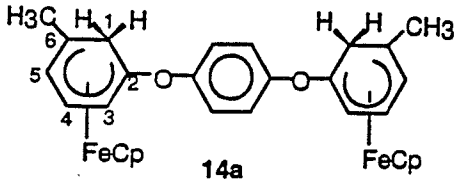

14a

+

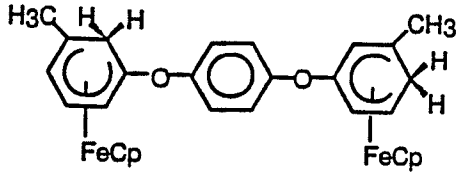

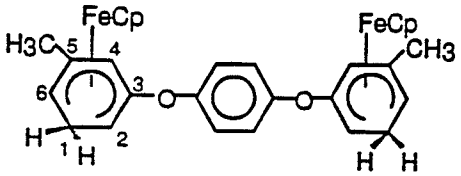

14b

+

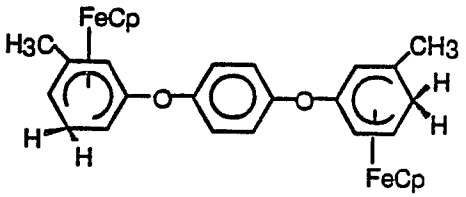

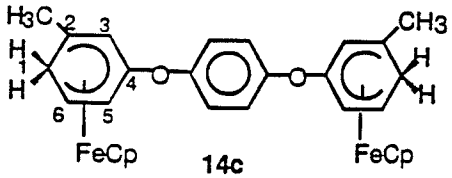

14c

+

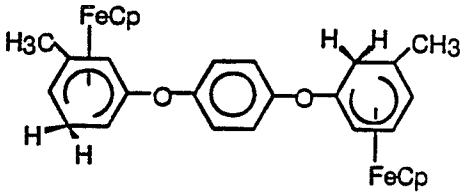

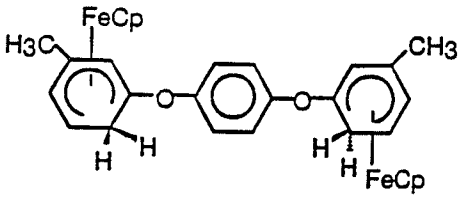

+

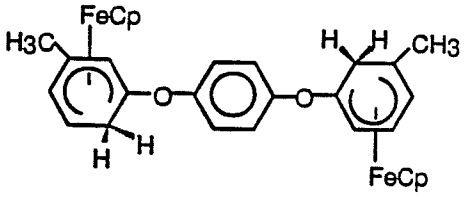

+

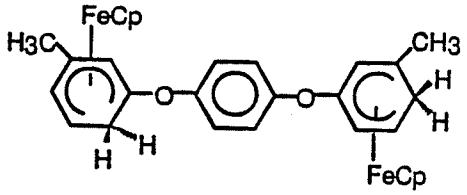

Scheme 20

The structure in which addition occurred at the position ortho to the ether link and para to the methyl group was present in trace amounts; therefore not all the peaks could be identified. The structures (**14a-f**) represent the symmetrical and asymmetrical products possible. The detailed NMR analyses are listed in Tables 3 and 4.

As part of this study, we blocked the two positions ortho to the etheric bridges by two methyl groups in order to enhance addition to the meta position. Hydride addition to 1,4-bis[(η^6-(2,6-dimethyl)phenoxy-η^5-cyclopentadienyl)iron]-benzene hexafluorophosphate, (**15**), resulted in the formation of three major isomers, as well as traces of a few minor isomers, as shown in Scheme 21.

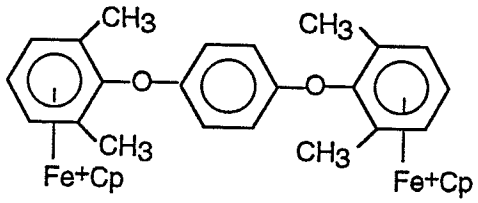

15

$NaBH_4$
THF/DMF

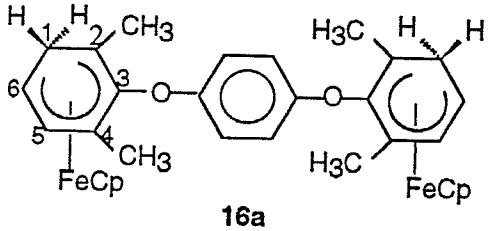

16a

+

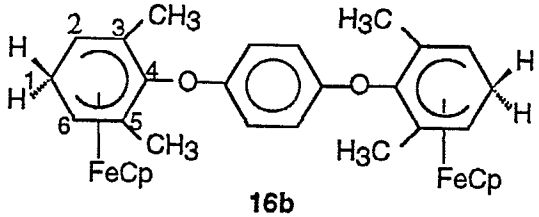

16b

+

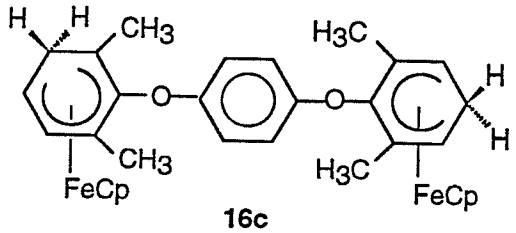

16c

+

Traces of ortho adducts

Scheme 21

Using the same strategy as described above, the predominant isomer was determined to be the meta adducts (51%); para (41%) and traces of ortho adducts (8%) were also present. The spectral analyses for these adducts are given in Tables 3 and 4. Figures 13 demonstrates the ^{1}H NMR of the adducts (**16**).

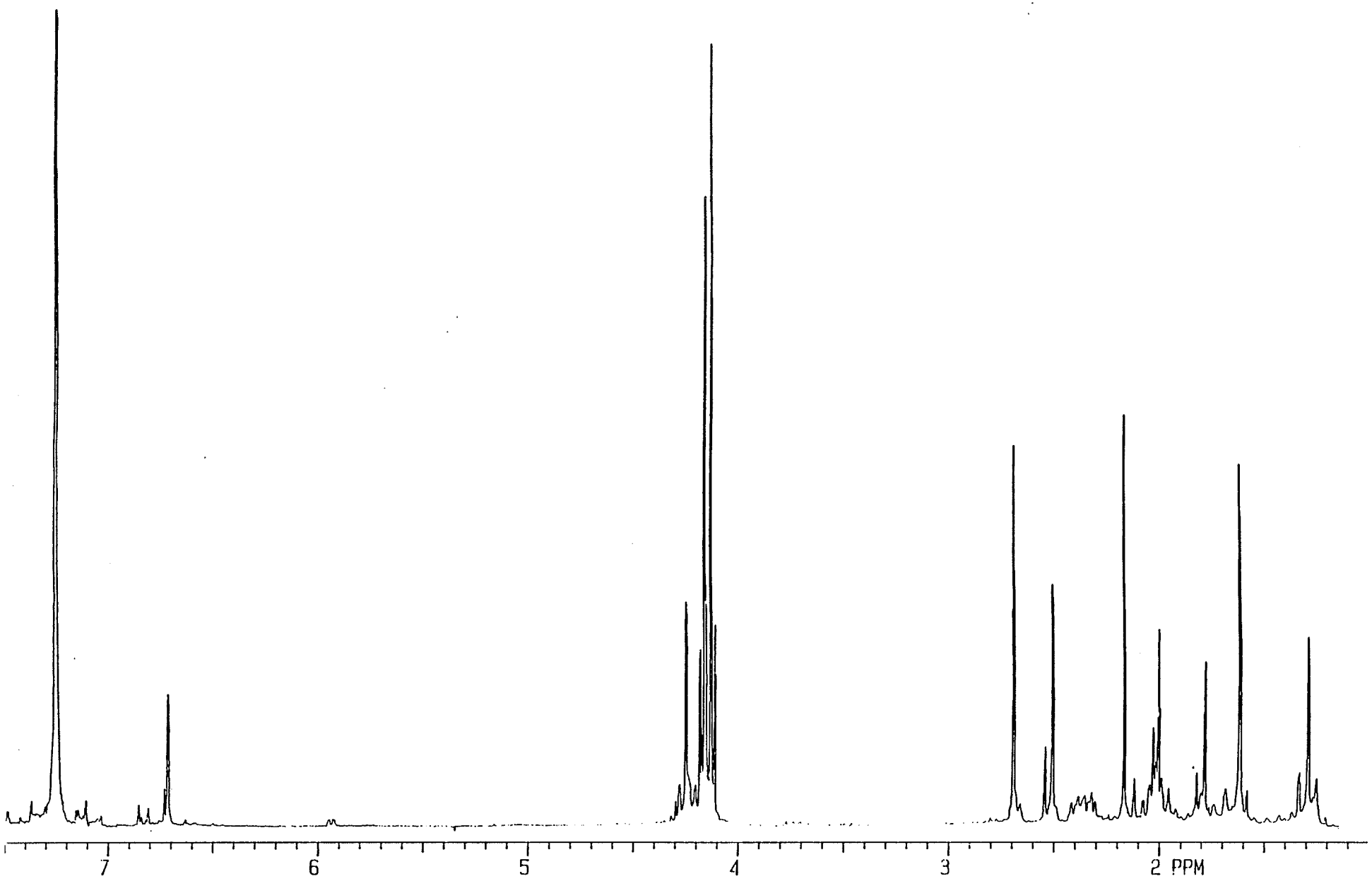

Figure 13: ^{1}H NMR of adduct (16).

Hydride addition to the bimetallic complexes resulted in the formation of isomers in which the site meta to the ether linkage was the preferred position of attack. The results are identical to those found with the analogous monoiron structures; thus the monometallic complexes serve as good models for larger systems. This is consistent for each case studied above. It was difficult to determine which uncomplexed aromatic peaks belonged to each isomer; therefore the data was summarized within the aromatic region for both ^{1}H and ^{13}C NMR. The position of hydride addition was found to be dependent on the substituents on the ring. In the case of the 4-methyl complexes (**1** and **4**), the primary position of addition was meta, illustrating the ortho directing effect of the methyl group and the meta directing ability of the phenoxy or thiophenoxy substituents.

2.2 Cyanide addition

2.2.1 Isomeric 1,4-bis(η6-methyl phenoxy-η5-cyclopentadienyliron) benzene dihexafluorophosphate.

Nitrile groups are unique in their ease of transformation to other functional groups such as acids, esters, amines and amides [73-76]. This versatility is valuable in the investigation of synthetic routes for the functionalization of organic and polymeric compounds. This versatility has been incorporated into the research of optically pure biological drugs such as antiulcer agents [76]; as well, this group can easily undergo cyclization reactions to extend ring systems [73]. In the past few years, we have been involved in the synthesis and characterization of polyaromatic ethers with or without pendent metallic moieties [10, 67, 70, 71]. In the present work, we report the cyanide addition to a number of $CpFe^+$ polyaromatic ether complexes.

Schemes 22, 23 and 24 show the relative distribution of adducts obtained from cyanide addition to isomeric bis(η^6-methylphenoxy-η^5-cyclopentadienyl)ironbenzene hexafluorophosphate (**11**, **13**, **15,** and **18**). In the case of complexes (**11**), (**18**), and (**15**), single pure products (**17**), (**19**), and (**20**) were obtained. Cyanide attack on (**11**) and (**18**) took place meta to the etheric bridge and ortho to the methyl group (Scheme 22).

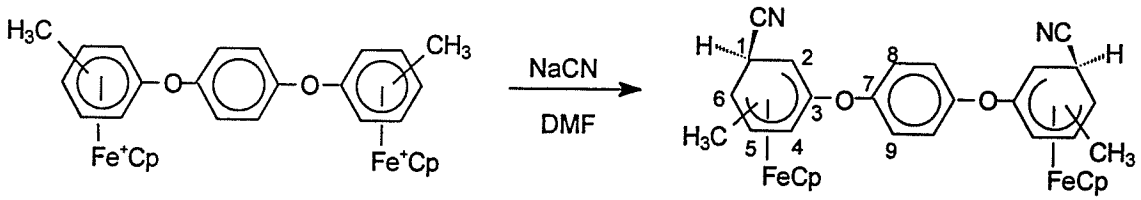

11 4-CH_3
18 2-CH_3

17 4-CH_3
19 2-CH_3

Scheme 22

Figures 14 and 15 illustrate the ^{1}H and ^{13}C NMR of the adduct (**17**). Reference to the hydride addition reactions shows that the most aromatic proton adjacent to the etheric linkage will appear at approx. 6.2 ppm whereas if a methyl group was adjacent to this same proton the chemical shift would be approx. 5.7 ppm. This information was used to solve the structure of the adduct after cyanide addition. The most aromatic proton appears as a doublet at 6.3 ppm (J=5.4Hz). The next peak along the spectrum is a doublet at 5.1 ppm (J=5.4 Hz), which would be the proton adjacent to the most aromatic proton. The Cp peak is a strong singlet at 4.7 ppm, and the methyl group is a singlet at 1.9 ppm. The last two peaks appear as two doublets; 3.5 ppm (J=5.5 Hz) and 3.0 ppm (J=5.5 Hz). All of the doublet peaks have an area of 2H, the Cp is 10H and the methyl peak 6H. There are only two possible products that could be formed: addition meta to the etheric substituent or meta to the methyl group. The only structure is the former due to the low field position where the most aromatic proton appears; as well, the methyl group is in the range of an ortho position, considering that the nucleophile is now cyanide, which will cause a downfield shift of all peaks. The ^{13}C spectral data illustrates similar trends to the di-iron hydride adducts in that the methyl groups appear at approx. 22 ppm and the Cp peaks are found at approx. 77 ppm. If we consider the most aromatic carbons on each ring, these display chemical shifts in the area of 75-84 ppm. The carbon which is the site of CN attack appears in the range of 28-31ppm. The proton coupled to the endo proton is slightly upfield from C1 at approx. 24 ppm. Quaternary carbons are dependent on the aromaticity of the ring at the position they are bonded to, and thus vary accordingly. Usually, the C-O carbon is found at approx. 96 ppm and the quaternary carbon (C-O) for the

uncomplexed ring is approx. 123 ppm. The CN carbon appears in the range of 116-119 ppm and the final quaternary carbon bonded to the methyl group is approx. 28 ppm assuming it is ortho to the site of addition. The uncomplexed aromatic carbons appear in the range of 126-130 ppm. There is no evidence that one ring influences the other, as determined from the hydride experiments. It is difficult to observe the uncomplexed phenyl peaks in the smaller bimetallic systems. This is a result of different relaxation times, but as will be shown, the peaks grow as the size of the complexes increase with exact integration. Figure 16 illustrates the ^{1}H NMR of (**19**).

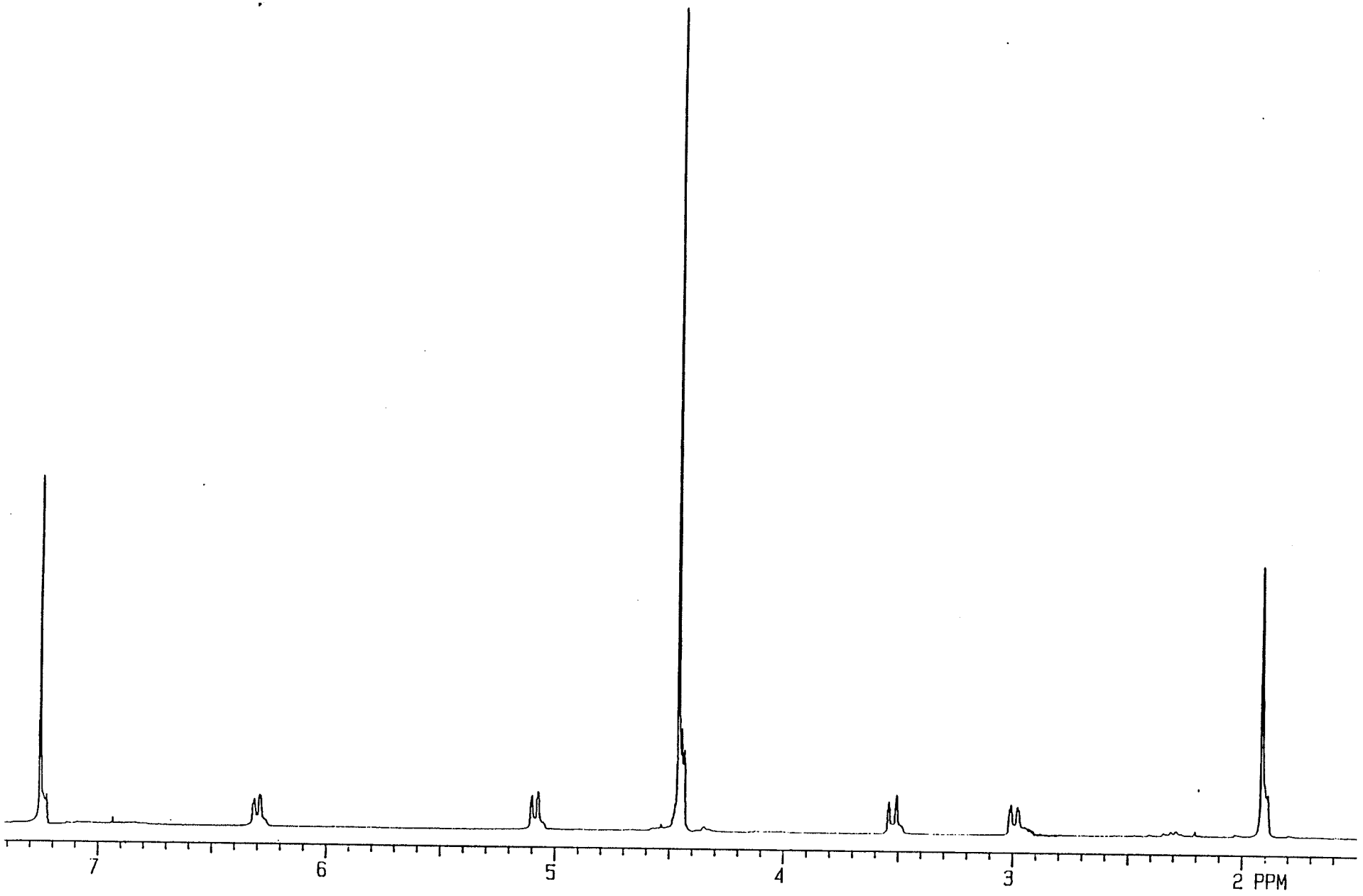

Figure 14: ^{1}H NMR of adduct (17)

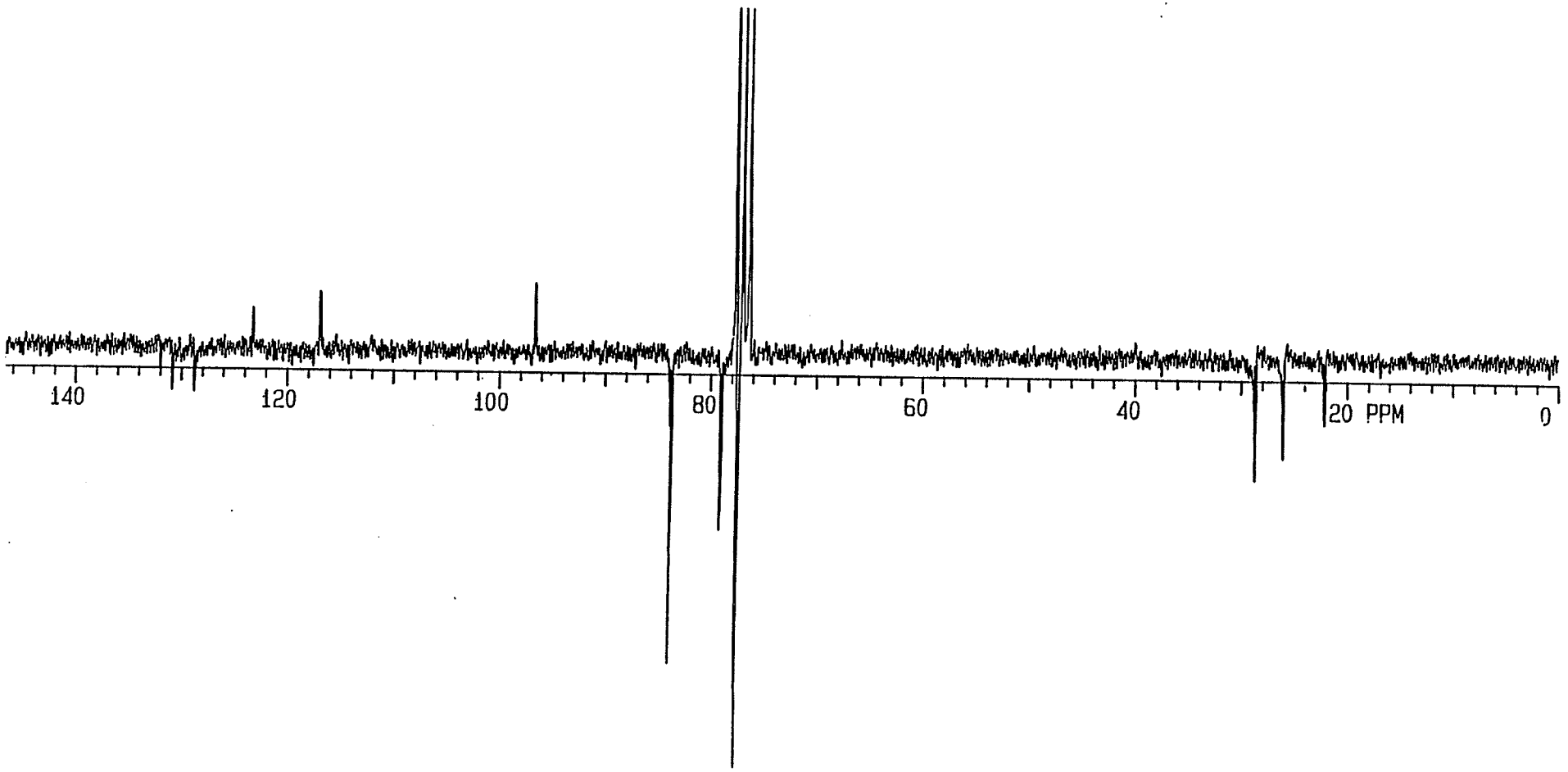

Figure 15: ^{13}C NMR of adduct (17).

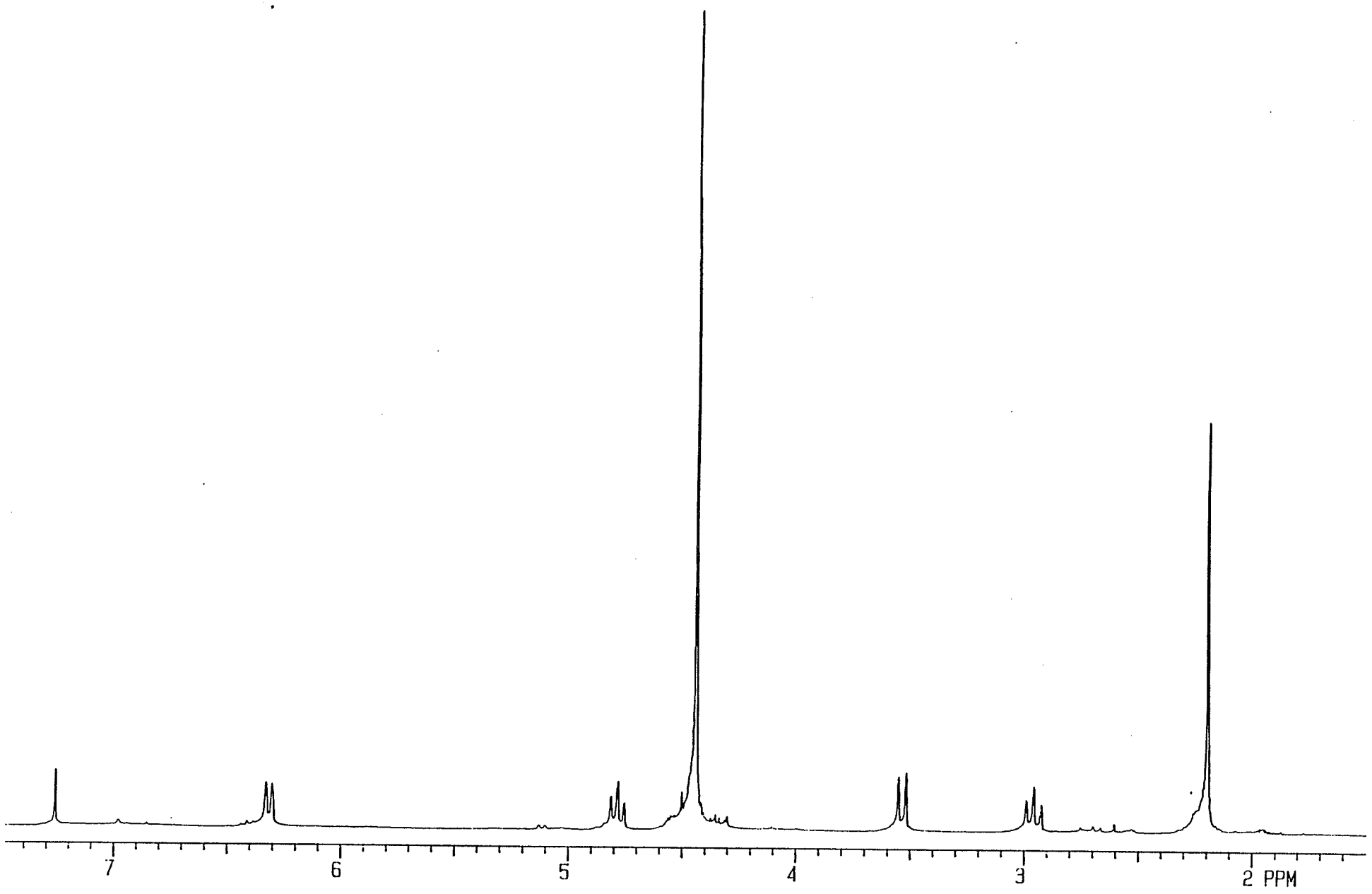

Figure 16: ^{1}H NMR of adduct (19).

In contrast, the 2,6-dimethyl ether complex gave selective addition ortho to the etheric bridge which is ipso to a methyl group (**20**) (Scheme 23). This is easily be verified with the recognition of a doublet at 6.35 ppm and a triplet at 4.79 ppm. These correspond to the aromatic protons on the structure illustrated in Scheme 23. There is no other possible structure that would produce this spectrum or splitting pattern. A similar result was obtained for the reaction of a monometallic complex substituted by an electron-withdrawing group and hindered at the ortho positions by methyl groups [29]. Steric effects have little relevance on site preference [28]. It should be noted that the only difference between the hydride and cyanide experiments is the nucleophile. The nature of the nucleophile seems to be a strong factor in the choice of the position of nucleophilic attack. The comparison of various nucleophiles with similar systems would be necessary before any further conclusions are made. Figure 17 illustrates the ^{1}H NMR spectrum of (**20**).

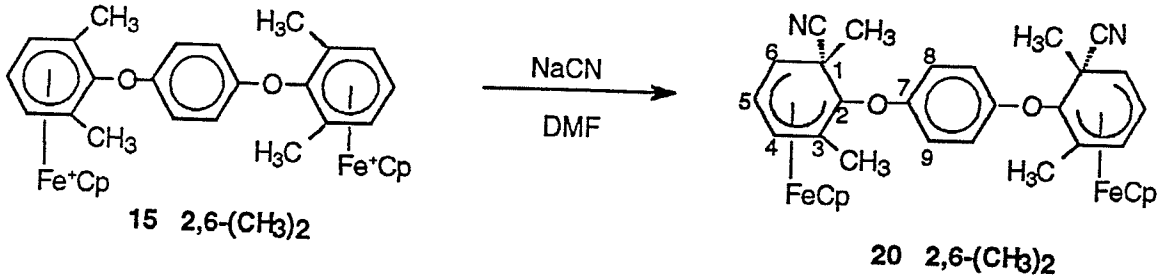

15 **2,6-(CH_3)$_2$** **20** **2,6-(CH_3)$_2$**

Scheme 23

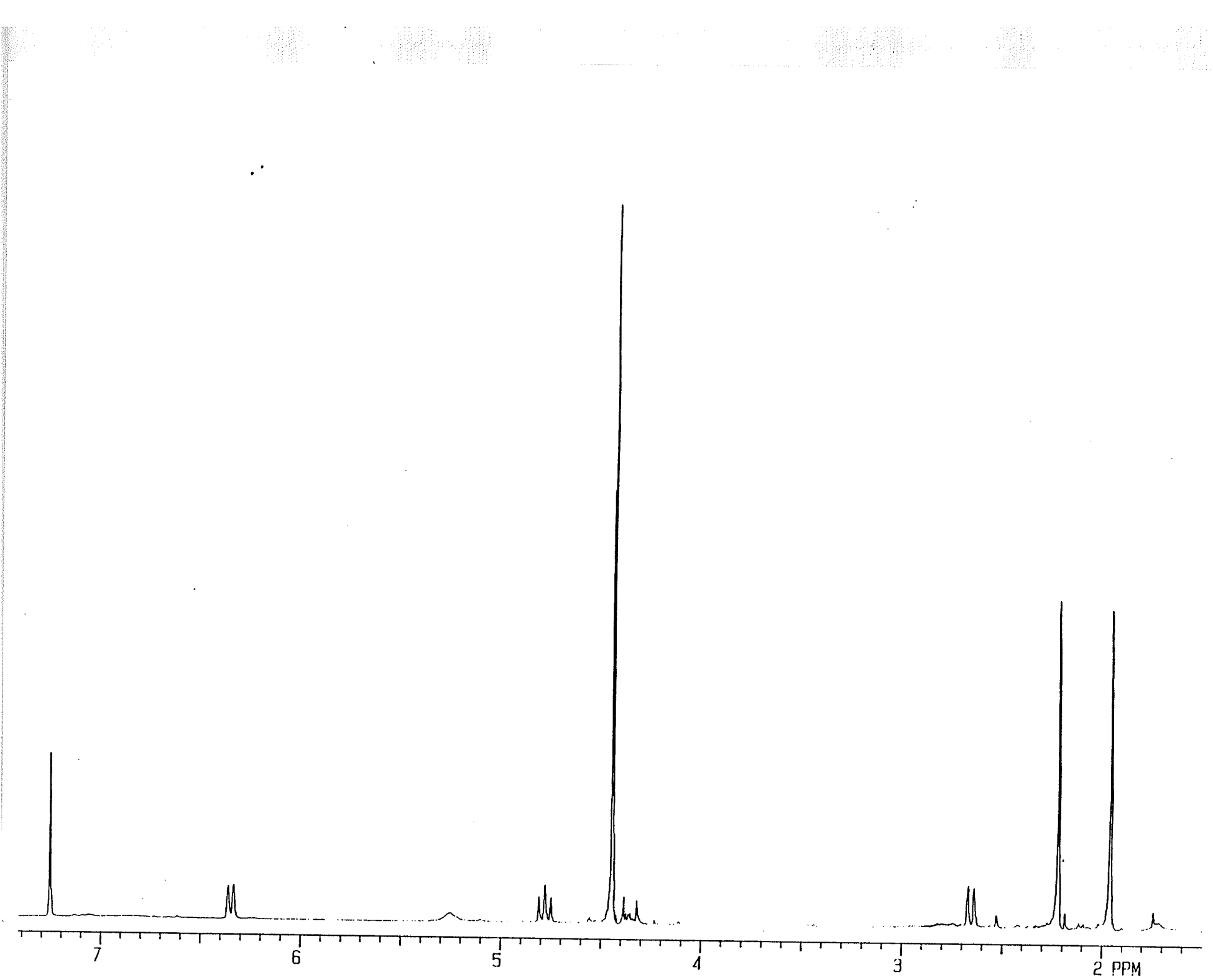

Figure 17: ^{1}H NMR of adduct (20)

The meta isomer (**13**) gave rise to three possible adducts (**21a-c**) (Scheme 24).

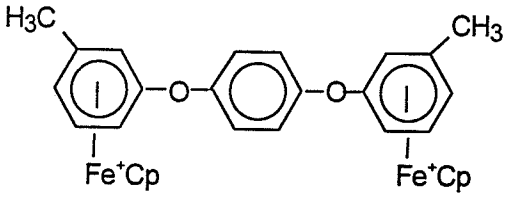

13

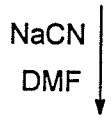

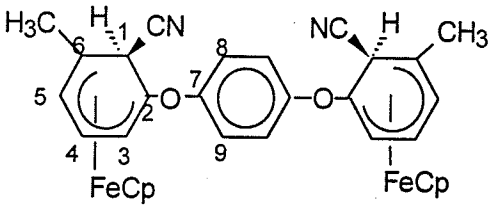

21a

+

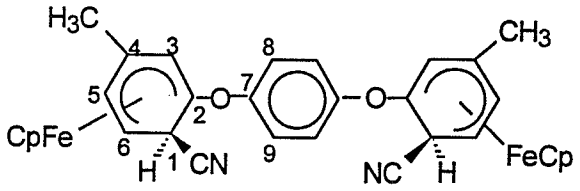

21b

+

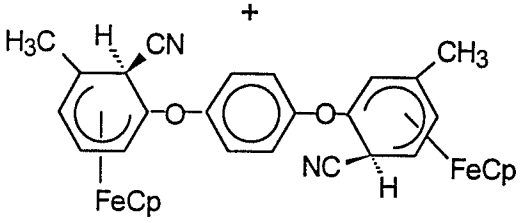

21c

Scheme 24

As in the case of the hydride addition reactions, it is difficult to ascertain if addition occurs in the same site on each ring; thus we can only conclude that symmetrical or asymmetrical products are produced. Therefore characterization of the products was based on the occurrence of a specific site of attack on one ring rather than both rings. These isomers displayed addition ortho with respect to both etheric and methyl substituents (**21a**) and

addition ortho to the etheric bridge and para to the methyl group (**21b**). As well, the asymmetrical isomer displayed addition ortho to one complexed arene ring with respect to both substituents and ortho to the etheric bridge, para to the methyl substituent for the second complexed arene (**21c**).

For the previous systems, we were able to conclude that both the rings displayed identical adduct formation but once mixtures of products appear we can no longer distinguish between the symmetrical products (addition the same on both rings) or asymmetrical products (addition different on both rings). Spectral data was assigned based on the total ortho addition detected (65%) for the adduct ortho to both substituents and the total ortho to the etheric bridge and para to the methyl group (35%) as in the hydride experiments with diiron systems. Statistically, there must be symmetrical products present but it is impossible to determine this quantity. The ^{1}H and ^{13}C NMR of the bimetallic adducts are listed in Tables 5 and 6. Figure 18 illustrates the ^{1}H NMR spectrum of adduct (**21**).

Table 5: ^1H NMR data for the adducts 17, 19, 20 and 21.

Adduct	CH_3	H(1endo)	H(2)	H(3)	H(4)	H(5)	H(6)	Cp	Ph
17	1.93	3.52	3.03	------	6.33	5.11	------	4.45	6.8-7.3
	s	*(d, 5.5, en-2)*	*(d, 5.5, 2-en)*		*(d, 5.4)*	*(dd, 5.4)*		*s*	*m*
19	2.19	3.54	------	------	6.33	4.79	2.96	4.44	6.8-7.3
	s	*(d, 5.6, en-6)*			*(d, 5.6)*	*(t,5.6)*	*(t, 5.6, 6-en; t, 5.6)*	*s*	*m*
20	1.97, 2.24	------	------	------	6.35	4.78	2.97	4.44	6.8-7.3
	s				*(d, 5.7)*	*(t, 5.8)*	*(d, 5.8)*	*s*	*m*
21a	1.71	3.51	------	5.08	6.25	4.57	------	4.47	6.8-7.3
	s	*s*		*(d, 5.4)*	*(t, 5.4)*	*(d, 5.4)*		*s*	*m*
21b	2.58	3.46	------	5.03	------	4.77	2.98	4.49	6.8-7.3
	s	*(d, 6.4, en-6)*		*s*		*(d, 6.4)*	*(t, 6.4, 6-en, t, 6.4)*	*s*	

All samples run in $CDCl_3$ (ppm from solvent peak at 7.26 ppm).

Coupling constants (Hz) are of adjacent protons unless otherwise indicated.

Table 6: ^{13}C NMR of the adducts 17, 19, 20 and 21.

Adduct	17	19	20	21a	21b
CH_3	22.08	20.47	24.94, 20.65	20.93	28.19
C (1)	28.66	28.59	32.21	33.62	23.39
C (2)	23.83	28.25	32.66	38.54	36.37
C (3)	96.66	94.49	96.03	81.14	81.76
C (4)	83.77	83.82	84.09	81.55	98.66
C (5)	79.00	80.02	79.86	78.36	80.16
C (6)	28.68	23.30	30.80	24.90	23.45
C (7)	123.4	122.8	121.2	123.6	123.4
C (8)	130.8	130.2	128.9	132.5	133.6
C (9)	128.8	126.2	127.8	129.2	129.0
CN	116.9	117.0	119.9	116.1	117.0
Cp	77.41	77.17	76.67	77.50	77.46

Samples were run in $CDCl_3$ (ppm from solvent peak at 77.03 ppm).

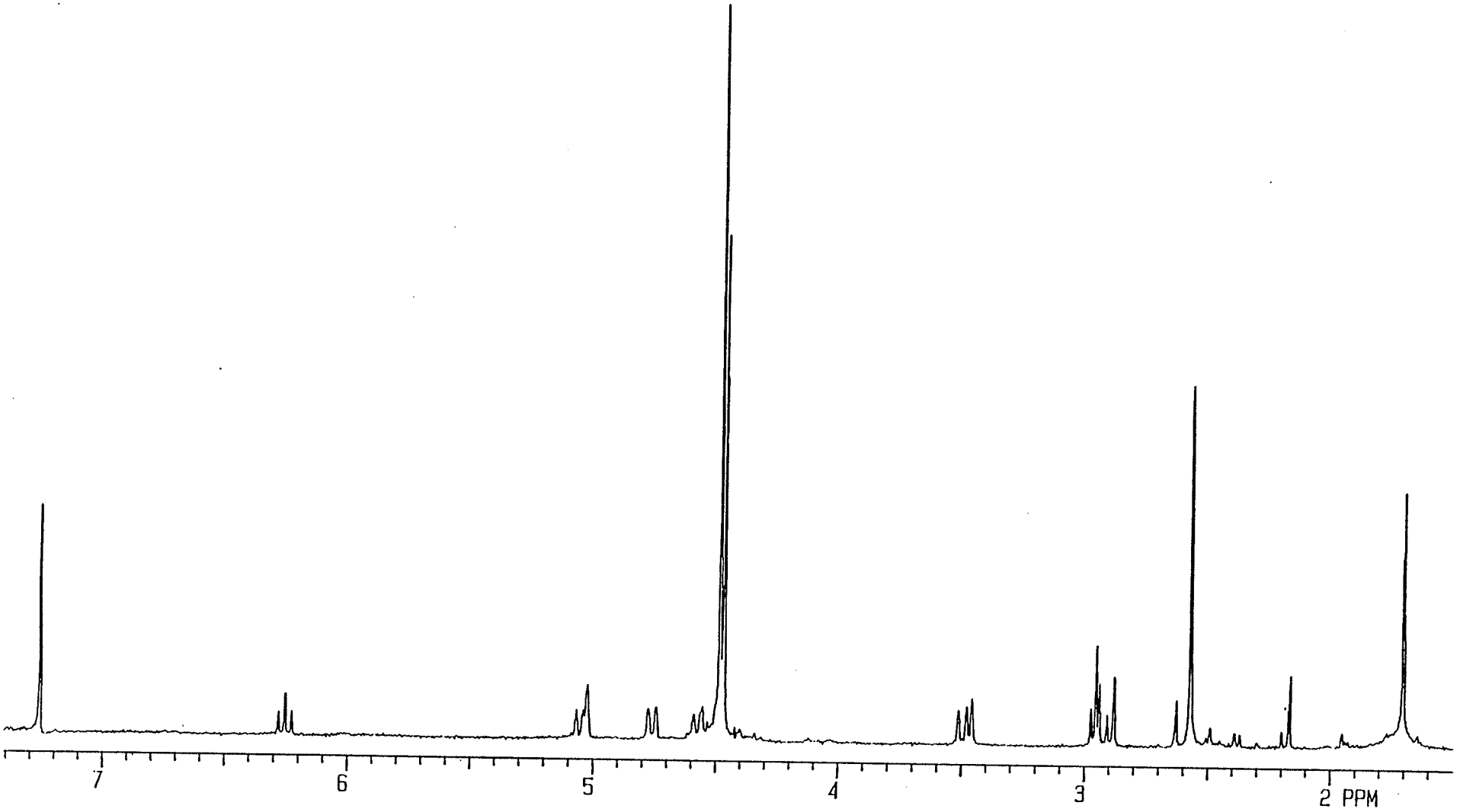

Figure 18: ^{1}H NMR of adduct (21).

2.2.2 Polyether complexes

The higher selectivity of cyanide addition was intriguing and prompted us to examine the polyiron systems. Polyaromatic ether complexes with pendent cyclopentadienyliron moieties **(22-27)** were treated with an excess of NaCN as described in Scheme 25.

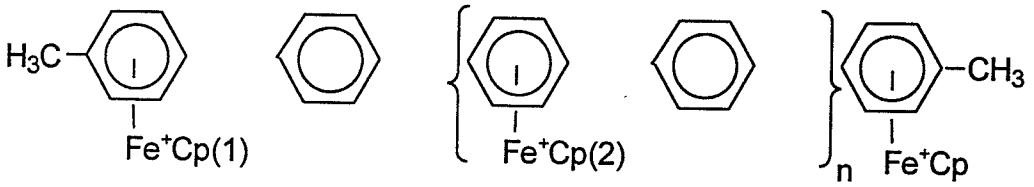

Complex	n
22	1
23	2
24	3
25	4
26	5
27	6

NaCN
DMF

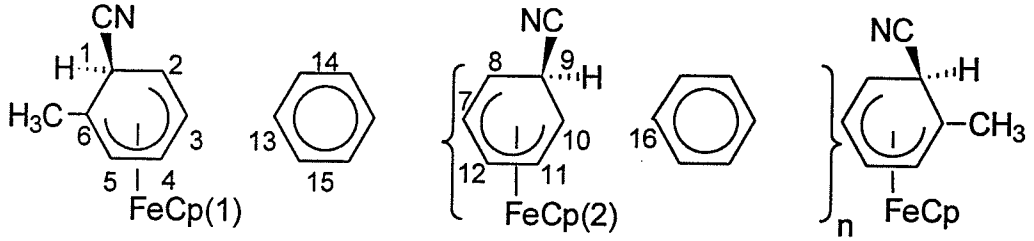

Complex	n
28	1
29	2
30	3
31	4
32	5
33	6

Scheme 25

Selective addition meta to the etheric bridges was obtained in all of these complexes leading to the formation of the neutral (cyclohexadienyl)FeCp systems (**28-33**) in yields of 72-81% (based on the recovered starting cationic complexes). Separation of these adducts from their starting cationic complexes was carried out simply by extracting the adducts from the mixture with chloroform. These results are consistent with those obtained for the analogous diiron complexes. We were able to assign inner and outer arene ring protons and carbons through the comparison between the diiron complex and the polyiron complexes; the inner peaks increase in intensity and integration as the units of the molecule grow. The most aromatic protons of the outer rings appear slightly upfield from those of the inner rings but exhibit similar J values and splitting patterns. In general, the chemical shift of the most aromatic proton is approx. 6.5 ppm for the inner ring and 6.3 ppm for the outer ring. These carbons appear at approx. 84 ppm. The protons adjacent to the most aromatic position, labelled H5 and H11 in Scheme 28, appear at approx. 5.1 and 5.2 ppm. The CH at the site of addition on both rings appears at approx. 3.5 and 3.6 ppm for the outer and inner rings respectively. The last protons (adjacent to the site of addition) are located at ca. 3.2 and 3.0 ppm for the inner and outer rings. The Cp rings show the same trend with the inner Cp at 4.6 ppm and the outer Cp at 4.4 ppm. ^{13}C NMR results in almost the same chemical shift values for the inner and the outer complexed rings. The uncomplexed aromatic peaks are difficult to assign as the number of metals increase, thus they are summarized as multiplets in the aromatic region. As an example, figures 19-23 illustrate the ^{1}H and ^{13}C NMR of adducts (**28, 29, 32 and 33**) respectively. The detailed NMR data for adducts (**28-33**) are given in Tables 7 and 8.

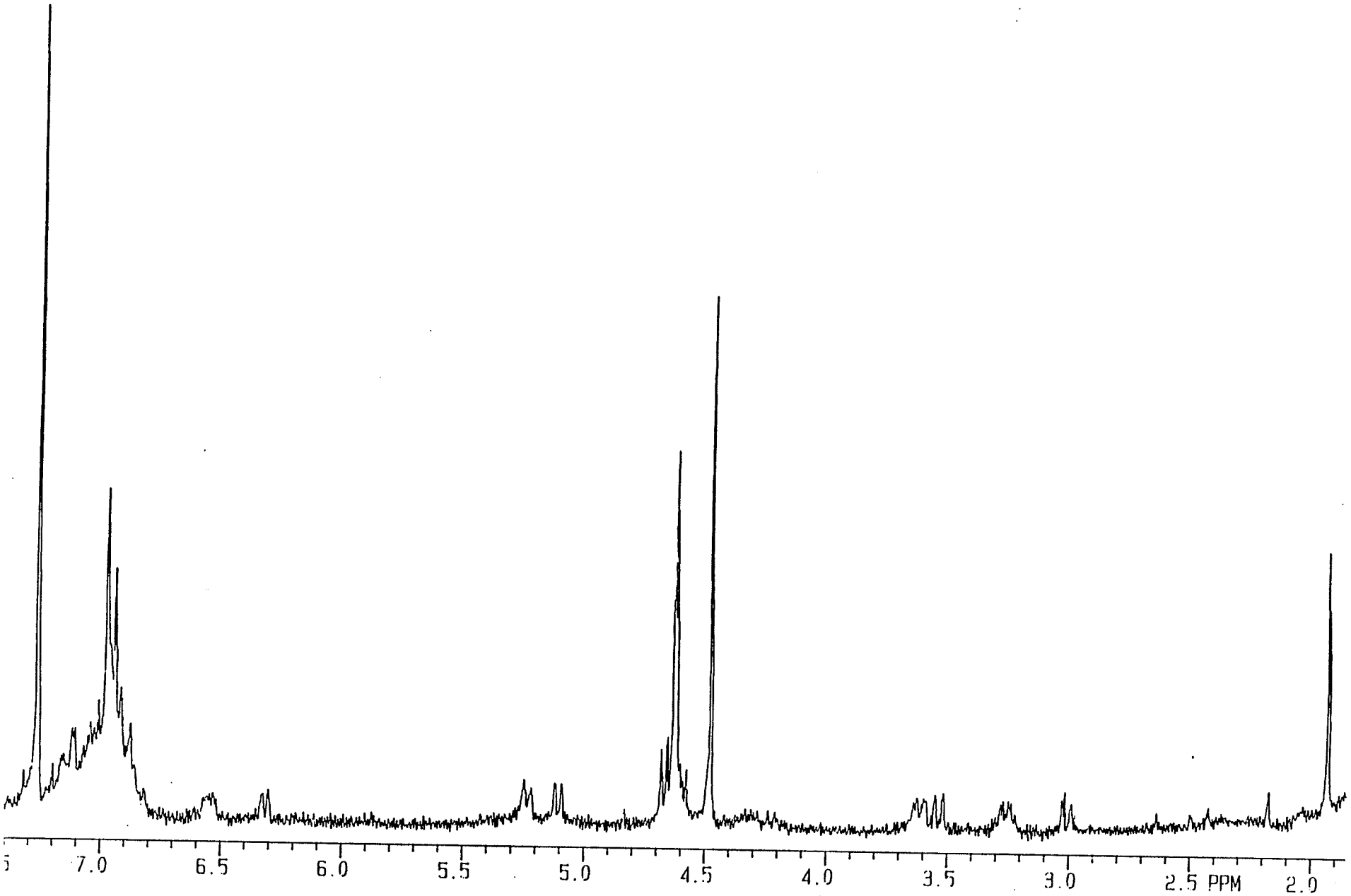
7.0
6.5
6.0
5.5
5.0
4.5
4.0
3.5
3.0
2.5 PPM
2.0

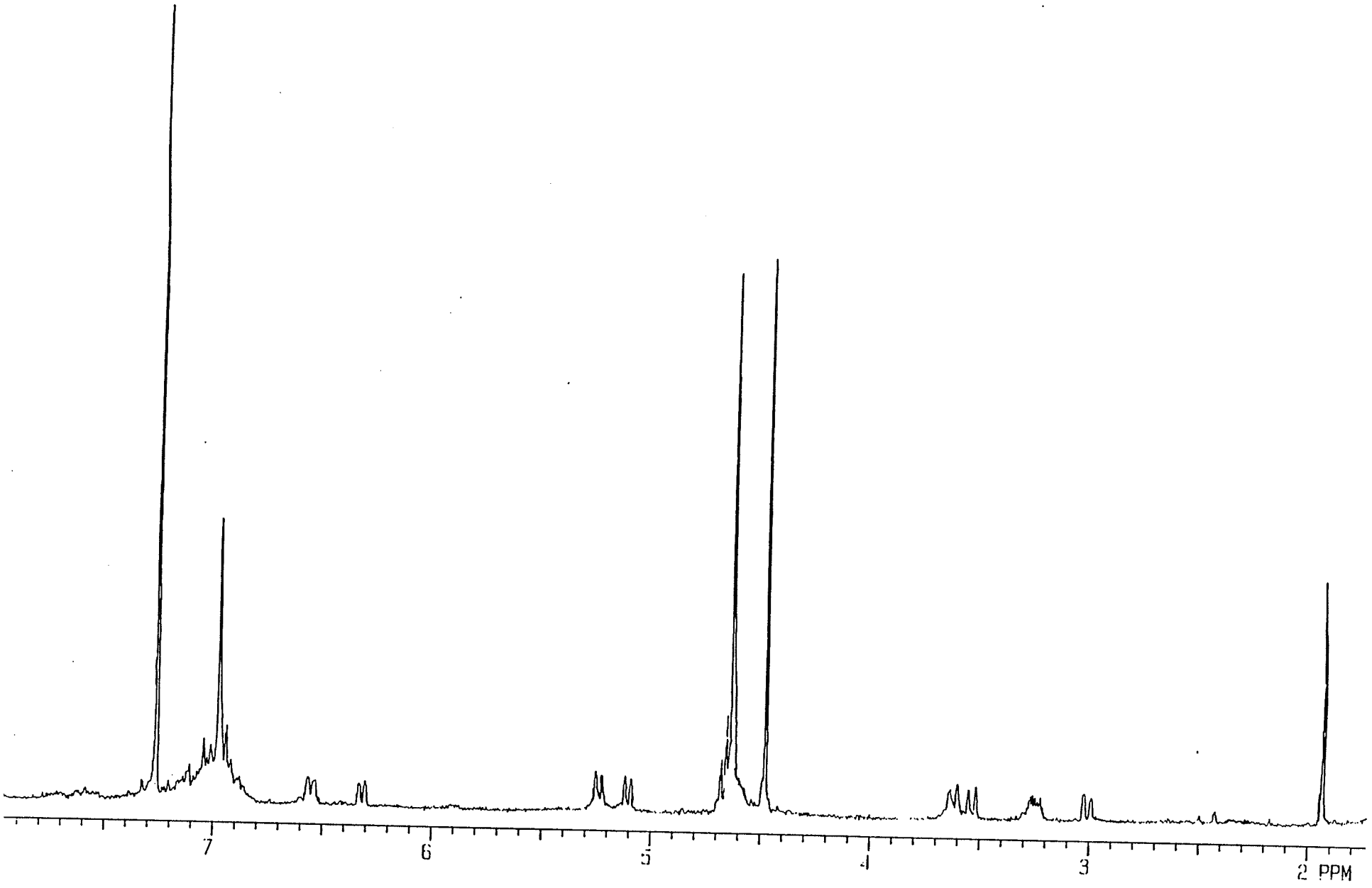

Figure 20: ^{1}H NMR of adduct (93)

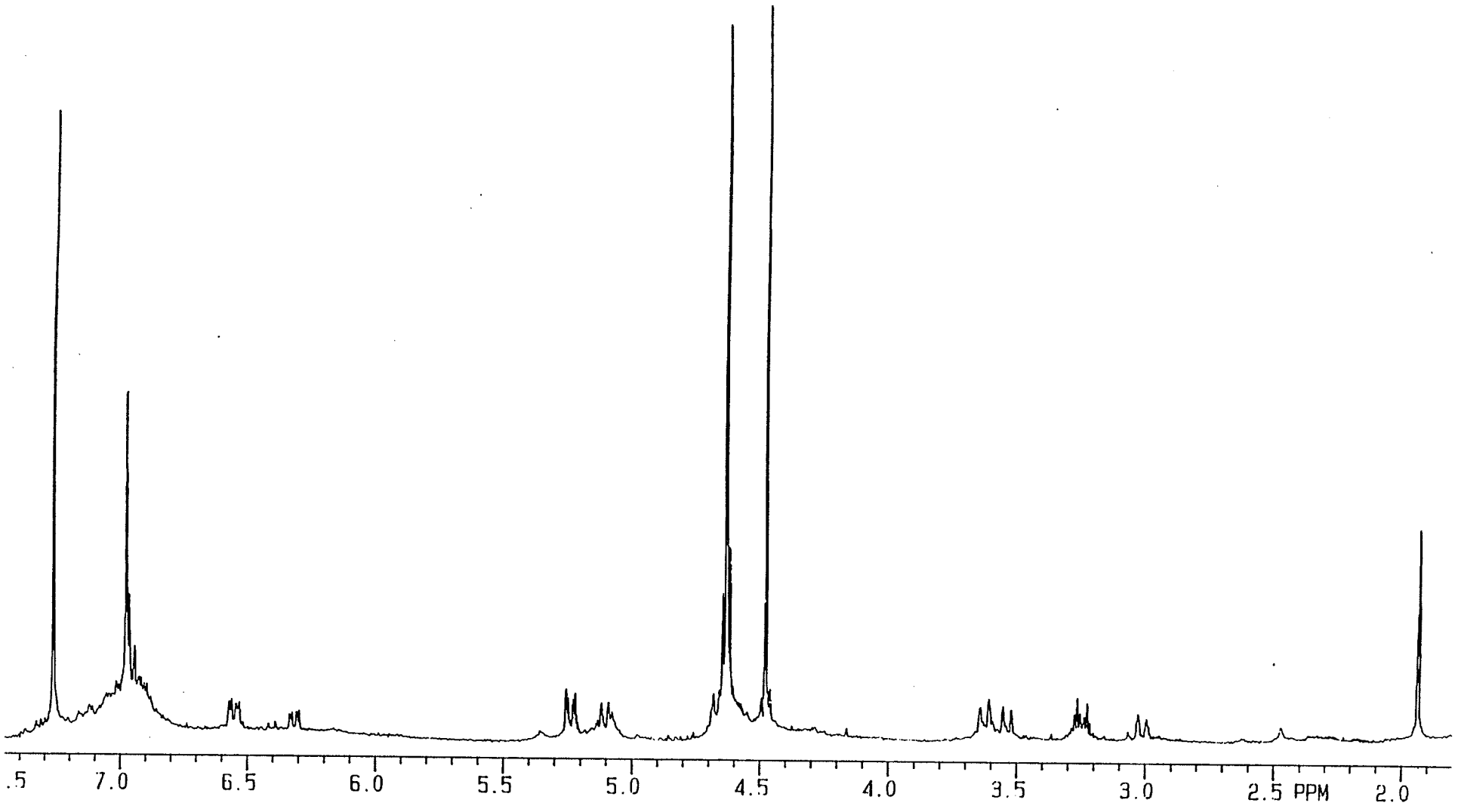
.5
7.0
6.5
6.0
5.5
5.0
4.5
4.0
3.5
3.0
2.5 PPM
2.0

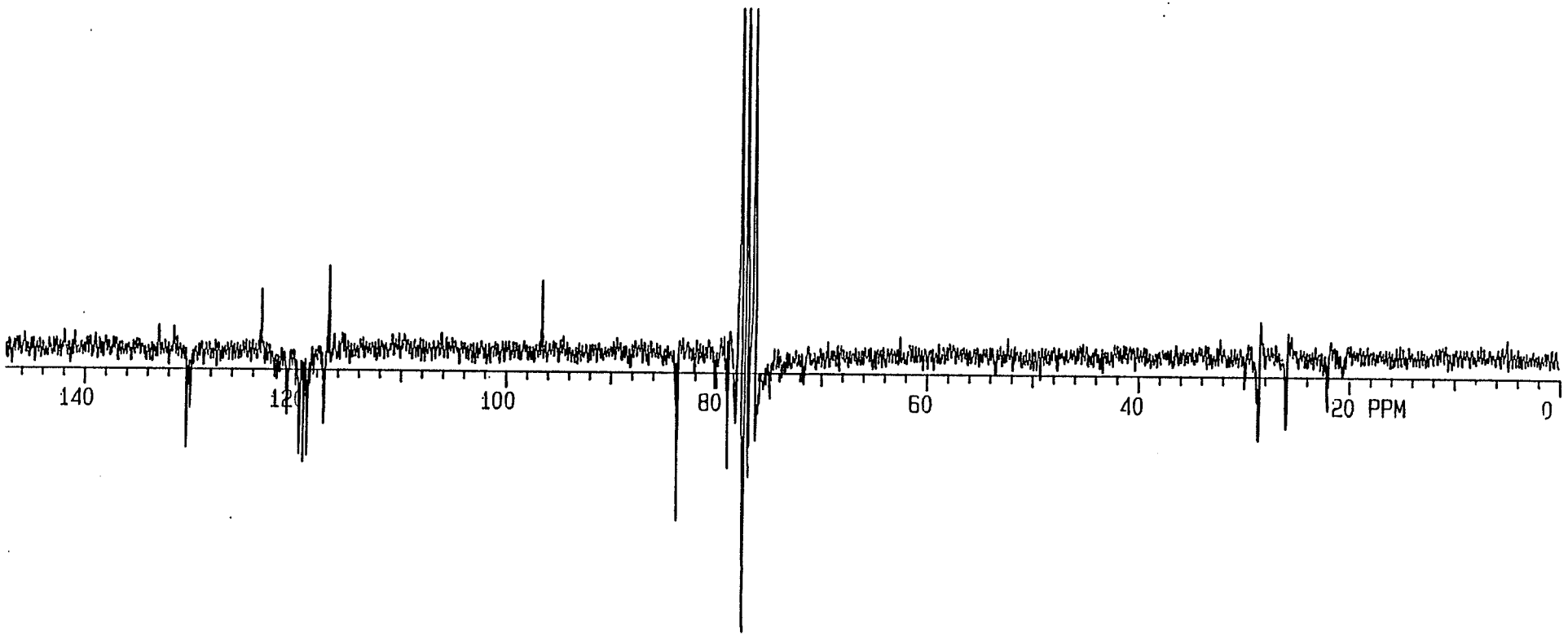

Figure 22: ^{13}C NMR of adduct (28).

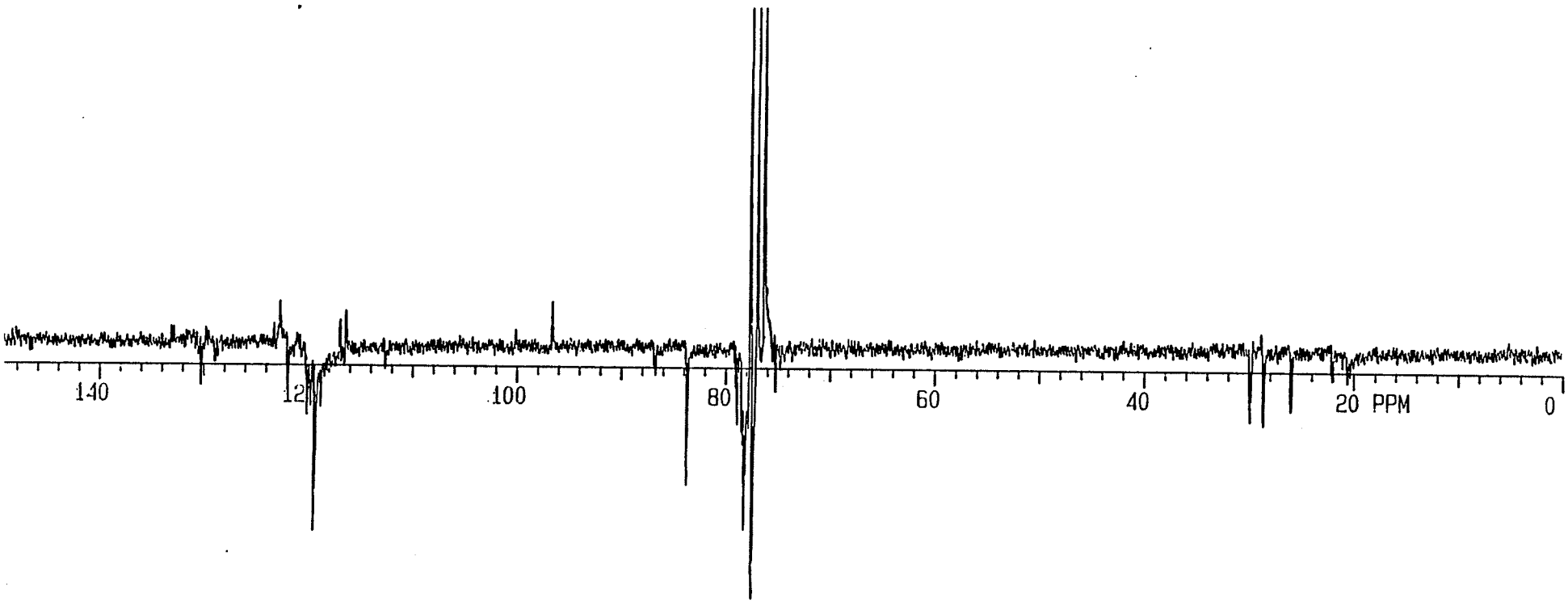

Figure 23: ^{13}C NMR of adduct (29).

Table 7: ^{1}H NMR of the Polymetallic Series Following Cyanide Addition.

Adduct	CH_3	H1	H2	H4	H5	H8	H9	H11	H12	Cp(1)	Cp(2)	ArH
28	1.93	3.53	3.01	6.31	5.10	3.24	3.61	5.21	6.54	4.48	4.60	6.8-7.4
	s	*(d, 6.6)*	*(d, 6.6)*	*(d, 5.4)*	*(d, 5.4)*	*m*	*(d, 6.4)*	*(d, 6.1)*	*(d, 6.1)*	*s*	*s*	*m*
29	1.93	3.55	3.02	6.31	5.12	3.25	3.63	5.25	6.55	4.48	4.62	6.8-7.4
	s	*(d, 6.4)*	*(d, 6.4)*	*(d, 5.5)*	*(d, 5.5)*	*(d, 6.3)*	*(d, 6.3)*	*(d, 5.8)*	*(d, 5.8)*	*s*	*s*	*m*
30	1.94	3.56	3.04	6.33	5.13	3.27	3.64	5.26	6.57	4.49	4.59	7.0-7.3
	s	*(d, 6.8)*	*(d, 6.8)*	*(d, 5.5)*	*(d, 5.5)*	*m*	*(d, 5.9)*	*(d, 5.8)*	*(d, 5.8)*	*s*	*s*	*m*
31	1.94	3.54	2.99	6.33	5.12	3.26	3.63	5.26	6.56	4.49	4.64	6.7-7.4
	s	*(d, 6.7)*	*(d, 6.7)*	*(d, 6.5)*	*(d, 6.5)*	*m*	*(d, 6.8)*	*(d, 6.8)*	*(d, 6.8)*	*s*	*s*	*m*
32	1.94	3.52	3.01	6.31	5.11	3.24	3.62	5.24	6.56	4.48	4.64	6.8-7.2
	s	*(d, 5.8)*	*(d, 5.8)*	*(d, 5.7)*	*(d, 5.7)*	*m*	*(d, 6.8)*	*(d, 5.6)*	*(d, 5.6)*	*s*	*s*	*m*
33	1.93	3.54	3.01	6.31	5.09	3.25	3.62	5.24	6.55	4.47	4.63	6.9-7.3
	s	*(d, 6.7)*	*m*	*(d, 6.5)*	*(d, 6.5)*	*(d, 6.9)*	*(d, 6.9)*	*(d, 6.7)*	*(d, 6.7)*	*s*	*s*	*m*

Chemical shifts were established based on the solvent peak ($CDCl_3$ at 7.26 ppm).
Coupling constants (Hz) are of adjacent aromatic protons unless otherwise indicated.

Table 8: ^{13}C NMR of the Polymetallic Series Following Cyanide Addition.

Adduct	28	29	30	31	32	33
CN(A)	116.93	116.96	116.34	115.95	116.30	115.91
CN(B)	116.33	116.39	116.38	116.35	116.34	116.27
CH_3	22.09	22.04	22.07	22.02	20.51	20.52
Cp(A)	77.37	77.35	77.38	77.36	77.38	77.41
Cp(B)	78.18	78.17	78.19	78.18	78.19	78.16
C(1)	28.69	28.61	28.88	28.34	28.64	29.71
C(2)	26.06	26.00	25.21	26.06	25.98	25.95
C(3)	96.63	96.63	96.60	96.62	97.21	96.86
C(4)	83.74	83.72	83.68	83.59	83.57	83.58
C(5)	78.94	78.39	78.27	78.40	78.51	78.38
C(6)	29.55	28.88	28.55	28.76	28.57	28.74
C(7)	96.63	96.63	96.60	96.62	97.21	96.86
C(8)	26.00	25.99	26.08	26.04	26.12	26.39
C(9)	29.88	29.87	29.87	36.43	29.90	29.95
C(10)	33.03	29.65	29.78	29.86	29.78	29.83
C(11)	80.12	78.93	78.96	78.96	78.98	78.99
C(12)	83.67	83.64	83.74	83.72	83.72	83.74
C(13)	123.35	122.67	123.35	122.86	123.78	122.52
C(14)	130.27	130.27	130.18	130.13	130.21	130.76
C(15)	129.95	129.01	129.80	129.67	128.75	128.80
C(16)	123.35	122.67	123.35	122.86	123.78	122.52
C(17)	119.26	120.12	119.79	119.87	119.81	119.73
C(18)	119.58	119.59	119.73	119.28	119.23	119.24

Chemical shifts from $CDCl_3$ at 77.00 ppm.

Overall, the meta position is influenced by both the etheric and methyl substituents. Infrared spectroscopy was used to confirm the presence of the cyano groups. The ν_{CN} for all cyano adducts studied were in the range of 2228-2229 cm^{-1}.

2.2.3 Substituted 1,4-bis(η^6-arylsulfoxide-η^5-cyclopentadienyliron) alkyl dihexafluorophosphate

Once selectivity of addition was established with the etheric complexes we were interested in discovering other systems that would exhibit these selective properties. Previous studies with cyanide addition reactions indicate selective ortho addition to monoiron complexes with one electron withdrawing group on the ring [29]. Our group has recently found an innovative approach to the synthesis of aromatic and aliphatic sulfides and their corresponding sulfones [77]. If addition is selective to the bimetallic series of these aliphatic sulfones, then it may also be applied to larger organic and polymeric systems. Scheme 15 illustrates the synthesis of a series of substituted aliphatic diiron complexes with sulfone linkages. The reaction of these complexes is depicted in Scheme 26.

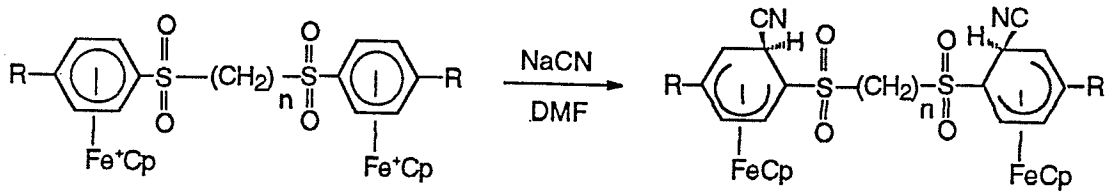

	R	n
34	Me,	2
35	Me,	4
36	Me,	6
37	Cl,	2
38	Cl,	4
39	Cl,	6
40	SPh	2
41	SPh	4
42	SPh	6

	R	n
43	Me,	2
44	Me,	4
45	Me,	6
46	Cl,	2
47	Cl,	4
48	Cl,	6
49	SPh	2
50	SPh	4
51	SPh	6

Scheme 26

As can be seen, the adducts formed are selectively ortho to the sulfone and meta to the methyl group. Sulfonyl substituents are extremely strong withdrawing groups, thus site activation is influenced primarily by this group. Cyanide is as selective with these complexes regardless of the nature of the second substituent. Complexes (**34- 36**) have identical arene rings and differ only in the length of the aliphatic chain; we see the same ortho adduct form in all cases. Therefore the length of the chain does not influence site activation, and the arene rings act independently. The position of attack is as expected, due to the inductive effect of the sulfonyl group. NMR assignments were based on the comparison of the addition products to those with etheric bridges. The most aromatic proton displays a downfield shift when adjacent to the sulfonyl group; we would also see a downfield shift of the endo proton if it is adjacent to the sulfonyl substituent. The chemical shift of the most aromatic proton did not differ greatly but the endo proton demonstrated a downfield shift from that of the etheric adducts from 3.5 ppm to 3.8 ppm; therefore, the site of nucleophilic

attack was ortho to the sulfonyl group. These results were compared to previous studies, and in fact a correlation was found [29]. A spectral example of the adduct (**45**) is listed in figures 24-25. ^{1}H and ^{13}C NMR of these products (**43-45**) was given in Tables 9 and 10.

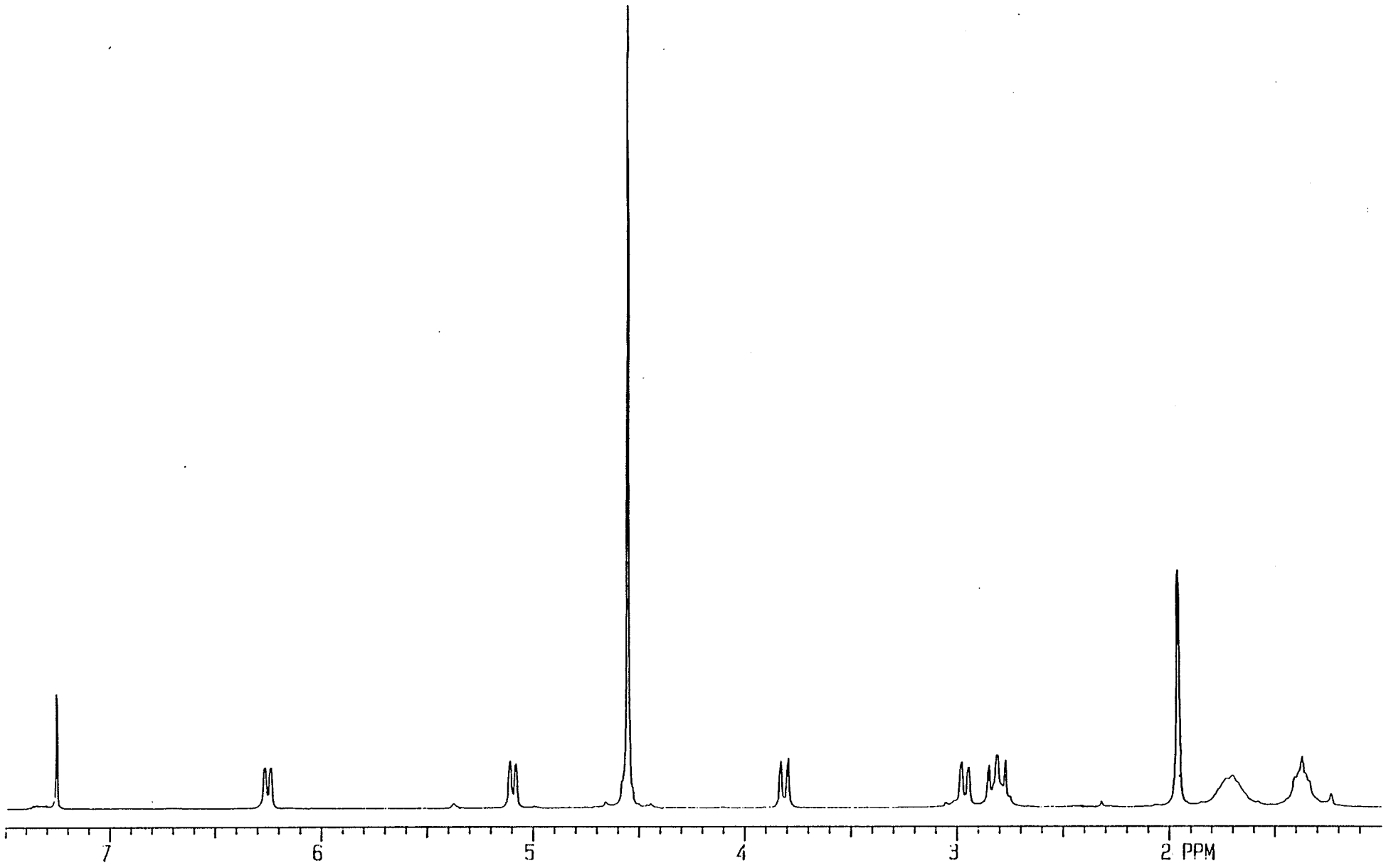

Figure 24: ^{1}H NMR of adduct (45).

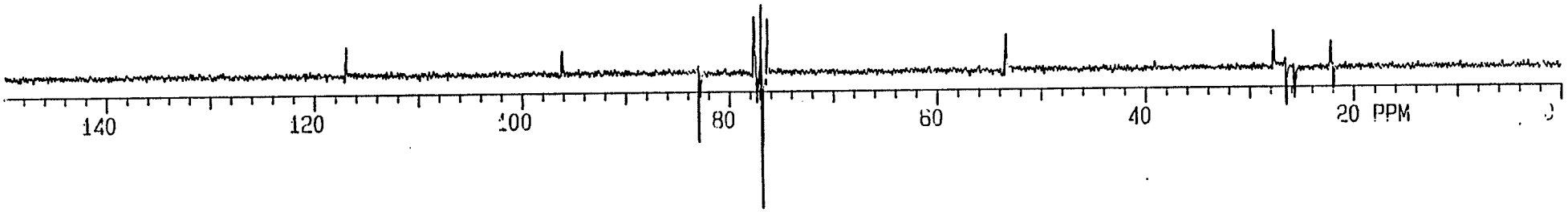

Figure 25: ^{13}C NMR of adduct (45).

Table 9: ^{1}H NMR of Bimetallic Complexes Containing Electron-Withdrawing Groups Following Cyanide Addition.

Adduct	CH_3	CH_2	H(1)	H(3)	H(4)	H(6)	Cp	ArH
43	1.98	2.83	3.84	5.13	6.25	3.00	4.56	--------
	s	*m*	*(d, 6.1)*	*(d, 5.5)*	*(d, 5.3)*	*(d, 6.0)*	*s*	
44	1.94	1.85, 2.84	3.80	5.09	6.24	2.95	4.53	--------
	s	*m*	*(d, 5.8)*	*(d, 5.5)*	*(d, 5.5)*	*(d, 5.9)*	*s*	
45	1.98	1.43, 1.72, 2.89	3.82	5.11	6.26	2.98	4.57	--------
	s	*m, m, (t, 7.1)*	*(d, 5.7)*	*(d, 5.5)*	*(d, 5.5)*	*(d, 5.8)*	*s*	
46	--------	2.85	3.91	5.20	6.62	3.42	4.72	--------
		(t, 7.2)	*(d, 5.9)*	*(d, 5.5)*	*(d, 5.5)*	*(d, 6.0)*		
47	--------	2.86, 1.86	3.92	5.21	6.63	3.42	4.72	--------
		(t, 7.0), m	*m*	*(d, 5.5)*	*(d, 5.6)*	*(d, 5.9)*	*s*	
48	--------	2.82, 1.71, 1.38	3.92	5.18	6.63	3.42	4.73	--------
		m	*(d, 6.0)*	*(d, 5.5)*	*(d, 5.5)*	*(d, 6.1)*	*s*	
49	--------	3.18	3.87	5.21	6.57	3.24	4.75	7.21-7.42
		m	*(d, 6.0)*	*(d, 5.4)*	*(d, 5.4)*	*(d, 6.1)*	*s*	*m*
50	--------	2.94, 1.92	3.89	5.21	6.56	3.33	4.74	7.30-7.40
		m	*(d, 6.1)*	*(d, 5.6)*	*(d, 5.6)*	*(d, 6.1)*	*s*	*m*
51	--------	1.41, 1.68, 2.85	3.87	5.19	6.59	3.28	4.74	7.25-7.44
		m	*(d, 6.0)*	*(d, 5.7)*	*(d, 5.7)*	*(d, 6.1)*	*s*	*m*

Chemical Shifts were established based on the solvent peak ($CDCl_3$ at 7.26 ppm).

Table 10: ^{13}C of the adducts 51-59 following cyanide addition to complexes which contain electron withdrawing groups.

Complex	43	44	45	46	47	48	49	50	51
CH_3	22.38	21.35	22.47	-------	-------	-------	-------	-------	-------
CH_2	52.35	52.77, 21.85	53.95, 28.26, 22.79	53.64	52.77, 21.26	53.32, 27.44, 22.04	54.21	52.94, 21.47	53.45, 28.31, 21.98
C(1)	28.94	26.37	27.00	27.78	27.80	27.82	28.05	27.63	28.14
C(2)	41.21	38.96	39.87	39.78	39.94	40.04	40.21	39.97	39.62
C(3)	79.28	77.28	77.89	77.15	77.10	77.09	78.34	78.97	78.60
C(4)	84.06	82.92	83.41	83.22	83.01	82.89	87.33	86.80	87.33
C(5)	96.96	96.25	96.69	104.6	104.6	104.5	95.47	94.66	95.15
C(6)	26.30	25.66	26.20	25.71	25.66	25.61	28.09	29.60	30.13
CN	117.3	117.0	117.6	116.1	116.1	116.1	116.6	116.2	116.7
Cp	77.70	76.87	77.39	79.05	79.09	79.04	79.10	78.50	79.02
ArH	-------	-------	-------	-------	-------	-------	131.2, 129.8, 127.4, 137.7	129.3, 128.8, 128.7, 137.2	130.5, 129.6, 129.2, 137.8

Chemical Shifts were established based on the solvent (7.26 ppm $CDCl_3$).

Complexes (**37-39**) contain a terminal chloro group, whose influence on the charge distribution of the arene with respect to the sulfonyl group was unknown. When these complexes were reacted with NaCN only one product was obtained; the ortho adduct formed (Scheme 26). There was a downfield shift of the most aromatic protons due to the presence of the chloro group. Figures 26-27 present the proton and carbon spectra of the adduct (**48**). The detailed analysis for adducts (**46-48**) are listed in Tables 9 and 10.

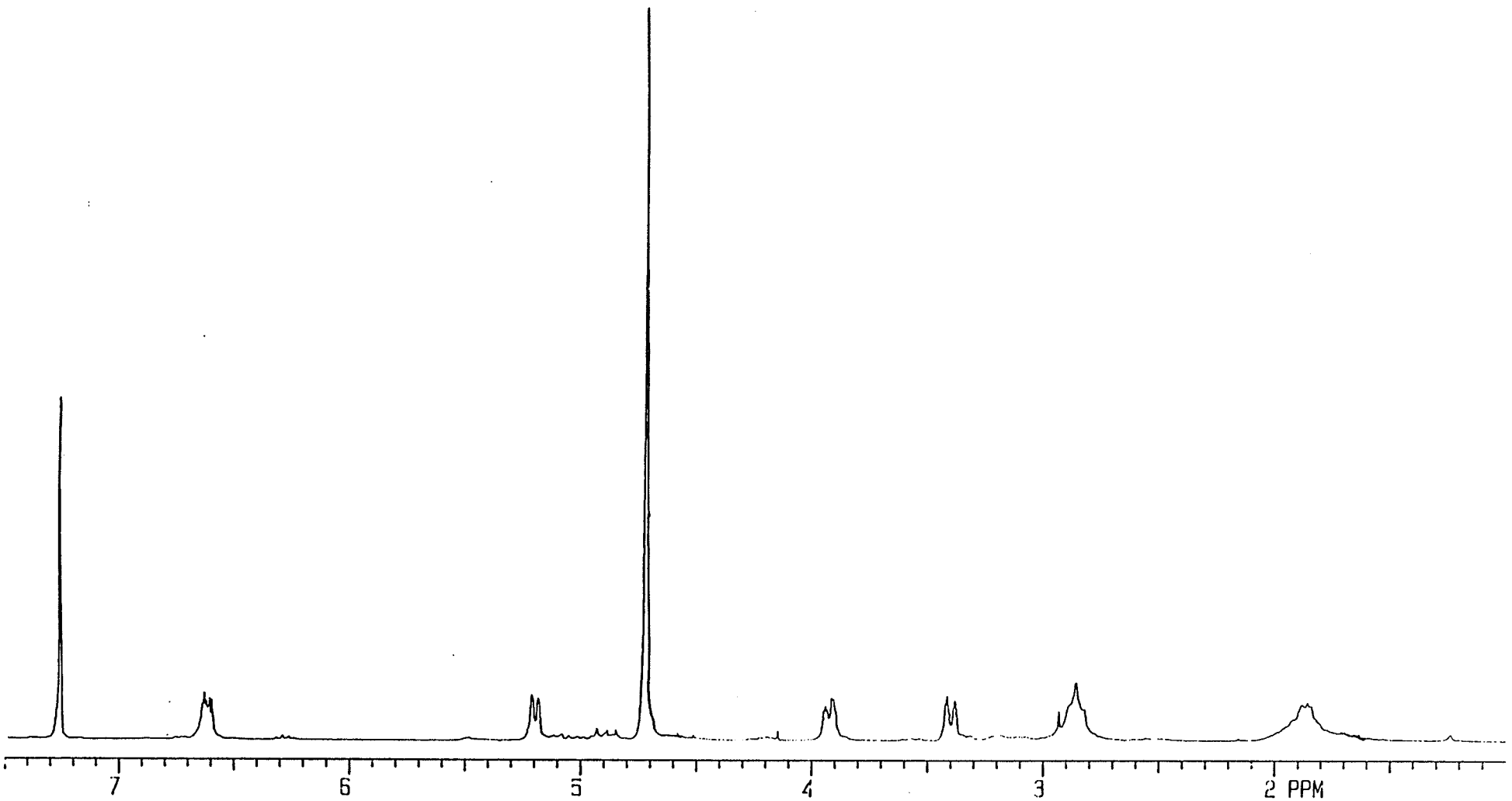

Figure 26: ^{1}H NMR

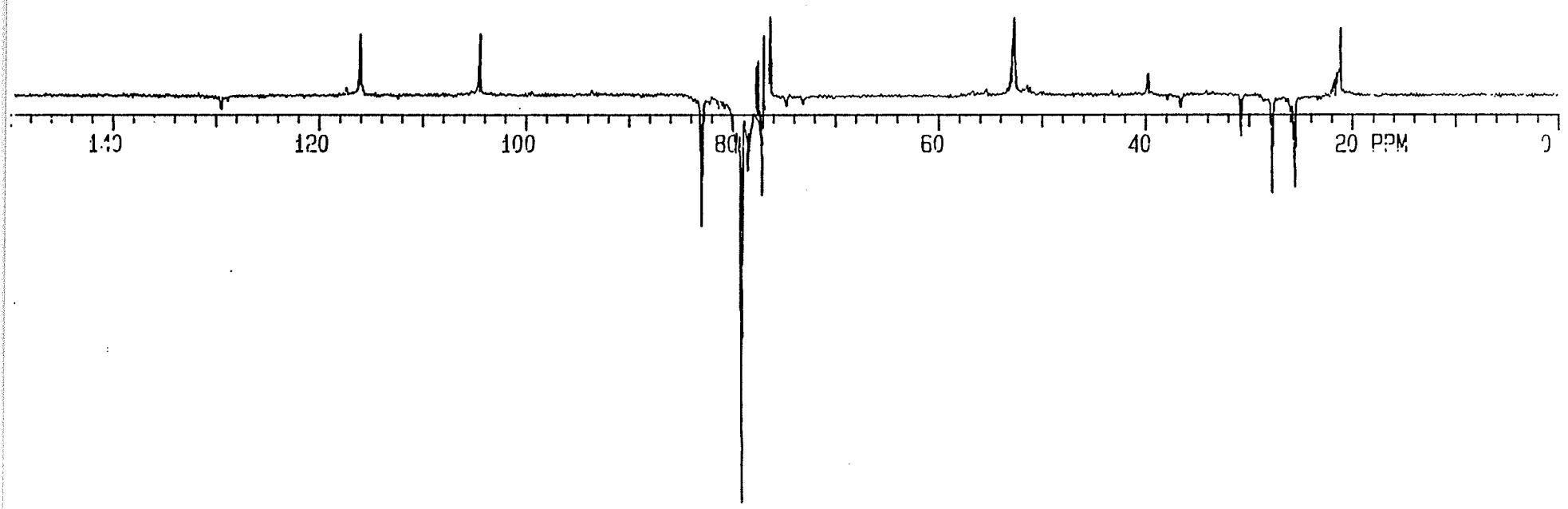

109

Figure 27: ^{13}C NMR of adduct (48).

The final counter substituent employed was a thiophenol group in the para position to the sulfonyl bridge (Scheme 26). Complexes (**40-42**) are prepared through the substitution of a terminal chloro group (as in complexes **37-39**) by thiophenol in the presence of a weak base [80]. Once prepared, they underwent reaction with NaCN yielding a single product with addition ortho to the sulfonyl group (**49-51**). The thioether group directs meta, as we have seen before, and the sulfonyl group directs ortho; thus these two groups complement each other. This result can be confirmed by the significant downfield shift of the aromatic protons due to the presence of the thiophenol group. The size of the aliphatic chain did not seem to cause any change in the site of addition. Figures 28-29 illustrate the ^{1}H and ^{13}C NMR of the adduct (**50**). Full spectral data is listed in Tables 9 and 10.

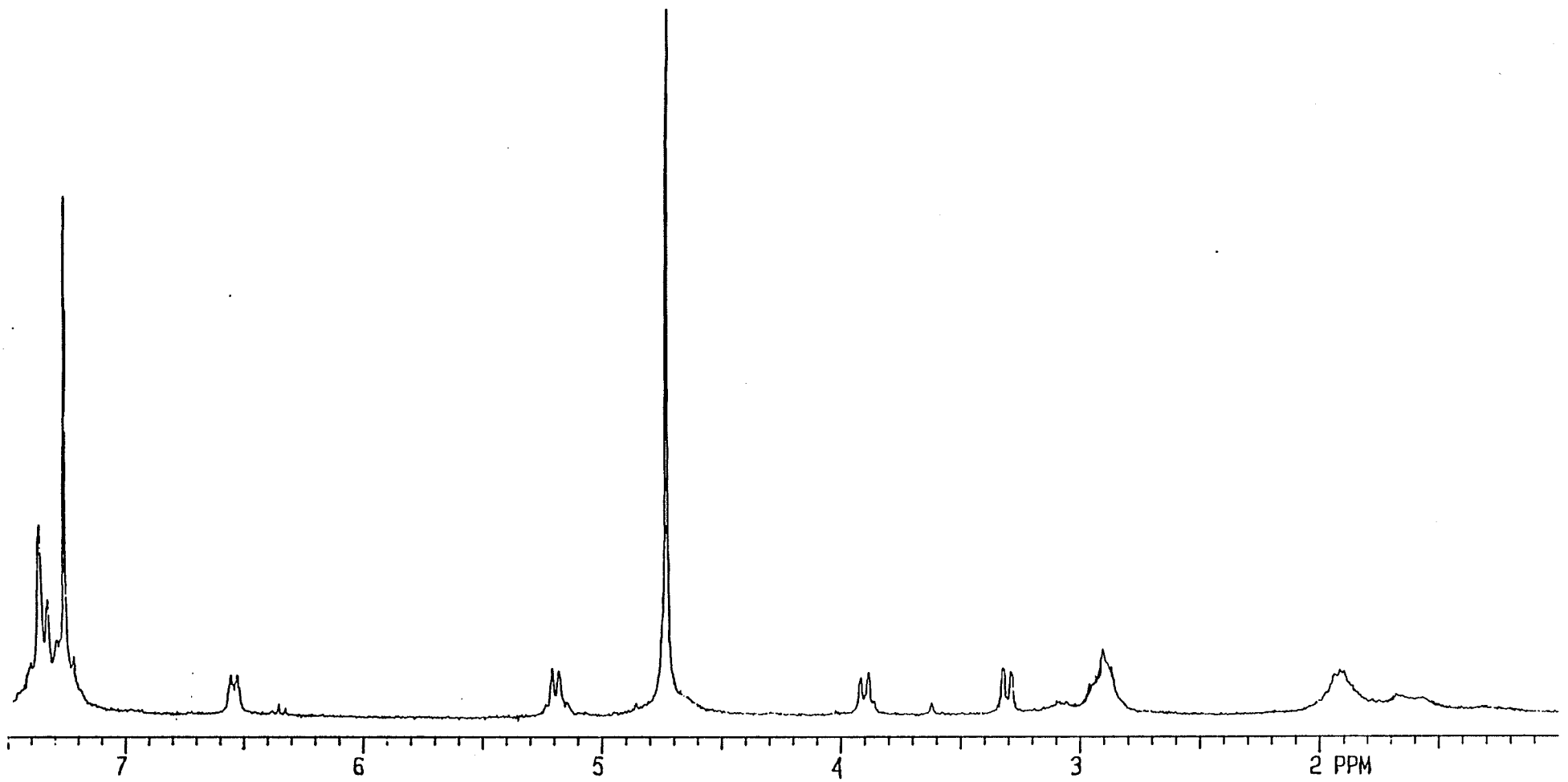
7
6
5
4
3
2 PPM

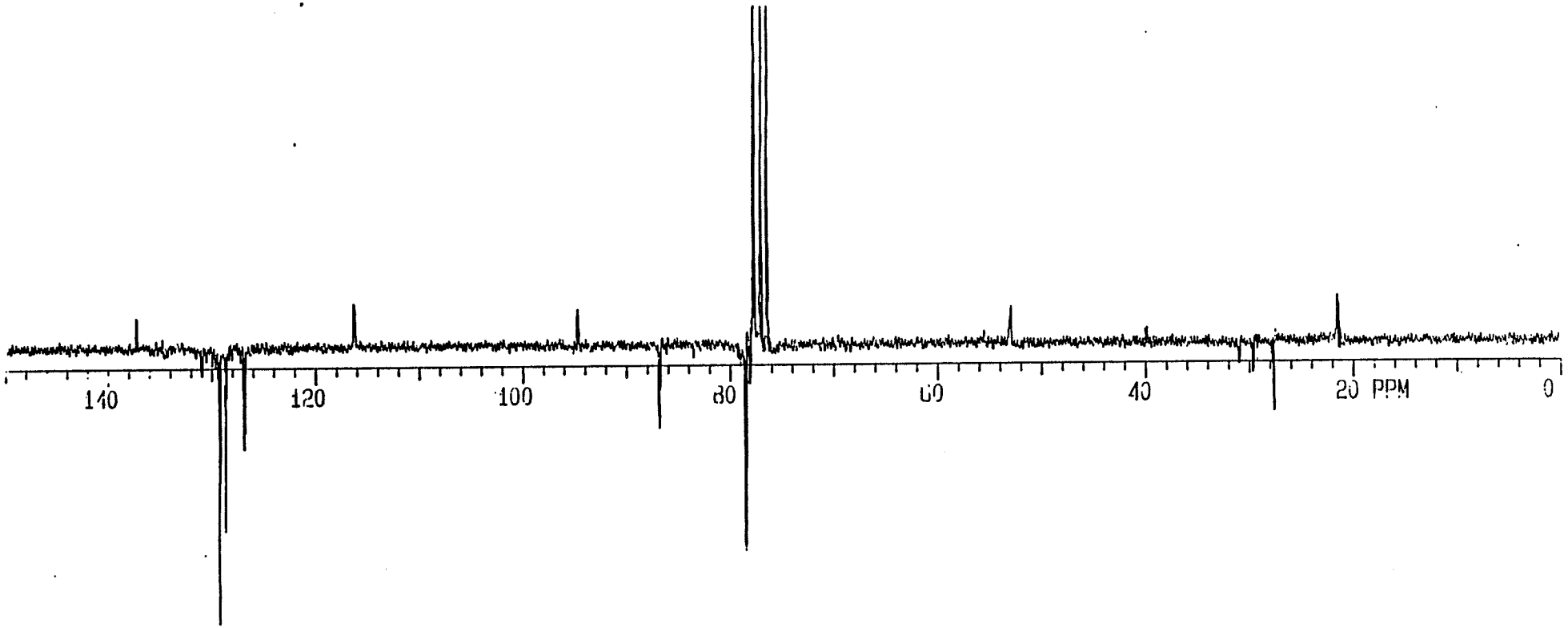

Figure 29: ^{13}C NMR of adduct (50).

The final experiment that was completed with cyanide addition is the reaction with complexes (**52**) and (**53**) as shown in Scheme 27 respectively.

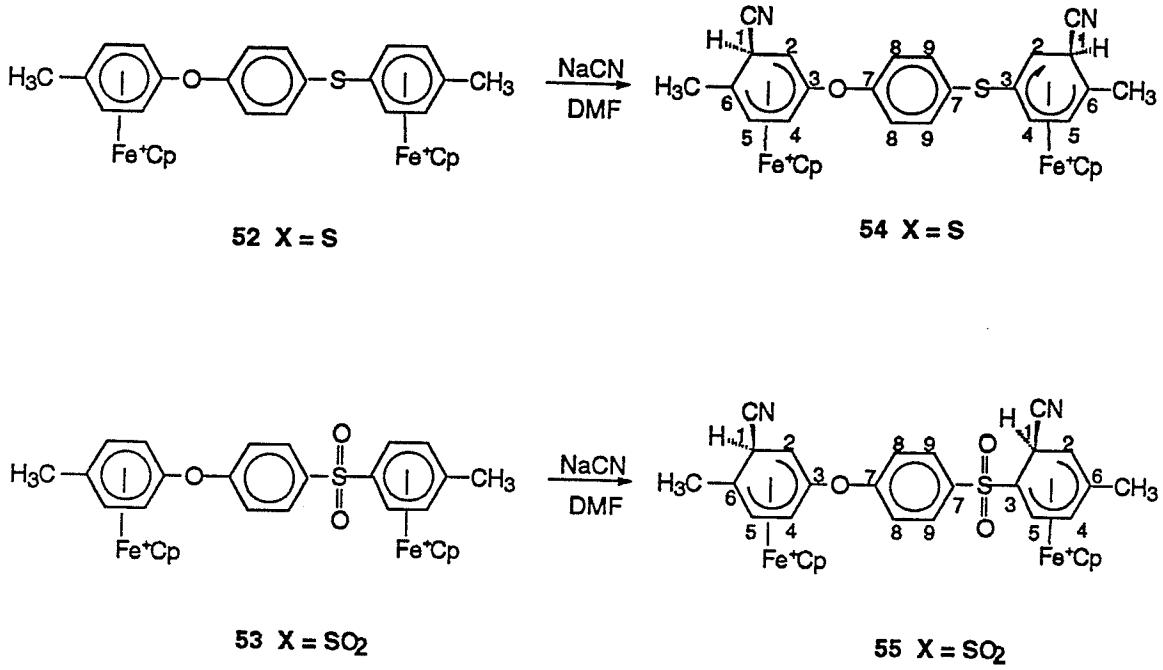

Scheme 27

It seems that the cyanide anion was selective with respect to each individual ring. The adduct (**55**) consisted of addition meta to the oxygen link, as well as ortho to the sulfonyl substituent. There is no possibility that addition occurred contrary to this or we would see a variety of peaks with different chemical shifts. Adduct (**54**) follows meta addition on both rings, which was expected based on the directing influence of the sulfur as established in the hydride addition experiment. Table 11 lists the spectral data of the adducts (**54 and 55**). Figures 30-31 represent the ^{1}H and ^{13}C NMR spectra.

Table 11: ^{1}H and ^{13}C NMR data for the adducts formed in 62 and 63.

Adduct	CH_3	H(1-endo)	H(2)	H(4)	H(5)	ArH	Cp
54	1.93	3.54	3.03	6.11	5.12	6.95-7.15	4.48
	s	*(d, 5.9)*	*(d, 5.8)*	*(d, 5.1)*	*(d, 5.1)*	*m*	*s*
55	1.93	3.53	3.02	6.32	5.19	6.85-7.19	4.47
	s	*(d, 6.5)*	*(d, 6.4)*	*(d, 5.2)*	*(d, 5.4)*	*m*	*s*

Complex	CH_3	C(1)	C(2)	C(3)	C(4)	C(5)	C(6)	C(7)	C(8)	C(9)	CN	Cp
54	22.26	29.17	26.54	123.87	84.25	79.48	97.14	123.87	120.57, 118.38	131.00, 129.98	117.48	77.89
55	22.08	28.63	26.00	123.35	83.73	78.97	29.75	123.35	129.64, 128.70	121.47, 120.38	116.96	77.37

All samples run in $CDCl_3$ (ppm from solvent peak at 7.26 and 77.00 ppm).

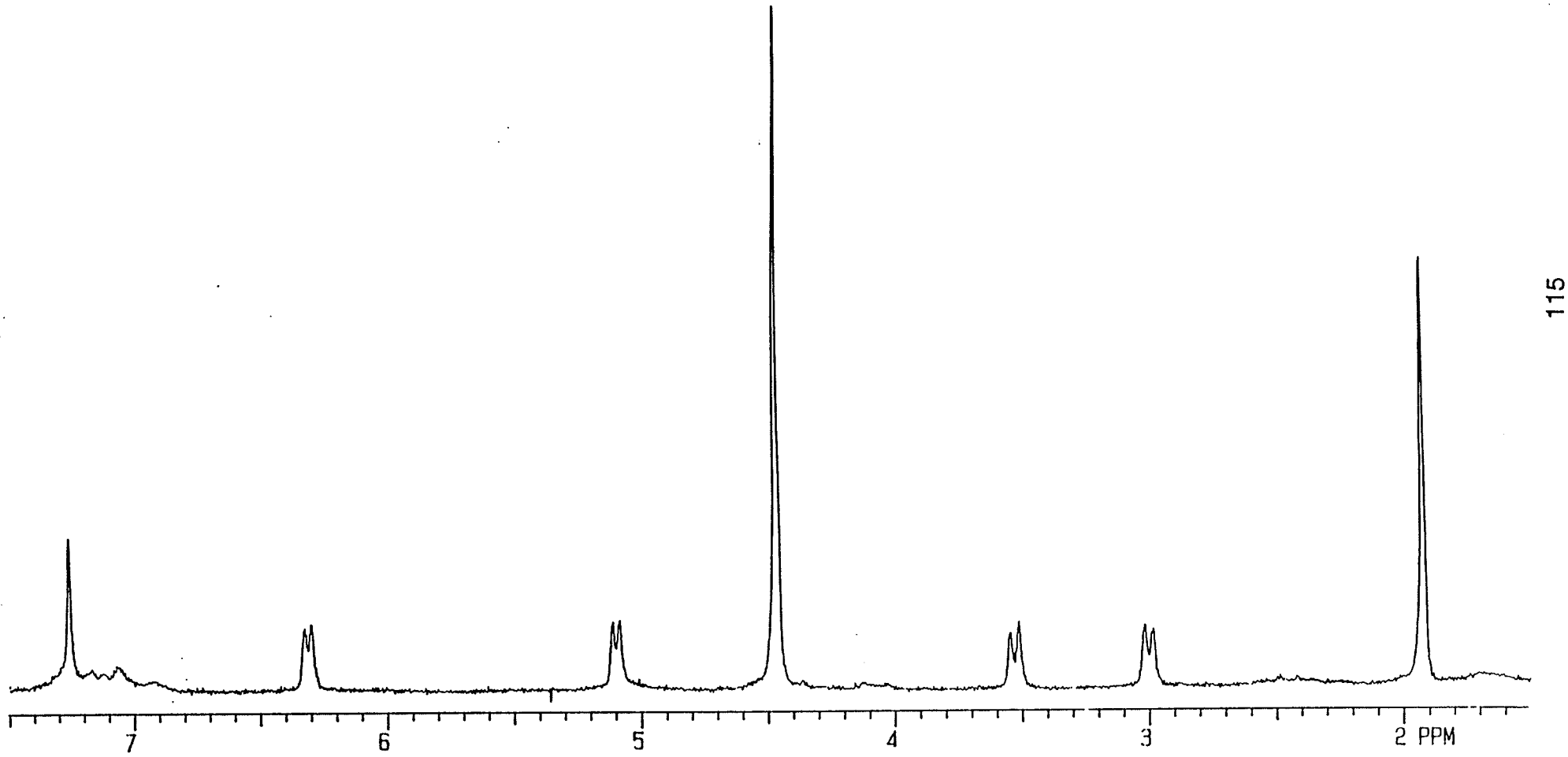

Figure 30: ^{1}H NMR of adduct (54).

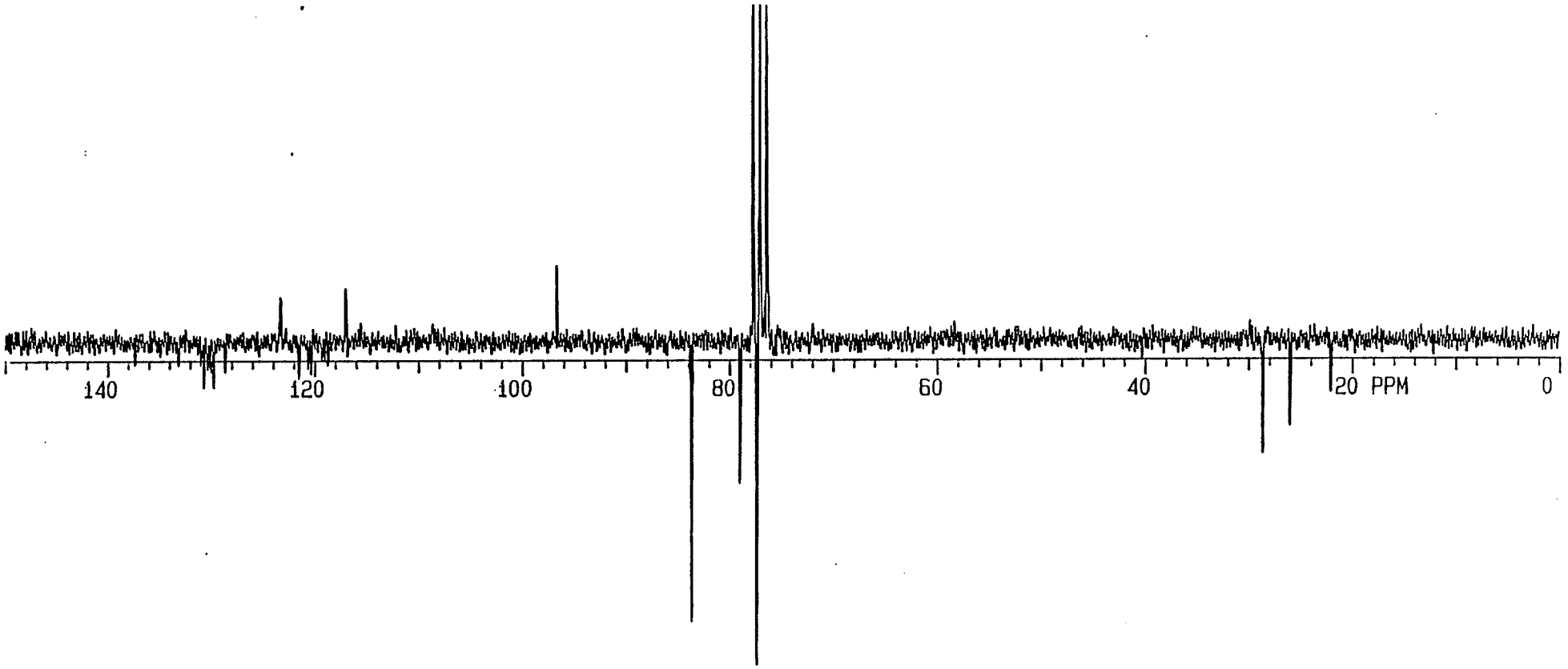

Figure 31: ^{13}C NMR of adduct (54).

2.2.4 Demetallation reactions of cyanide adducts

The free functionalized organic product can be obtained through a simple oxidative demetallation step using 2,3-dichloro-5,6-dicyano-1,4-benzoquinone (DDQ). The adducts (**17, 19, 28-33**) underwent reaction in acetonitrile with DDQ for 30 minutes leading to the free organic compounds (**34-41**) in 75% yield (Scheme 28 and 29).

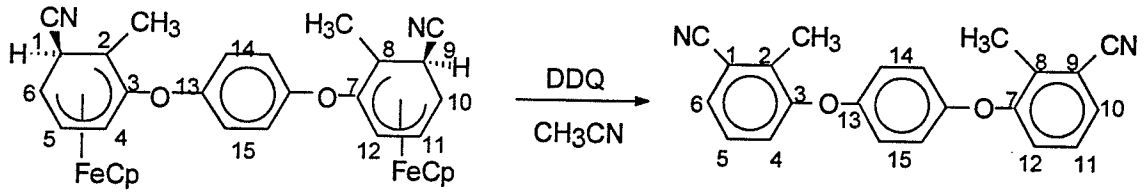

19 **56**

Scheme 28

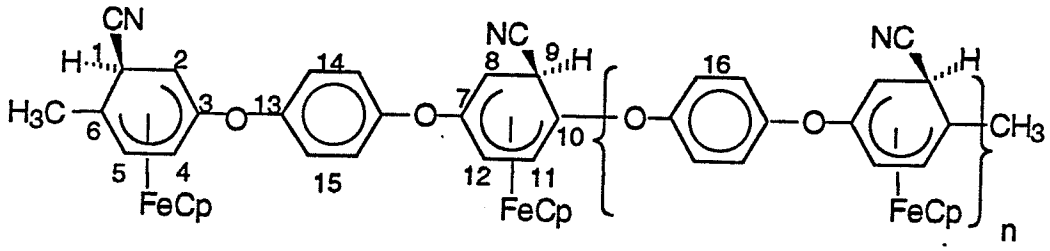

Complex	n
17	0
28	1
29	2
30	3
31	4
32	5
33	6

DDQ
CH_3CN

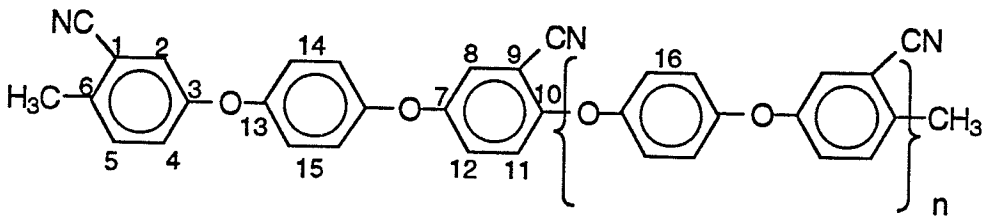

Complex	n
57	0
58	1
59	2
60	3
61	4
62	5
63	6

Scheme 29

Figures 32-36 illustrate the ^{1}H and ^{13}C NMR for products (**56-59**).

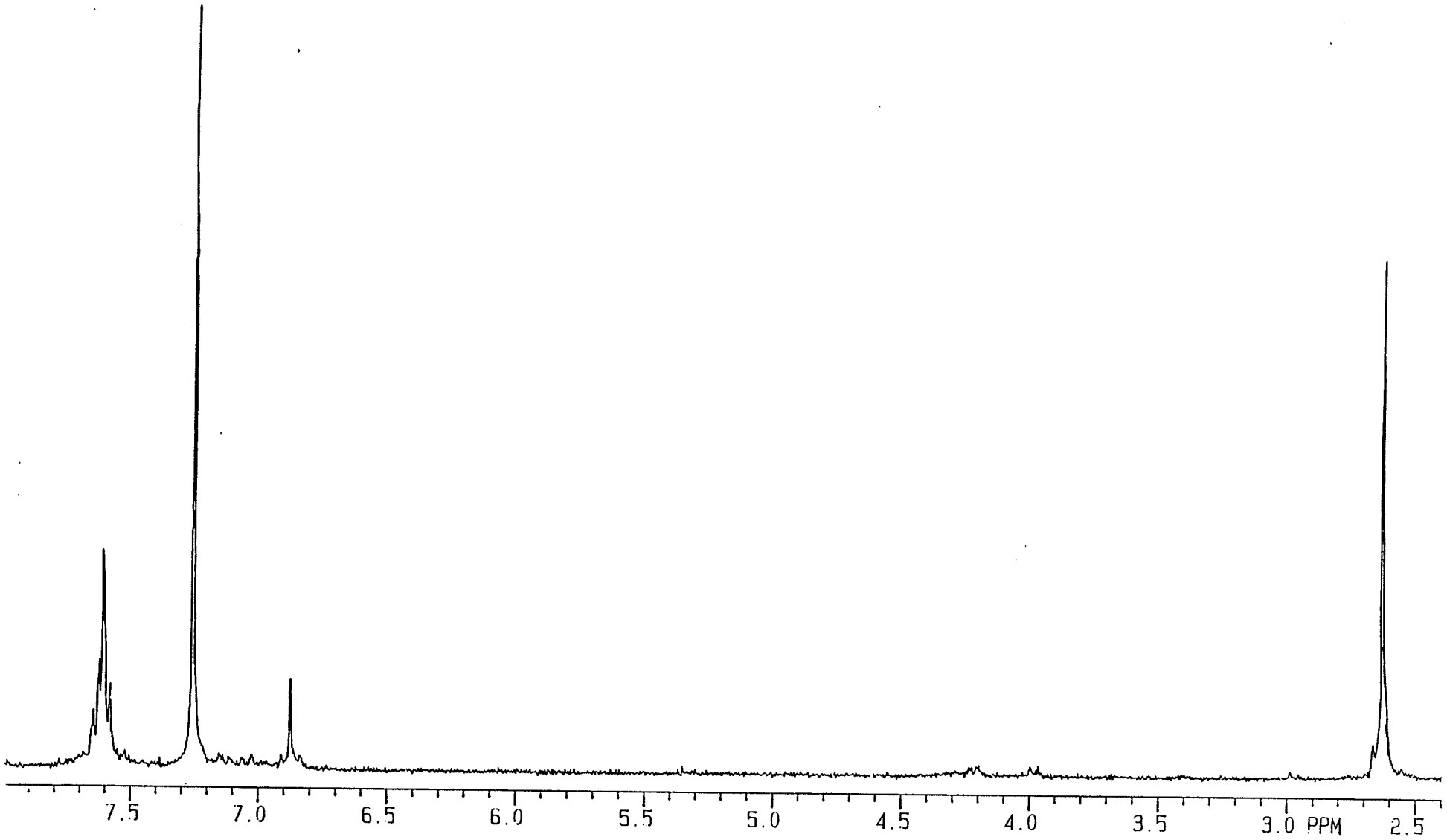

Figure 32: ^{1}H NMR of adduct (56).

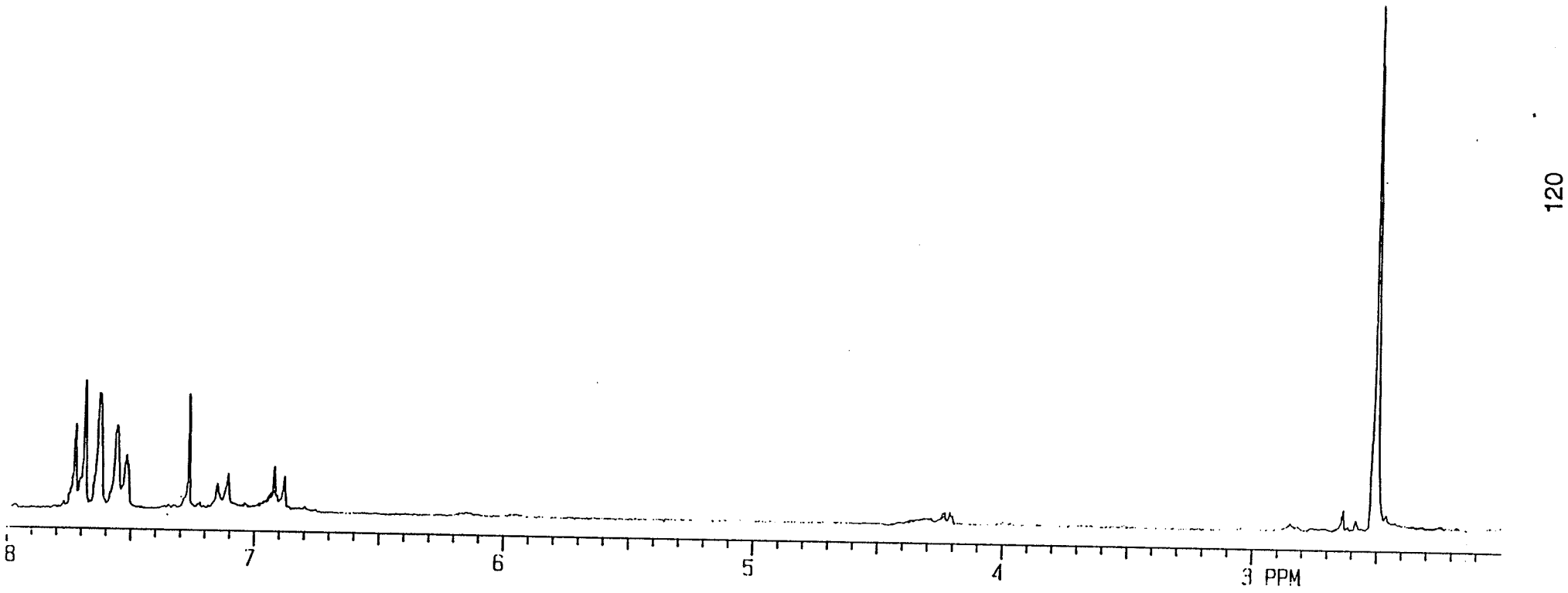

Figure 33: ^{1}H NMR of adduct (57).

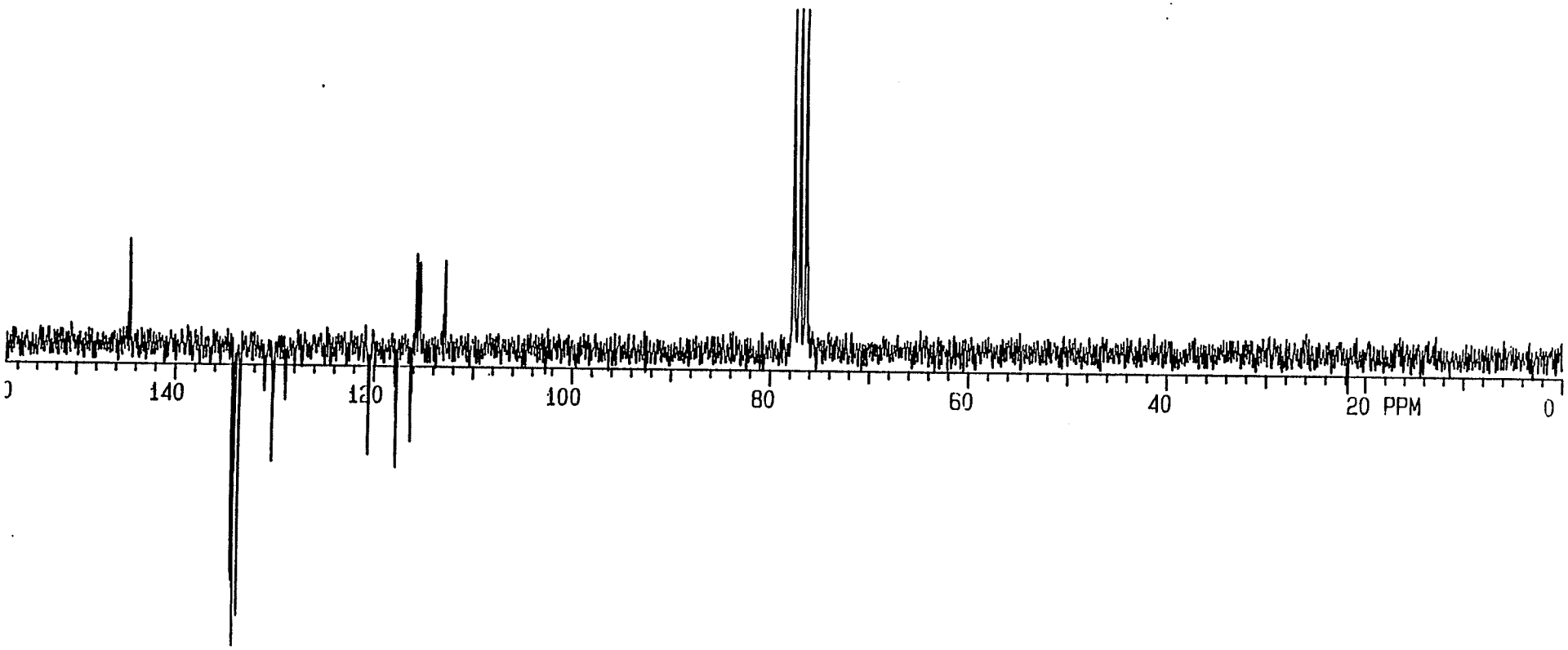

Figure 34: ^{13}C NMR of adduct (57).

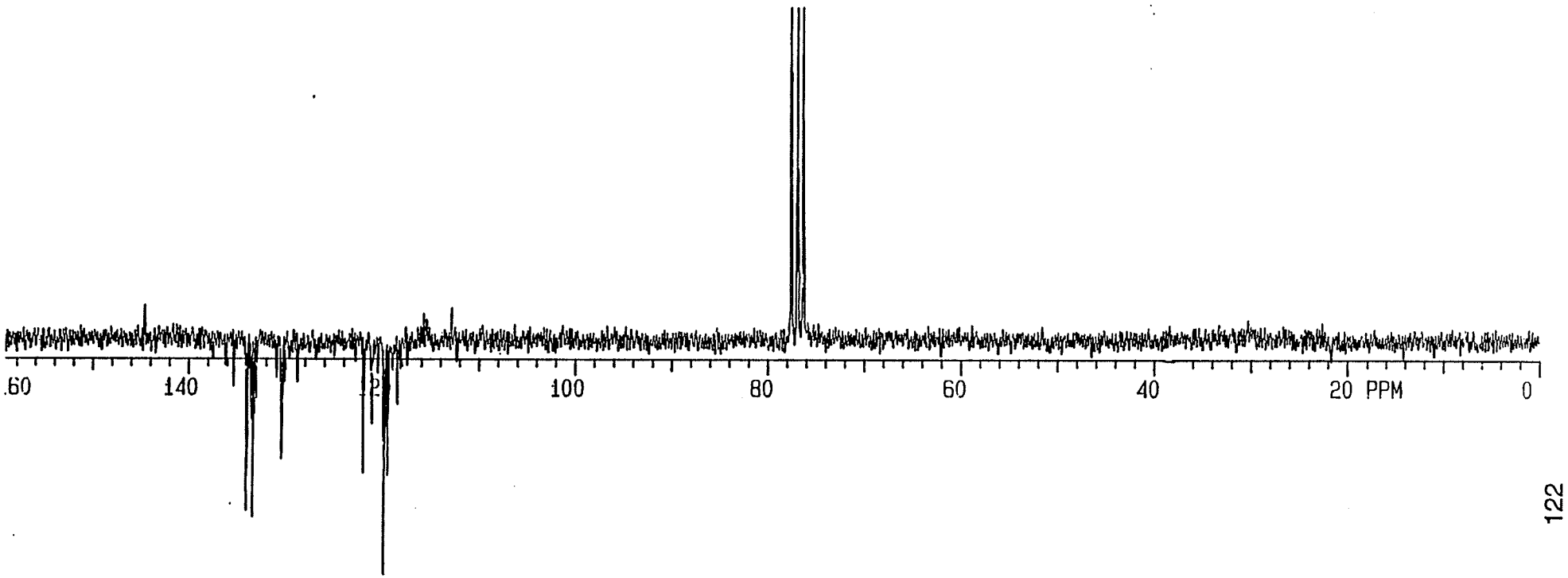

Figure 35: ^{13}C NMR of adduct (58).

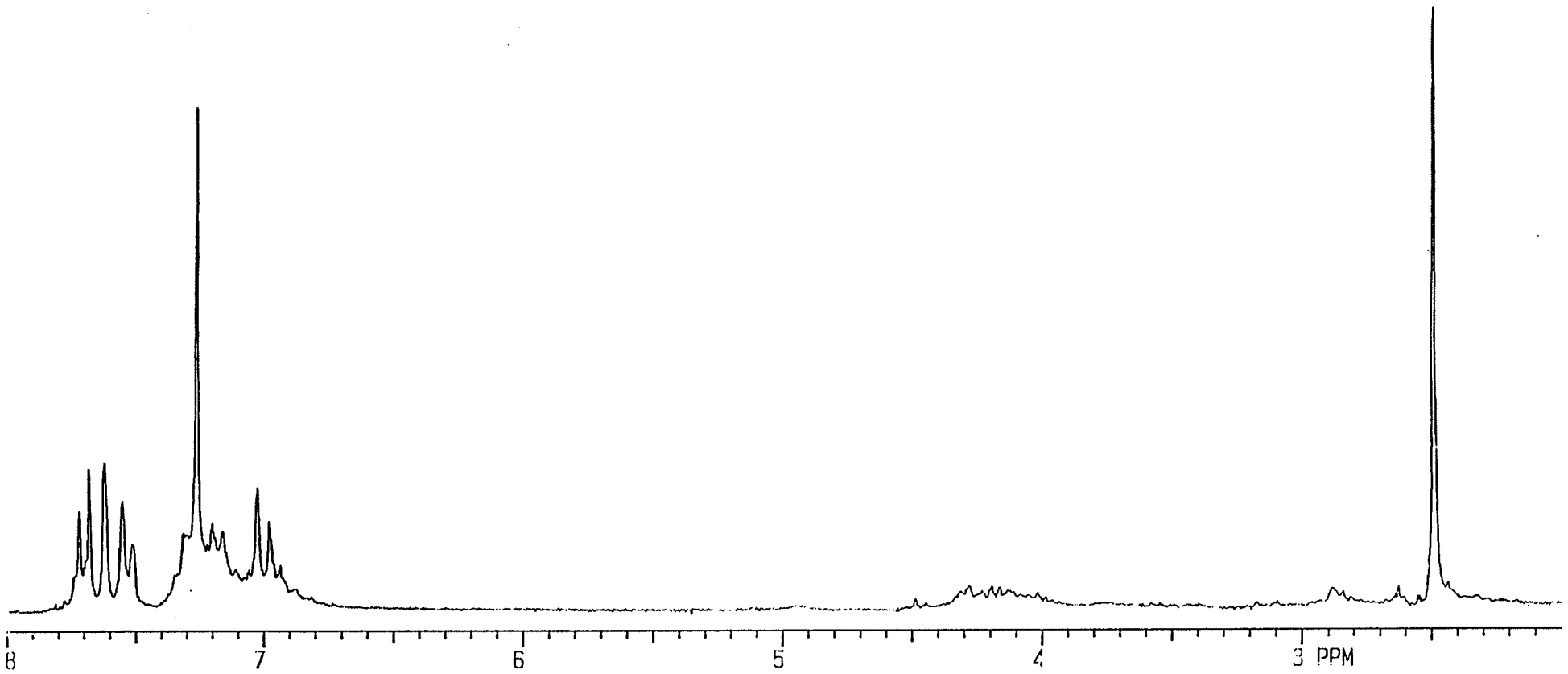

Figure 36: ^{1}H NMR of adduct (59).

The chemical shift trend found in the polyiron series was approx. 1.96 ppm (^{13}C: 21 ppm). The CH on the aromatic rings containing CN are at slightly higher field than the linking aromatic rings in the region of 7-8 ppm. The corresponding carbon peaks appear at approx. 117-130 ppm for the rings containing CN and approx. 133-135 ppm for the bridging aromatic ring. As the size of the iron complex increases, we see a proportional increase in these areas on the NMR spectra. Quaternary carbons appear approx.144 ppm for the C-O carbon, CN at approx. 116 ppm, C-CN at ca. 115 ppm, and finally at 112 ppm for the C-Me carbon peak. Detailed NMR data was listed in Tables 12 and 13. Analytical data for these compounds (**57**) and (**62**) are listed in Table 14.

Table 12: ^{1}H NMR of the Functionalized Organic Compound in the Polymeric Series.

Adduct	CH_3	H(2)	H(4)	H(5)	H(6)	H(8)	H(9)	H(11)	H(12)	ArH
52	2.53	------	7.59	7.62	7.63	6.89	6.87	------	------	------
	s		*m*	*m*	*m*	*m*	*m*			
53	2.50	7.63	7.71	7.54	------	7.11	6.90	------	------	------
	s	*s*	*(d, 7.7)*	*(d, 7.7)*		*(d, 8.6)*	*(d, 8.6)*			
54	2.33	7.58	7.70	7.52	------	7.62	------	7.55	7.73	6.81-7.03
	s	*s*	*(d, 8.2)*	*(d, 8.2)*		*s*		*(d, 8.9)*	*(d, 8.9)*	*m*
55	2.50	7.62	7.70	7.53	------	7.62	------	7.53	7.70	7.01-7.23
	s	*s*	*(d, 9.1)*	*(d, 9.1)*		*s*		*(d, 8.5)*	*(d, 8.6)*	*m*
56	2.37	7.69	7.74	7.58	------	7.69	------	7.59	7.74	6.84-7.25
	s	*s*	*m*	*m*		*s*		*m*	*m*	*m*
57	2.49	7.69	7.78	7.54	------	7.64	------	7.72	7.82	6.86-7.20
	s	*s*	*m*	*m*		*s*		*m*	*m*	*m*
58	2.49	7.64	7.76	7.54	------	7.63	------	7.57	7.73	6.77-7.13
	s	*s*	*(d, 8.1)*	*(d, 8.1)*		*s*		*(d, 8.2)*	*(d, 8.1)*	*m*
59	2.50	7.75	7.76	7.72	------	7.63	------	7.55	7.68	6.85-7.36
	s	*s*	*(d, 8.2)*	*(d, 8.1)*		*s*		*(d, 8.4)*	*(d, 8.3)*	*m*

Chemical Shifts were established with reference to the solvent peak ($CDCl_3$ at 7.26 ppm).

Table 13: ^{13}C NMR of the Functionalied Organic Compound.

Complex	52	53	54	55	56	57	58	59
CN	116.15	115.81	115.82, 115.50	115.53, 115.85	115.89, 115.47	115.11, 115.23	115.23, 115.40	115.77, 116.06
CH3	21.03	21.66	21.58	21.83	21.32	21.70	21.73	21.69
C(1)	115.95	115.52	115.35	115.38	115.28	114.88	115.22	115.26
C(2)	112.30	130.04	130.48	128.79	130.90	130.90	130.53	130.50
C(3)	144.17	144.67	144.63	144.63	144.40	144.97	144.31	145.05
C(4)	119.36	120.46	121.93	121.92	122.06	122.08	121.90	121.17
C(5)	118.38	117.74	119.77	119.75	119.91	119.83	119.42	119.33
C(6)	127.17	112.90	113.00	112.97	112.56	112.18	112.57	112.20
C(7)	144.17	144.67	144.63	144.63	144.40	144.97	144.31	145.05
C(8)	112.30	130.04	130.22	128.93	130.18	129.95	130.53	130.92
C(9)	115.95	115.52	115.42	115.44	115.46	114.88	115.30	115.26
C(10)	127.17	112.90	144.63	144.63	144.40	144.97	144.31	145.05
C(11)	118.38	117.74	119.42	119.40	120.34	120.37	119.82	119.79
C(12)	119.36	120.46	121.11	121.07	121.93	122.04	122.71	122.77
C(13)	144.14	144.67	144.63	144.63	144.40	144.97	144.31	145.05
C(14)	129.68	133.88	133.88	133.85	134.15	134.12	134.02	133.90
C(15)	130.57	133.38	133.40	133.38	134.08	134.04	133.87	133.43
C(16)	------	------	134.08	134.06	135.38	134.26	134.23	134.11

Chemical Shifts from $CDCl_3$ at 77.00 ppm.

Table 14: Yields and IR data.

Complex	Yield(%)	CN υ (cm^{-1})
6	76	------
7	72	------
8	65	------
9	88	------
10	85	------
12	88	------
14	92	2199
16	85	2228
17	72	2229
19	69	2228
20	65	2230
21	71	2228
28	68	2228
29	73	2228
30	67	2229
31	81	2229
32	73	2229
33	79	2228
43	82	2240
44	80	2239
45	83	2245
46	78	2245
47	74	2250
48	81	2245
49	83	2245
50	77	2250
51	79	2245
54	74	2245
55	76	2250
56	81	2236
57	82	2234
58	70	2240
59	78	2235
60	75	2234
61	79	2234
62	76	2232
63	68	2230

3.0 Conclusions

In conclusion, spectral data for the hydride reactions of mono- and di-iron arene complexes show that the etheric substituent has a larger overall effect on the charge distribution on the ring in comparison to the methyl substituent(s). The proportions of the isomers for the bimetallic complexes were in agreement with their analogous monoiron species. In contrast, the reactions of cyanide anion with di- and poly-iron arenes were selective, with addition at the meta position to the etheric bridges. The only isomer that gave a mixture of adducts was the bis[(η^6-3-methylphenoxy-η^5-cyclopentadienyl)iron]benzene hexafluorophosphate (**13**). In this case, the addition was ortho and para to the methyl group and ortho to the etheric bridges. Oxidative demetallation proved to be successful, allowing for the liberation of the functionalized nitrile compounds from their corresponding iron moieties. The selectivity of the cyanide addition to the poly-iron system provides a unique route to the functionalization of polyaromatic ethers. The selective cyanide product that was found with the sulfur and sulfonyl bimetallic complexes also proves that this is a useful route in the functionalization of polymeric systems that contain electron withdrawing groups. Finally, the bridging groups, aliphatic or aromatic, do not effect addition, nor do they facilitate communication between the complexed rings.

4.0 Experimental

Measurements

^{1}H and ^{13}C NMR spectra were recorded at 200 and 50 MHz (Gemini 200), respectively, while HH COSY and CH COSY were recorded on a Bruker 500 NMR Spectrometer, with chemical shifts calculated from $CDCl_3$ (7.26 for proton and 77.00 for carbon). Coupling constants were measured in Hz. IR spectra were recorded with an FT-IR Bomem MB102 spectrometer.

Reagents

Starting complexes (**1-5, 11, 13, 15, 18, 22-27, 34-42, 52, and 53**) were prepared by established procedures [10, 67, 70-72]. Sodium borohydride (Alfa), DDQ and sodium cyanide (Aldrich) are commercially available and were used without further purification. All solvents (reagent grade) were used without further purification, with the exception of THF, which was freshly distilled. Silica gel, 60-100 mesh, was used in the column chromatographic purification of the liberated arenes.

Ligand Exchange

The following procedure outlines a general synthesis of the chloroarene complexes. In a 500 ml 3-necked round bottom flask were placed 100 mmol of ferrocene, 200 mmol of aluminum trichloride ($AlCl_3$) and 100 mmol of aluminum powder (Al). To this 60 ml of decalin was added and finally 250 mmol of p-dichlorobenzene or p-chlorotoluene was stirred at

135°C for 5 hours under a nitrogen atmosphere. Once the mixture was cooled to 50°C it was slowly poured into 200 ml of ice water to render the $AlCl_3$ inactive. This mixture was then filtered through sand to remove the Al(s). Washing with petroleum ether (2 x 50 ml) then with diethyl ether (1 x 50 ml) to remove any unreacted ferrocene and excess benzene compound. Aqueous NH_4PF_6 (75 mmol) was added slowly to the aqueous layer inducing a partial precipitation of a green solid. To this solution CH_2Cl_2 was added (3 x 70 ml) and all the product was dissolved. This organic layer was dried over $MgSO_4$ and filtered. The solution was concentrated via rotary evaporation and the product was precipitated with a small amount of diethyl ether. Filtration and washing with diethyl ether yielded the green solid. After drying under vacuum the product was characterized by ^1H and ^{13}C NMR [5-8].

Monoiron Complexes

The formation of the monometallic complexes that contain etheric or thioetheric linkages are described in the following routes [20, 65, 66]: In a 50 ml round bottom flask, a mixture of 1 mmol of the chloroarene complex and 1.2 mmol of phenol were added followed by 2.5 mmol of K_2CO_3 to this mixture of 5 ml of THF and 5 ml of DMF. The solution was left to stir for 5 hours at 65 °C. The reaction mixture was filtered into 10 ml of 10% HCl to which an aqueous solution of NH_4PF_6 was added inducing a yellow precipitate. The purified solid was recovered by filtration, washed with water and rinsed with diethyl ether.

The reaction with thiophenol followed the same ratio of 1:1.2 complex to nucleophile in the presence of a weak base and placed in a 50 ml round bottom flask containing the solvent mixture of a 1:1 DMF to THF. The

reaction was left to stir for 18 hours under nitrogen. The work-up consisted of filtration into 10% HCl, followed by the addition of the aqueous NH_4PF_6 solution which caused partial precipitation of the product. To achieve the highest yields, extraction with CH_2Cl_2 and washing this organic layer with water. The organic layer was dried over $MgSO_4$ and filtered. The solvent was concentrated and the solid product was precipitated out upon addition of diethyl ether. The solid was collected by filtration, washed with ether and dried under vacuum. This was the method followed to prepare complexes (**1-5**).

Diiron Complexes

The synthesis of the dicyclopentadienyliron arene complexes with etheric bridges (**11**, **13**, **15** and **18**) was carried out according to published procedures [10, 67, 70-72]. To a mixture of 1 mmol of chloroarene cyclopentadienyliron complex, 0.5 mmol of the aliphatic or aromatic oxygen dinucleophile and 2.5 mmol of K_2CO_3 in 10 ml of DMF. The mixture was stirred for 15 hours under nitrogen. The brown/green solutions were then filtered through a sintered glass crucible into 10% (v/v) HCl solution resulting in a yellow precipitate. This solution was then washed with water and rinsed with diethyl ether. After drying under vacuum the yellow products were characterized by ^{1}H and ^{13}C NMR [10, 67, 70-72].

Polyiron Complexes

The trimetallic complex (**22**) was prepared from the reaction of the p-dichloroarene complex with the monometallic complex consisting of a free hydroxyl group in the presence of K_2CO_3 in DMF. The reaction was left to stir for 16 hours under a nitrogen atmosphere. The procedure for product isolation was an initial filtration into 10% HCl and then the addition of a concentrated aqueous solution of ammonium hexafluorophosphate yielded a yellow precipitate. The product was purified by filtration, washed with water and rinsed with ether. Characterization was accomplished after drying under vacuum [77].

The even polyiron series such as the tetrametallic (**23**), hexametallic (**25**), and octametallic (**27**) complexes were prepared from the reaction of the corresponding complex with one terminal chloro group in a 2:1 ratio to the desired dinucleophilic complex. In the presence of K_2CO_3 and DMF the reaction was left to stir for 16 hours under nitrogen. The solution was filtered into 10% HCl and then an aqueous NH_4PF_6 mixture was added which caused a yellow precipitate to form. The product was isolated by filtration and purified by washing with water and rinsing with diethyl ether. Once dried under vacuum the yellow solid product could be characterized by NMR [77].

The odd polyiron series that were used in this work such as the pentametallic (**24**) and heptametallic (**26**) complexes were prepared using a 2:1 ratio of the terminal chlorinated complex with the dihydroxy nucleophile. These were added to a 50 ml round bottom flask containing base and DMF. Under nitrogen, the reaction was left to stir at room temperature for 16 hours. The solution was filtered into 10% HCl and then an aqueous ammonium hexafluorophosphate solution was added to precipitate the product. The

yellow solid was isolated by filtration and purified by washing with water and rinsing with diethyl ether. After drying under vacuum the product could be characterized by NMR [77].

Hydride Addition Reactions

Monoiron system:

In a 25 ml flask, 0.5 mmol of a monoiron arene complex and 1.25 mmol of $NaBH_4$ in 10 ml of THF and 1.0 ml of DMF were stirred for 3 hours under nitrogen. The bright orange product was then filtered through sintered glass, washed with 10 ml of water and extracted with $CHCl_3$ (3 x 20 ml). The bright orange extract was washed with water, dried over $MgSO_4$ and the solvent was removed by rotary evaporation yielding a red/orange oil. This methodology was used in the preparation of the adducts (**6-10**). The yields are listed in Table 14.

Diiron system:

When 0.5 mmol of the bimetallic complexes was employed 2.5 mmol of $NaBH_4$ was used for complete reaction to occur in a 25 ml round bottom flask that contained 10 ml of THF and 1 ml of DMF. The reaction was left to stir for 3 hours under an nitrogen atmosphere. The product was isolated by extraction with chloroform (3 x 20 ml) and purified with water washings. The

organic layer was dried over $MgSO_4$ and filtered. The solvent was removed via rotary evaporation, resulting in a red/orange oil. This procedure was followed in order to obtain the adducts (**12-16**). The yields are listed in Table 14.

Cyanide Addition Reactions

Diiron systems:

An example of the cyanide addition reactions for the bimetallic series is as follows. In a 25 ml flask, 0.5 mmol of 1,4-bis[(η^6-4-methylphenoxy-η^5-cyclopentadienyl)iron]benzene hexafluorophosphate and 3.0 mmol of NaCN in 5 ml of DMF and 1 drop of water were stirred for 3 hours. The red solution was extracted with $CHCl_3$ (2 x 20 ml), washed with water to remove the DMF, and dried over $MgSO_4$. The solvent was evaporated off, yielding a red oily product. In the case of the complex where both ortho positions were hindered with methyl groups, the reaction time was 12 hours. This may be due to the steric position at which nucleophilic attack occurs. Reaction times of 3, 5, and 8 hours were attempted but only starting material was recovered. This procedure led to the production of adducts (**17**, **19**, **20** and **21**). Recoveries are listed in Table 14.

Polyiron systems:

Reaction ratios varied according to complex size; 0.1 mmol of the trimetallic complex (**22**) with 0.9 mmol of NaCN immediately turned orange when introduced to 5 ml of DMF in a 25 ml round bottom flask. The water is introduced to the reaction mixture last to aid in the solubility of the NaCN. The product was isolated by extraction with $CHCl_3$ (2 x 20 ml) and the highly interacting solvent (DMF) was removed by washing with water. The organic solution was dried over $MgSO_4$ and filtered. The red product (**28**) was obtained once the chloroform was removed by rotary evaporation. The yields and υ_{CN} are listed in Table 14.

The isolation techniques for the remaining cyanide addition products follow the procedure outlined above. The ratio of 1:3 of complexed arene ring to nucleophile was found to be the ideal ratio. An increase in the amount of NaCN resulted in the identical products obtained with the 1:3 ratio with no change in yields. However if the amount of NaCN was used was lower, the yields decreased and there was some unreacted products detected.

The tetrametallic complex (**23**) (0.1 mmol) was reacted with 1.2 mmol of NaCN which initially gave a yellow/orange solution only later to become orange/red in color. The work-up consisted of separating the unreacted starting material from the adduct. This was completed using chloroform to extract the adduct then purification through water washings. The unreacted complex in each case was recovered by the extraction of the aqueous layer with dichloromethane and all DMF was removed by the washing with water. The organic layer was dried over $MgSO_4$ and filtered. Once the solvent was removed by rotary evaporation the final yellow solid was recovered upon precipitation with diethyl ether. Never was there 100% reactivity occurring

even if the reaction time was extended to a maximum of 12 hours. The highest yield and most pure samples were obtained when the reaction time was 3 hours. Longer reaction times resulted in lower yields due to the increased amount of decomposition therefore uncharacterizable products present so once cleaned the yields based on recovery decreased. This was the method used in order to determine the yields based on full recovery. The yields and υ_{CN} of adduct (**29**) are listed in Table 14.

The following oligomeric species follow the same reaction pattern as outlined above where 0.1 mmol of the pentametallic complex (**24**) reacted with 1.5 mmol of NaCN in 5 ml of DMF and 1 drop of water. The adduct formed selectively (**30**) and the unreacted starting complex was isolated and purified as described above. As the length of these oligomeric complexes increase the more they interact with the DMF therefore an increased number of water washings is required. The increased number of washings can also greatly effect the yield if the product becomes slightly soluble. If for some reason the sample was not DMF free as shown by ^{1}H NMR, dissolution of the product in ether and transfer to a new flask then removal of the solvent proved to be a sufficient method of purification. The cyanide adducts are more stable than the hydride products but will decompose within two days at room temperature.

For the remaining oligomeric complexes the ratio used is as follows, 0.1 mmol of the hexametallic complex (**25**) was reacted with 1.8 mmol of NaCN, 0.1 mmol of heptametallic complex (**26**) was reacted with 2.1 mmol of NaCN, and finally 0.1 mmol of the octametallic complex (**27**) with 2.4 mmol of NaCN. These were the best ratios giving the highest yields and the highest quality of the product. The yields and υ_{CN} of the adducts (**31, 32 and 33**) are listed in Table 14.

Aliphatic sulfonyl systems:

In the case of the aliphatic sulfonyl bimetallic complexes, the reaction ratios were found to be ideal in a 1:3 ratio. An example of the reaction between the aliphatic complex and sodium cyanide is as follows. In a 25 ml round bottom flask, 0.5 mmol of the substituted aliphatic sulfonyl diiron complex (**34-42**) was dissolved in 5 ml of DMF. To this solution 3.0 mmol of NaCN and a drop of water were added. The dark red solution was left to stir for 30 minutes under nitrogen. The reaction mixture was then extracted with chloroform (3 x 20 ml) and washed well with water. The organic layer was dried over $MgSO_4$ and filtered to remove the drying agent. The product was recovered after the solvent was removed by rotary evaporation as a red oil. The reaction time was an important factor for the complexes that consisted of electron withdrawing groups. If time was increased to 3 hours all that could be recovered were decomposition products that were soluble in water and could not be recovered. Therefore reactivity is increased when electron withdrawing groups are present. This method was used to prepare the adducts (**43-51**). The yields and υ_{CN} are listed in Table 14.

Mixed ether and thioether systems:

The reaction of NaCN with the mixed ether/thioether bimetallic complex (**52**) followed the above procedure in which the ratio of complex to nucleophile was 1:3. The reaction was carried out in DMF with one drop of water and was allowed to stir for 3 hours under nitrogen. The product was recovered using $CHCl_3$ (3 x 20 ml) and purified by washing with water. Once

the product had been dried over $MgSO_4$ and filtered the red oil product was recovered after rotary evaporation. The yields and υ_{CN} of the adduct (**54**) are listed in Table 14.

The final system that underwent cyanide functionalization was the aromatic ether/sulfonyl diiron complex (**53**). The reaction ratios were 1:3 complexed arene ring to NaCN. The reactions were carried out at room temperature for 1 hour under nitrogen. The dark red solution was extracted with $CHCl_3$ (3 x 20 ml) and washed with water. The organic layer was dried over $MgSO_4$ and then filtered. The pure product was isolated by removal of the solvent via rotary evaporation. Decomposition occurred if the reaction time was extended past one hour. The unreacted complex was recovered by extraction of the water layer with dichloromethane and the DMF was removed with water. The resulting organic layer was dried over $MgSO_4$ and filtered. The solvent was removed by rotary evaporation and the yellow product was recovered on precipitation with diethyl ether. The yields and υ_{CN} of adduct (**55**) are listed in Table 14.

Demetallation Reactions

Diiron systems:

To a solution of the bimetallic adduct (**17** and **19**) (0.2 mmol) in 10 ml of acetonitrile was added 0.4 mmol of DDQ (2,3-dichloro-5,6-dicyano-1,4-benzoquinone), and the resulting mixture was left to stir for 30 minutes at room temperature. The ratio of oxidant to adduct or complexed cyclohexadienyl ring always followed a 1:1 reaction ratio. The black solution

was then filtered through sintered glass and evaporated to dryness. The product was dissolved in CH_2Cl_2, placed on a short silica gel column and eluted with $CHCl_3$ and CH_2Cl_2; the resulting solutions were dried over $MgSO_4$ and evaporated to dryness to give the free functionalized aromatic ether. This procedure was used in the production of the compounds (**56** and **57**). Yields are listed in Table 14.

Polyiron systems:

In the case of the trimetallic cyclohexadienyl product (**28**), the ratio of complex to oxidant was 1:3 and the work up procedure follows as described above. For the tetrametallic (**29**) and pentametallic (**30**) adducts the ratio of complex to DDQ was 1:4 and 1:5 respectively and the organic product was recovered via column chromatography in the chloroform and dichloromethane layers. The remaining reactions of the hexametallic (**31**), heptametallic (**32**) and octametallic (**33**) adducts followed the same trend in ratio of adduct to oxidant. For the hexametallic adduct the ration was 1:6 adduct to DDQ. In the case of the heptametallic and octametallic adducts the ratios of adduct to oxidant were 1:7 and 1:8 respectively. The methodology of recovery of these products followed the same procedure as outlined for the smaller systems. The difference that was encountered with these latter systems is their position of elution, all were present in only the dichloromethane layer. The recovery of compounds (**56-63**), was effective with the use of DDQ. The yields and υ_{CN} are listed in Table 14.

Photolysis of these adducts was carried out in 30 ml of CH_2Cl_2 and 10 ml of CH_3CN and left to purge for 30 minutes under nitrogen. The photolytic tube was left under a xenon lamp for 5 hours then evaporated to dryness.

The product was dissolved in 4 ml of CH_2Cl_2 and put on a silica gel column prepared in hexane. The ferrocene was eluted in the hexane layer and the product was recovered in both the $CHCl_3$ and CH_2Cl_2 fractions. The yellow/white solid was recovered once the solvent was removed following rotary evaporation. This technique gave lower product yield and was more difficult to separate from the ferrocene than in the DDQ reaction. In addition, the reaction time and work-up time for the DDQ reaction was far more efficient.

The aliphatic sulfonyl adducts produced confusing results when demetallated with DDQ. Photolytic degradation of these addition products was also attempted in 30 ml of CH_2Cl_2 and 10 ml of CH_3CN which were purged for 30 minutes under nitrogen then placed under a xenon lamp for 5 hours. The free organic compound was not recovered. In both instances, either the CN group or the aliphatic bridge was not present spectroscopically. Further work is necessary in this area in order to establish conditions.

NMR parameters

All samples were run in $CDCl_3$ and this was the reference point of 7.26 ppm for proton and 77.00 ppm for carbon NMR. For the CH COSY experiments, the system at equilibrium is subjected to a 90^o pulse, which is then allowed to evolve for a variable period t_1. The end of the evolution period is marked by a second 90^o pulse, after which the data is acquired over t_2. The relaxation delay was set to 0.2 sec and 11.5 μsec after the first pulse and 17 μsec as the second delay during acquisition. The acquisition time to complete one scan was set to 0.56527 sec. The incremented delay in the second dimension was set to 0.0000030 μsec and the sweep width covered

was 3623.19 Hz (152.898 ppm). The number of dummy scans was 32 which allows for steady state to be reached before the acquisition and processing of 64 actual scans. The time domain data size which defines the number of points to be sampled and digitized before processing occurs was 4096 points. The composite pulse decoupling is the program used to process the data and this program is referred to as the Garp program. The HH COSY experiments follow the same general route of acquisition but the parameters are slightly different. The resolution delay was set to 3 sec and the acquisition time was set to 0.113684 sec. The sweep width covered 4504.50 Hz (9.007 ppm). The number of dummy scans was 4 and the number of actual scans was 16. The time domain data set included 1024 points. The delays were the same as outlined for the CH COSY. The delay employed for the evolution of long range couplings was 0.20000 sec.

Waltz16 is the composite pulse decoupling program used in data processing for the one dimensional experiments. Carbon NMR spectra were obtained with a relaxation delay of 3.0 sec after the 90^{o} pulse with delay of 70.0 μsec. The number of dummy scans was 2 with 5000 processed scans. The sweep width was 29411.77 Hz and the time domain data set included 65536 points. The acquisition time was set to 1.114132 sec. Proton NMR had a relaxation delay of 5.0 sec after the 90^{o} pulse with a delay of 12.5 μsec. The time domain data set included 32768 points and the sweep width encompassed 7575.78 Hz. The number of dummy scans used was 2 and the actual number of scans was 32.

5.0 References

[1] D. Astruc. Tetrahedron, **39**, 4027 (1983).

[2] J. March. Advanced Organic Chemistry: Reactions, Mechanisms, and Structure., Fourth Ed., John Wiley and Sons, New York, 1992.

[3] S.G. Davies, M.L. Green, M.P. Mingos. Tetrahedron, **34**, 3047 (1978).

[4] M.F. Semmelhack. Comprehensive Organic Chem. Eds: B.M. Frost and I. Fleming, Oxford, Pergamon, 4, 531 (1991).

[5] A.N. Nesmeyanov, N.A. Vol'kenau, I.N. Bolesova. Dokl. Akad. Nauk. SSSR, **149**, 615 (1963).

[6] A.N. Nesmeyanov, N.A. Vol'kenau, I.N. Bolesova. Tetrahedron Lett. 615 (1963).

[7] A.N. Nesmeyanov, N.A. Vol'kenau, I.N. Bolesova. Dokl. Akad. Nauk. SSSR, **169**, 1327 (1965).

[8] D. Astruc, R. Dabard. J. Organomet. Chem. **111**, 339 (1976).

[9] A.N. Nesmeyanov, I.F. Leshchova, Yu.A. Ustynyuk, Ye. I. Sirotkina, I.N. Bolesova, N.A. Vol'kenau. J. Organomet. Chem. **22**, 689 (1970).

[10] A.S. Abd-El-Aziz, D.C. Schriemer, and C.R. de Denus. Organometallics, **13**, 374 (1994).

[11] D. Astruc, Top. Curr. Chem., **180**, 48 (1991).

[12] C.C. Lee, R.G. Sutherland and B.J. Thomson. Tetrahedron Lett. **26**, 2625-2626, (1972).

[13] A.N. Nesmeyanov, N.A. Vol'kenau, L.S. Shilovtseva and V. A. Petrakova. J. Organomet. Chem. **85**, 365 (1975).

[14] M.R. Churchill, R. Mason. Proc. Chem. Soc. 112 (1963).

[15] M.R. Churchill, R. Mason. Proc. Roy. Soc. 191 (1964).

[16] M.R. Churchill. J. Organomet. Chem. **4**, 258 (1965).

[17] P.E. Baikie, O.S. Mills, P.L. Pauson, G.H. Smith, J. Valentine. Chem. Comm. 425 (1965).

[18] M.R. Churchill, R. Mason. ibid. 777 (1967).

[19] I.U. Khand, P.L. Pauson and W.E. Watts. J. Chem. Soc. (C) 2257 (1968).

[20] I.U. Khand, P.L. Pauson and W.E. Watts. J. Chem. Soc. (C) 116 (1969).

[21] I.U. Khand, P.L. Pauson and W.E. Watts. J. Chem. Soc. (C) 2261 (1968).

[22] P. Michaud, D. Astruc, J. H. Ammeter. J. Am. Chem. Soc. **104**, 3755 (1982).

[23] J.F. McGreer and W.E. Watts. J. Organomet. Chem. **110**, 103 (1976).

[24] R.G. Sutherland, C.H. Zhang, R.L. Chowdhury, A. Piorko, and C.C. Lee. J. Organomet. Chem. **333**, 367 (1987).

[25] R.G. Sutherland, R.L. Chowdhury, A. Piorko and C.C. Lee. Can. J. Chem. **64**, 2031(1986).

[26] R.G. Sutherland, R.L. Chowdhury, A. Piorko and C.C. Lee. J. Organomet. Chem. **319**, 379 (1987).

[27] R.G. Sutherland, R.L. Chowdhury, A. Piorko and C.C. Lee. J. Chem. Soc. Chem. Comm. 1296 (1985).

[28] C.H. Zhang, R.L. Chowdhury, A. Piorko, C.C. Lee, and R.G. Sutherland. J. Organomet. Chem. **346**, 67 (1988).

[29] R.G. Sutherland, C.H. Zhang, A. Piorko and C.C. Lee. Can. J. Chem. **67**, 137 (1989).

[30] R.G. Sutherland, R.L. Chowdhury, A. Piorko and C.C. Lee. J. Org. Chem. **52**, 4618 (1987).

[31] D.W. Clack and L.A.P. Kane-Maguire. J. Organomet. Chem. **174**, 199 (1979).

[32] D.W. Clack and L.A.P. Kane-Macguire. J. Organomet. Chem. **107**, C40 (1976).

[33] E.P. Kundig, P. Jeger, and G. Bernardineli. Angew. Chem. Int. Ed. Engl. **19**, 34, (1995).

[34] S.L. Grundy, A.R.H. Sam, and S.R. Stobart. J. Chem. Soc. Perkin Trans. I. 1663 (1989).

[35] F. Terrier. Chem. Rev. **82**, 77 (1982).

[36] R.G. Sutherland, C. Zhang, A. Piorko. J. Organomet. Chem. **419**, 357 (1991).

[37] M.F. Semmelhack, G.R. Clark, J.L. Garcia, J.J. Harrison, Y. Thebtaranonth, W. Wulff, and A. Yamashita. Tetrahedron. **23**, 3957 (1981).

[38] R.D. Pike, D.A. Sweigart. Synlett. 565 (1990).

[39] M.F. Semmelhack, H.T. Hall, R. Farina, Jr.,M. Yoshifuji, G. Clark, T. Bargar, K. Hirotsu and J. Clardy. J. Am. Chem. Soc. **13**, 3535 (1979).

[40] P.J.C. Walker, R.J. Mawby. Inorg. Chim. Acta. **7**, 621 (1973).

[41] R.D. Pike, W.J. Ryan, N.S. Lennhoff, J. Van Epp, and D.A. Sweigart. J. Am. Chem. Soc. **112**, 4798 (1990).

[42] W.J. Ryan, P.E. Peterson, Y. Cao, P.G. Williard, D.A. Sweigart, C.D. Baer, C.F. Thompson, Y.K. Chung, and T.M. Chung. Inorganica Chimica Acta. **211**, 1 (1993).

[43] G.R. Krow, W.H. Miles, P.M. Smiley, W.S. Lester and Y.J. Kim. J. Org. Chem. 14, 4040 (1992).

[44] W.H. Miles and H.R. Brinkman. Tetrahedron Lett. 5, 589 (1992).

[45] W.H. Miles, P.M. Smiley and H.R. Brinkman. J. Chem. Soc., Chem. Commun. 1897 (1989).

[46] A.J. Pearson, T.R. Perrior. J. Organomet. Chem. **285**, 253 (1985).

[47] A.J, Birch, L.F. Kelly. J. Organomet. Chem. **285**, 267 (1985).

[48] A.J. Pearson. Pure and Appl. Chem. **55**, 1767 (I983).

[49] A.J. Pearson. J. Chem. Soc., Chem. Comm. 339 (1977).

[50] R.P. Alexander, and G.R. Stephenson. J. Of Organomet. Chem. **299**, C1 (1986).

[51] A.J. Pearson. Acc. Chem. Res. **13**, 463 (1980).

[52] P.J. Domaille, S.D. Ittel, J.P. Jesson and D.A. Sweigart. J. Organomet. Chem. **202**, 191 (1980).

[53] J.F. Helling, G.G. Cash. J. Organomet. Chem. **73**, C10 (1974).

[54] T.S. Cameron, M.D. Clerk, A. Linden, K.C. Sturge, and M.J. Zaworotko. Organometallics. **7**, 2571 (1988).

[55] J.R. Hamon, J.Y. Saillard, A. Le Beuze, M. McGlinchey, D. Astruc. Ibid. **104**, 7549 (1982).

[56] Y.K. Chung and D.A. Sweigart. J. Organomet. Chem. **308**, 223 (1986).

[57] S.L. Grundy and P.M. Maitlis. J. Organomet. Chem. **272**, 265 (1984).

[58] Y.H. Lai, W. Tam, P.C. Vollhardt. J. Organomet. Chem. **216**, 97 (1981).

[59] R.D. Pike, W.J. Ryan, G.B. Carpenter, and D.A. Sweigart. J. Am. Chem. Soc. **111**, 8535 (1989).

[60] R.G. Sutherland, A. Piorko, U.S. Gill, C.C. Lee. J. Heterocyclic Chem. **19**, 801 (1982).

[61] R.G. Sutherland, B.R. Steele, K.J. Demchuk, C.C. Lee. J. Organomet. Chem. **181**, 411 (1979).

[62] R.G. Sutherland, A. Piorko, C.C. Lee, S.H. Simonsen, V.M. Lynch. J. Heterocyclic Chem. **25**, 1911 (1988).

[63] R.G. Sutherland, C.C. Lee, U.S. Gill, M. Iqbal, C.I. Azogu. J. Organomet. Chem. **231**, 151 (1982).

[64] C.C. Lee, R.L. Chowdhury, A. Piorko, R.G. Sutherland. J. Organomet. Chem. **310**, 391 (1986).

[65] A.N. Nesmeyanov, N.A. Vol'kenau, I.N. Bolesova. Dokl. Akad. Nauk. SSSR. **183**, 834 (1968).

[66] A.N. Nesmeyanov, N.A. Vol'kenau, I.S. Isaeva, I.N. Bolesova. Dokl. Akad. Nauk. SSSR. **175**, 606 (1967).

[67] A.S. Abd-El-Aziz, C.R. de Denus, C.R. Zawortko, and L.R. MacGillivray. J. Chem. Soc, Dalton Trans. 3375 (1995).

[68] A.E. Derome. Modern NMR Techniques for Chemistry Research., Pergamon Press, New York, 1987.

[69] R.M. Silverstien, G.C. Bassler, T.C. Morrill. Spectrometric Identification of Organic Coumpounds., Fifth Ed., John Wiley and Sons, New York, 1991.

[70] A.S. Abd-El-Aziz, K.M. Epp, C.R. de Denus, and G. Fisher-Smith. Organometallics, **13**, 2299 (1994).

[71] A.S. Abd-El-Aziz, Y. Lei, and C.R. de Denus. Polyhedron, **14**, 1585 (1995).

[72] A.S. Abd-El-Aziz, and K.M. Epp. Polyhedron, **14**, 957 (1994).

[73] W.C. Christopfel and L.L. Miller, J. Org. Chem. **51**, 4160 (1986).

[74] L. Anzalone and J.A. Hrisch, J. Org. Chem. **50**, 2128 (1985).

[75] W.D. Rounds, J.T. Eaton, J.H. Urbanowicz, G.W. Gribble. Tetrahedron Lett. **29**, 6557 (1988).